REACTIVE OPTIMIZATION OF TRANSMISSION AND DISTRIBUTION NETWORKS

A Thesis
Presented to
The Academic Faculty

by

Branislav Radibratovic

In Partial Fulfillment
of the Requirements for the Degree
Doctor of Philosophy in the
School of Electrical and Computer Engineering

Georgia Institute of Technology
May 2009

REACTIVE OPTIMIZATION OF TRANSMISSION AND

DISTRIBUTION NETWORKS

Approved by:

Dr. Miroslav Begovic, Advisor
School of Electrical and Computer Engineering
Georgia Institute of Technology

Dr. Deepak Divan
School of Electrical and Computer Engineering
Georgia Institute of Technology

Dr. Bonnie Heck
School of Electrical and Computer Engineering
Georgia Institute of Technology

Frank Lambert
NEETRAC
Georgia Institute of Technology

Dr. John Dorsey
School of Electrical and Computer Engineering
Georgia Institute of Technology

Date Approved: November 20, 2008

ACKNOWLEDGEMENTS

I would like to thank to my wife Jelena for continuous support and understanding on this endless road, to my adviser dr. Miroslav Begovic for making this road possible and to my colleague, graduate student, George Stefopoulos for numerous interesting discussion during all of these years.

I would like to especially thank to Dr. John Dorsey for his guidance and friendship. Without his help this document will never be written.

TABLE OF CONTENTS

LIST OF TABLES

Page

LIST OF FIGURES

Page

SUMMARY

The objective of this research is to address some of the challenges associated with the multi-objective optimization on a modern power system. In particular, optimization of reactive resources was performed in order to simultaneously optimize several criteria: transmission losses, distribution losses, voltage stability, etc. The optimization was performed simultaneously on the entire power system; transmission and distribution subsystems included.

The inherent physical complexity of modeling together transmission and distribution systems is considered first. After considering all pros and cons for such a task, a model of the entire power system is successfully established using the available test system explained in Section 9.

The inherent mathematical complexity of high-dimensional optimization space is resolved by introducing the decoupling principle. System is first decoupled in several independent models (transmission system and distribution subsystems) and independent optimizations are performed on each part of the system. An algorithm is developed that properly combines the independent solutions to reach the overall system optima.

Even with the decoupled systems the multi-objective optimization space was immense for any conventional optimization algorithm. The principle of algorithm synthesis is used to reduce the size of the solution space. Deterministic algorithms are used to locate the local optima which are subsequently refined by probabilistic algorithm. All the algorithms are customized for the problem at hand and the multi-objective

optimization framework.

The algorithm is applied on a real-life test system and it is shown that the obtained solutions outperform the solution obtained with the conventional algorithm.

CHAPTER 1

1. INTRODUCTION

Modern electric utilities face the problem of load growth along with a strict limitation on investment resources which severely limits upgrades to the transmission and distribution (T&D) network infrastructure. One method for increasing system performance is investment in reactive resources. They are deployed in both the transmission and distribution networks. Table 1 summarizes the objectives usually considered when reactive resources are applied to the system.

Table 1. Transmission and distribution system objectives for installation of reactive resources.

Transmission system objectives	**Distribution system objectives**
Maximize transmission capacity	Minimize distribution losses
Minimize transmission losses	Flatten voltage profile
Improve voltage stability	Improve power factor
Improve transient stability	

Historically, utility companies have developed reactive resource planning policies that address each of these objectives separately, without optimizing the entire system performance. Therefore, various algorithms have been proposed to solve the capacitor placement problem, either on the transmission network or on the distribution feeders, when only one of the above objectives is optimized [1-22]. These types of problems are referred to as single-objective optimization problems.

In recent years, multi-objective optimization problems have been formulated in many engineering applications [23]. In these problems, two or more objectives need to be simultaneously optimized. Few multi-objective algorithms have already been proposed

for allocation and sizing of reactive resources [24-29]. However, these algorithms treat only one portion of the power systems (usually the distribution feeder). The problem of simultaneous optimization of reactive resources on the transmission and distribution systems represents a further step in the generalization of the problem.

A new approach of multi-objective optimization of reactive resources in T&D networks is demonstrated in the following sections. The reason such an algorithm is not already available is simple: modern power systems are of immense size. Pareto-optimal techniques, genetic algorithms, linear programming and system decoupling have been combined to overcome badly behaved optimization functions and very large solution spaces. This research considers only the steady-state phenomena of power systems; the dynamic reactive resources and transient system behavior are not considered.

The research illustrates the simultaneous optimization of a chosen subset of objectives (Table 1) with a limited budget dedicated for reactive support. The outcome of the multi-objective T&D optimization is, typically, a set of solutions rather than a single solution. While the choice of a single solution is left to the system owner (electric utility company), one possible procedure for its selection is discussed as well.

CHAPTER 2

2. ORIGIN AND HISTORY OF THE PROBLEM

Optimization of reactive resources in power systems is an important and well-researched topic [1-29]. However, to the best of the author's knowledge, no published literature considers the problem on the entire power system (transmission and distribution system). Moreover, models of entire systems are unavailable. Numerous physical difficulties (Section 4.1) and anticipated mathematical obstacles (Section 4.2) prevent the system owners from setting up these models and researchers from investigating them. Therefore, published algorithms tackle the problem either only on the distribution or only on the transmission side of the system. This section gives a brief overview and comparison of the available capacitor allocation techniques, for both transmission and distribution subsystems, along with an outline of multi-objective optimization. After a literature review, a motivational example is presented to illustrate how the proposed integral approach yields better results than the current practice.

Transmission optimization. Most of the transmission literature treats the capacitor allocation problem as a single-objective optimization problem. Researchers are usually concerned with stability (voltage or frequency) or transmission capacity issues; system losses are usually considered as an objective of secondary importance.

The optimization of *transmission line transfer capability* has been addressed by a number of authors [1-3]. The foundations of the problem are set by Saied [1]; Ojo builds on it [2]. Both efforts study a long tie-line between two networks or between a remote generator and a load. A series reactive device is applied to the line to increase its transfer

capacity. The maximum receiving-end power is obtained by placing a series capacitor near the receiving end of the line. A positive effect of series compensation to voltage stability is also reported. Five proposed compensation schemes of a long tie-line are evaluated in [3]. Maximum power transfer limits of all schemes are compared for the system operating on the verge of voltage stability. The effect of the degree of compensation, load power factor and line length on the maximum power transfer, critical angular separation and critical voltage is investigated as well.

Voltage stability of power systems is discussed in [4-7]. The effect of static reactive support on the voltage stability margin is investigated in [4]. The minimum singular value of the system Jacobian and the total generated reactive power are used as indications of stability margin. An algorithm for the calculation of the sensitivity of total generated reactive power with respect to system loads is presented. Sensitivity information is used for allocation of recitative support. It is found that the allocation and amount of reactive support have a strong effect on voltage stability margin.

The amount and allocation of reactive support needed for a system to operate at maximum reliability against voltage collapse is investigated in [5]. Continuation power flow (CPF), originally developed to overcome ill-conditioning near the point of voltage collapse, is utilized to obtain sensitivity information and augmented to find the minimum amount of support that delays voltage collapse (this methodology is partially adopted in the research presented in this proposal). Bus sensitivities are used to identify a small set of buses for possible reactive compensation. A non-linear constrained optimization problem (minimization of shunt reactive injection) is formulated and solved using sequential quadratic programming.

Prevention of voltage collapse via reactive support is extended to a system under contingencies [6-7]. A methodology for finding the optimal location of static-var compensator (SVC) is presented, [6]. Based on the system loading and contingency analysis, several indices are defined. They are used to identify the buses that need the SVC installment in order to increase the voltage stability margin. Indices measure proximity to voltage collapse, with or without SVC installed, in the normal regime, as well as under contingencies. CPF combined with eigenvalue analysis is used to access the voltage stability margin. Reactive dispatch practice of a modern electric utility (NGC – National Electric Grid, UK) is described in [7]; the author reports the development of a contingency constrained optimal reactive dispatch. The full set of NGC controls (generator and synchronous compensator vars, SVC, shunts and taps) is considered. The problem is solved using combination of heuristic techniques and linear programming. Minimization of the reactive losses and minimization of control actions are considered as objective functions. The author only briefly explains the technical details of the optimization process; the focus is on its practical implementation.

Numerous papers address *transient stability* issues. Reactive resources are frequently installed to improve damping of oscillations due to disturbances in the system. However, dynamic problems are beyond the scope of the research presented in this dissertation.

Distribution optimization. The reactive optimization problem in distribution systems is usually formulated as optimization of the position and size of capacitor banks in order to minimize power/energy loss and investment in reactive support. Various capacitor placement techniques have been proposed, [8]. Historically, the first choice for

capacitor placement was the point where the substation is connected to the distribution feeder. During the late 50's, the benefits of placing shunt capacitors along the primary feeder were observed [8]. The "two-thirds" rule (for maximum reduction of losses, a capacitor rated at two-thirds of the reactive peak should be placed at two-thirds of feeder length) was established. These early optimization techniques are analytical, easy to understand and implement. Unfortunately, they consider only the feeders with a constant conductor size and uniform loading. More accurate analytical techniques, based on nonlinear programming, have been suggested [9-13]. An example, in [10], shows how the "two-thirds" rule produces negative "savings" in the case of non-uniform loading. A common weakness of all the techniques discussed above is modeling of the capacitor sizes and locations as continuous variables.

With advancements in computing technology, numerical programming methods have been increasingly used in various optimization problems. Dynamic programming is used for capacitor allocation for feeder loss minimization [14]. The capacitor placement problem is solved using mixed integer programming [15, 16]; peak power and energy loss reduction are used as objectives. The location, size and type of capacitors, voltage constraints and load variations are also considered.

A heuristic technique is used in [17] to iteratively compensate the most "sensitive" node on a distribution feeder in order to reduce feeder losses. This algorithm was further improved in [18]. Heuristic techniques are intuitive and easy to understand and implement. They produce results very fast, but their weakness is the lack of guarantee of optimality.

Artificial intelligence (AI) - based methods have become popular during the last

two decades [8]. The capacitor allocation problem is usually solved using genetic algorithms (GA's), expert systems, simulating annealing or fuzzy set theory. Numerous AI-based methods are also used in other engineering applications. A major benefit in all AI-based methods is the capability of locating the global optima; their common weakness is high computational expense. Moreover, unlike other techniques, some of the AI-based methods are naturally suitable for multi-objective optimization.

Integral T&D optimization has not yet been proposed, partially because of the large size of its solution space. The necessity to reduce the solution space, even in the case of distribution systems, has been recognized [17-22]. A heuristic procedure for capacitor placement on a small number of sensitive nodes, selected by identifying branches with large losses due to reactive power, has been proposed [17]. A two-stage algorithm is applied in [19]; an expert system is used to find a local optimum, which is later improved by a simulated annealing technique. A genetic algorithm (GA) is proposed as an optimization tool in [20]. A sensitivity analysis (SA) based method is used to identify nodes for capacitor placement and therefore reduce the computational burden of GA. An opposite approach is also derived, [21]. GA is applied first and terminated after a specified number of iterations. The obtained result is improved via SA. Successive linearization of the nonlinear capacitor problem is applied in [22]. The problem is solved in three ways: using a deterministic procedure, by GA, and by a hybrid method combining the previous two techniques.

The majority of the researchers treat the reactive problem on a single feeder; a few engage in distribution networks. The case of a radial MV network has been solved [24]; a network of feeders fed from the same substation has also been considered [25].

Multi-objective optimization. The research presented here is performed in a multi-objective framework. Andersson, [23], presents a useful survey on multi-objective optimization in engineering design; he presents and compares available multi-objective optimization tools. Most of the capacitor placement techniques are developed using single objective optimization; they maximize economic gain considering capacitor price and power and energy losses. Some of the early efforts, claiming to perform capacitor allocation optimizing several objectives, simply combine different objectives into a new one. Ma et al. use, [26], a modified GA to minimize feeder losses and capacitor cost. Cost of losses and capacitors are simply added. Jwo et al. [19] use a similar approach. They translate different objectives into a single one via fuzzy logic and then apply simulating annealing to find the optimal solution.

The existence of several objectives has been recognized [24], [27-29]. Voltage deviation and security margin are added to the objective-list [27]. An iterative trade-off technique is proposed to help the decision maker to proceed from one to another (more preferable) Pareto-optimal solution. Agugliaro et al. [24] optimize power losses and voltage regulations using shunt capacitors, tap changers and tie switches as control actions. A specifically designed GA relying only on a mutation operator is applied. A complete multi-objective approach, with resulting Pareto fronts is shown in [28]. Here the authors propose voltage reduction as an additional control action. Baran et al., [29], simultaneously optimize a set of objectives (investment, losses and voltage deviation) and obtain a Pareto optimal front of solutions.

Motivational example. A power system model is set using the IEEE 9-bus system (Figure 1). Two of the system loads are modeled using the real-field three-phase

feeder models. The third load is assumed to be customer owned; no reactive support can be assigned to its distribution circuit. It is supposed that system owner plans to apply 45 MVAr of support, to reduce the system losses or increase the voltage stability margin. The owner could do the following:

1. Use integral T&D algorithm proposed in this research to minimize total system losses (Table 2: first row, cells 1 to 3), or to maximize the voltage stability margin (first row, last cell).
2. Let the transmission division spend the entire budget on transmission loss minimization (second row, cells 1 to 3) or to maximize stability margin (second row, last cell).
3. Allow the distribution division to spend the entire budget to minimize distribution losses (last column).

Table 2. Verification of integral T&D approach.

	Integral T&D compensation	Compensation of transmission system	Compensation of distribution system
Transmission losses [MW]	3.33	**3.32**	3.46
Distribution losses [MW]	5.44	5.61	**5.42**
Total losses [MW]	**8.77**	8.93	8.88
Voltage stability margin [pu]	**3.15**	3.01	-

Review of the obtained results, Table 2, favors integral T&D compensation. Both transmission and distribution planners manage to minimize losses in their systems; however, the total system losses are the lowest for the proposed integral approach. The highest voltage stability margin is also obtained using the proposed algorithm.

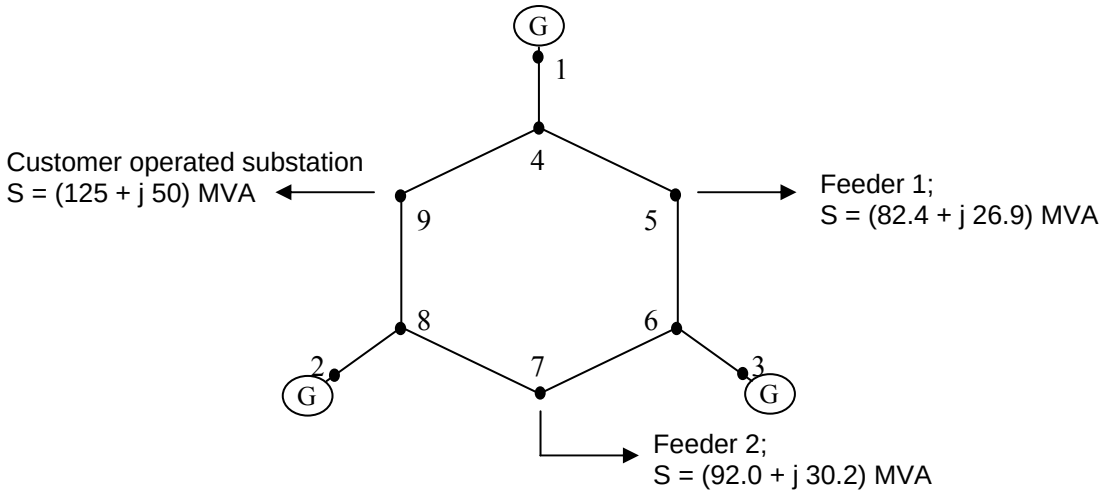

Figure 1. IEEE 9-bus system; one-line diagram.

The integral T&D algorithm achieves **both** of the above solutions (Loss = 8.77 MW and λ = 3.15 pu) in a single run. These are distinct solutions, the first minimizes losses and the second maximizes stability; the algorithm also finds the set of solutions in-between them. These solutions are called Pareto-optimal; they represent the different trade-offs between the two starting solutions.

A brief cost-benefit analysis of the proposed approach is performed. Stability is ignored; only the system losses are analyzed. The cost of the reactive support is estimated to be 10$/kVAr. Table 2 illustrates the peak system loading. To model the yearly load fluctuation, utilities usually use peak, shoulder (92% of peak) and valley (20% of the peak) load cases. These loads typically last for 5%, 70% and 25% of the year, respectively. Assuming the gain of the proposed method, 0.11 MW, distributed accordingly, and assuming the cost of system losses of 6 cents/kWh, an annual income of $43,015 is obtained. The investment in reactive resources pays-off after 10.5 years. It should be understood that the income obtained by reactive support is higher; the pay-off is obtained only by choosing the integral T&D approach instead of current practices.

Even though the above results seem enticing, the cost of the approach should be carefully analyzed. The integral T&D method has three stages: transmission optimization, distribution optimization, and results coupling. The time spent on transmission and distribution optimization is comparable to the time utilities spend using current practices. If the proposed routines are organized as a multi-objective search, they last longer but give more (or better) results. If a distribution/transmission planner intends to achieve several objectives, his repetitive use of single-objective procedure might last even longer.

The coupling of T&D systems requires time in addition to other utility activities. The duration of this stage highly depends on the availability and accuracy of the system data; the difficulties encountered are elaborated in Section 4.1. The fact that these calculations are done off-line and their encouraging economic results have motivated this research. Moreover, after the coupling was performed on a real system several beneficial side-effects have been discovered. Coupling of T&D systems has determined errors in both models; errors that would not be found unless both systems had undergone the scrutiny of the integral approach. Consequently, if the physical and mathematical obstacles are overcome, the integral T&D compensation is expected to yield better results than the current practice. Its beneficial results and side effects are expected to significantly outweigh its computational cost.

CHAPTER 3

3. CONCEPT OF MULTI-OBJECTIVE OPTIMIZATION

In most real-world problems several optimization criteria exist. Usually, it is not opportune to combine them in a single objective. If the criteria are optimized simultaneously their artificial addition is avoided. Moreover, the result of single-objective optimization is a single solution while the multi-objective optimization yields a solution set. The latter provides better insight to possible alternatives and consequently enables the choice of the solution with superior overall performance. A rigorous overview of multi-objective optimization (MO) methodology has been given by Coello et al. [30]. Basic mathematical definitions related to the topic are presented next.

Decision vector. The decision (control) vector consists of decision variables. It is represented by:

$$\vec{u} = [u_1, u_2, ..., u_q]^T .$$

Here u_j *(j = 1, ..., q)* represent a decision variable. The values of u_j are chosen during an optimization process.

Constraints. A set of physical limitation exists in any optimization problem. These limitations, referred to as constraints, are usually divided into equalities and inequalities.

$$\vec{g}(\vec{u}) = [g_1(\vec{u}), g_2(\vec{u}), ..., g_n(\vec{u})]^T = 0$$

$$\vec{h}(\vec{u}) = [h_1(\vec{u}), h_2(\vec{u}), ..., g_m(\vec{u})]^T \geq 0$$

Any constraint h_j *(j = 1, ..., m)* of type $h_j \leq 0$ can fit in the above formulation via multiplication with *-1*. The number of equality constraints n must be less than q; otherwise the problem becomes over-constrained.

Objective functions. Goals of MO problem are referred to as objectives or criteria. A set of objective functions f_j *(j = 1,...,k)* of a particular MO problem form a vector function denoted as:

$$\vec{f}(\vec{u}) = [f_1(\vec{u}), f_2(\vec{u}),..., f_k(\vec{u})]^T .$$

Multi-objective optimization problem. The general MO problem is formulated as follows:

Minimize: $\vec{f}(\vec{u}) = [f_1(\vec{u}), f_2(\vec{u}),..., f_k(\vec{u})]^T .$ (1)

Subject to: $\vec{g}(\vec{u}) = [g_1(\vec{u}), g_2(\vec{u}),..., g_n(\vec{u})]^T = 0 ,$

$\vec{h}(\vec{u}) = [h_1(\vec{u}), h_2(\vec{u}),..., g_m(\vec{u})]^T \geq 0 .$

Similar to handling inequality constraint, maximization of any objective function can be represented as minimization of its negative value. An alternative, compact, representation of (1) is given with (2).

Minimize: $\vec{f}(\vec{u}).$ (2)

Where $\vec{f} : \Omega \to R^k ,$

$\Omega = \{\vec{u} \in R^q \mid \vec{g}(\vec{u}) = 0, \vec{h}(\vec{u}) \geq 0\}.$

Convex set. A convex set is a collection of points such that the line segment connecting any two points entirely lays in the same set. Therefore, if for $\forall \vec{u}_1, \vec{u}_2 \in \gamma$ $\vec{u} \in \gamma$ $(\vec{u} = \kappa\vec{u}_1 + (1-\kappa)\vec{u}_2, 0 \leq \kappa \leq 1)$ then the set γ is convex.

Pareto optimality. While the notion of optimality in single-objective problems is intuitively clear, the multi-objective optimization forces a new definition of optimality. The concept of Pareto optimality has to be introduced. The solution is said to be Pareto optimal (belongs to a Pareto-optimal set) if no other solution can be found with better (or equal) performance with respect to all objectives. All of the solutions that make up the

Pareto-optimal set are said to be *non-dominated* (by other solutions). Therefore:

- $\vec{u}* \in \Omega$ is **Pareto optimal** if $for\ \forall \vec{u} \in \Omega\ and\ \forall j \in \{1,2,...,k\}\ stands\ f_j(\vec{u}) \geq f_j(\vec{u}*)$.
- $\vec{u}_1$ **dominates** $\vec{u}_2$ (denoted by $\vec{u}_1 \prec \vec{u}_2$) if for $\forall j \in \{1,2,...,k\}$ stands $f_j(\vec{u}_1) \leq f_j(\vec{u}_2)$.
- **Pareto-optimal set** is defined as $P := \{\vec{u} \in \Omega \mid \neg\exists \vec{y} \in \Omega, \vec{y} \prec \vec{u}\}$.

Concepts related to Pareto-optimal sets are further illustrated in Figure 2. Solutions are represented as points in the objective plane (f_1 and f_2 are two objectives).

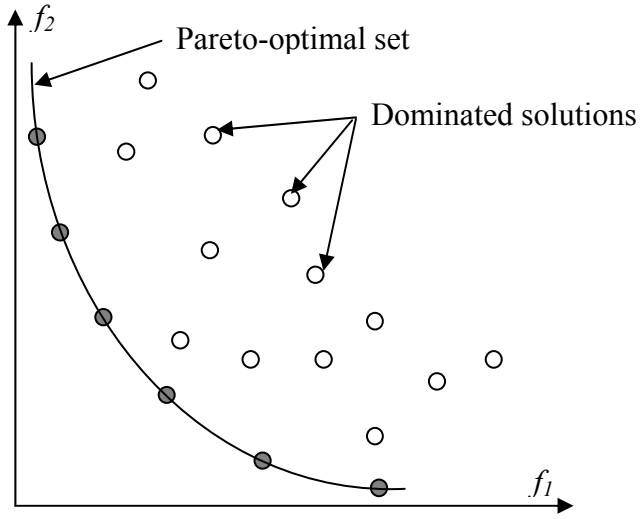

Figure 2. Pareto-optimality, non-dominated and dominated solutions, bi-objective case.

3.1. Multi-objective Optimization in Power System

The reactive power optimization problem is a multi-objective, integer, non-differentiable optimization problem. It is formulated as:

$$\begin{aligned}
&\text{Minimize:} && \vec{f}(\vec{x},\vec{u},\vec{p}) && f\text{: } R^N \rightarrow R^k. && (3)\\
&\text{Subject to:} && \vec{g}(\vec{x},\vec{u},\vec{p}) = 0 && g\text{: } R^N \rightarrow R^n,\\
& && \vec{h}(\vec{x},\vec{u},\vec{p}) \geq 0 && h\text{: } R^N \rightarrow R^m,\\
& && I_R(\vec{u}) = \vec{C}^T \cdot \vec{Q}_c = constant && \vec{Q}_c \subseteq \vec{u}\ ,\ \vec{Q}_c(i) \in N^n,\\
& && \vec{p} = \vec{p}(t)\,. &&
\end{aligned}$$

Here:

$\vec{x}$ - state vector; $dim(\vec{x}) = n$

$\vec{u}$ - control vector; $dim(\vec{u}) = q$

$\vec{p}$ - parameter vector; $dim(\vec{p}) = r$

N - $N = n + q + r$

I_R - investment resources [$]

$\vec{C}$ - vector of unit costs of reactive support [$]

$\vec{Q}_c$ - vector of reactive support [kVAr]

The above formulation is derived from (2) by explicit consideration of the system states and parameters. To avoid complicated notations, from this point on, vector signs will be neglected. Explanations of variables and functions in problem (3) are given in the following paragraphs.

State vector, *x*, in power system consists of positive sequence voltage phasors at all the buses in the system. Once the system states are calculated the rest of the quantities of interest (currents, line flows, etc.) are easily computable. For the problem at hand, the control vector, *u*, may include generator voltages and active power injections, transformer taps, and vector of reactive support. In the most general case the vector of reactive support may include static and dynamic VAr resources installed as shunt or series devices. Parameter vector, *p*, includes system impedances, topology (different breaker states) and loads. Explicit dependence of parameter vector on time, shown in (3), takes into consideration changes in the system topology and loading over the year.

Set of objective function, *f*, can include any subset of objectives from Table 1. Different objective sets are discussed in this document; exact mathematical formulation

of the objective functions are presented during these discussions. Set of inequality constraints, *h*, contains typical power system operational constraints (line flow limits, voltage limits and limitations on power injection of system generators). The mathematical formulation of these constraints is deferred to the following sections.

This research assumes that an electric utility has a limited budget dedicated for system improvement via reactive support. This limitation is expressed by economic constraint on investment resources (3). Cost of reactive support, *C*, is a function of the voltage level at the place of installment and type of the control. Reactive support vector, Q_c, is an integer vector; it accounts for the discrete increments in capacity of reactive support apparatus.

States of electric power systems are calculated using equations (4). The equations show power balance at bus *k*. If the equations are written for every bus in the system, the "power flow" system of equation is obtained. This system coincides to the set of equality constraints, *g*, in (3). If the system control and parameters, *u* and *p*, are known and fixed the power flow system of equations is referred to as the power flow problem. The power flow problem is a nonlinear system of equations; an iterative algorithm is required to find its solution. To that end, several algorithms are used; the Gauss-Seidel, the Newton-Raphson and the Fast-decoupled Power Flow are the most frequently utilized. The choice of the algorithm depends of the size and topology of considered system and desired speed of the algorithm.

$$\begin{aligned} P_{gk} - P_{dk} &= V_k^2 \left[g_k + \sum_{m \in M(k)} \left(g_{km} + g_{skm} \right) \right] - V_k \sum_{m \in M(k)} \left[g_{km} \cos(\delta_k - \delta_m) + b_{km} \sin(\delta_k - \delta_m) \right] \cdot V_m \\ Q_{gk} - Q_{dk} &= -V_k^2 \left[b_k + \sum_{m \in M(k)} \left(b_{km} + b_{skm} \right) \right] - V_k \sum_{m \in M(k)} \left[g_{km} \sin(\delta_k - \delta_m) - b_{km} \cos(\delta_k - \delta_m) \right] \cdot V_m \end{aligned} \tag{4}$$

The following notations are used in (4):

P_{gk}, Q_{gk}	-	Active and reactive generation at bus k
P_{dk}, Q_{dk}	-	Active and reactive demand at bus k
g_k, b_k	-	Shunt conductance and susceptance at bus k
g_{km}, b_{km}	-	Conductance and susceptance of the line between buses k and m
g_{skm}, b_{skm}	-	Shunt conductance and susceptance of the same line
V_i, δ_i	-	Voltage magnitude and angle at the bus i ($i = k$ or m)
$M(k)$	-	Set of buses connected to bus k

CHAPTER 4

4. OPTIMIZATION ALGORITHM; HIGH-LEVEL OVERVIEW

The goal of this research was to design an algorithm that will perform multi-objective optimization of reactive resources on a model of the entire power system. Literal accomplishment of the above task was impossible. First, accurate modeling of the entire power system is practically impossible. Second, no single optimization algorithm can efficiently explore the high-dimensional solution spaces of such models. To overcome these problems the *system decoupling* and *algorithm synthesis* are introduced.

4.1. Modeling Difficulties

Electric utilities favor strict separation between transmission and distribution models. Different types of data are considered in T&D systems. Developed operational procedures enable running the system without having its centralized model. Setting together T&D models is a demanding, though not impossible task. This section discusses the physical obstacles that may be encountered during the process.

The mathematical model of the power system built on equation (4) assumes symmetric systems and voltage-independent loads (constant power loads). Transmission systems, operating in steady state, are practically symmetric. Transmission operators usually neglect the voltage dependence of loads as well. For most of the practical problem the above mathematical model accurately represents transmission systems. The system's owner records the peak (maximum) and the valley (minimum) load for a given year. Shoulder load, used in numerous calculations, is derived from the peak load by

scaling it down by 8%. The peak load usually does not correspond to electric utility peak but the system operator peak (not Georgia Power peak for instance, but the peak of the entire Southern Company). Moreover, a system operator may ask the utility to scale up or scale down, the peak loads to account for any unusual ambient temperature (uncommonly hot or cold peak day). Finally, the system loads are measured at the HV side of HV/LV transformers; the loads are usually measured several times during 15 minutes and then averaged.

The asymmetry of distribution networks (asymmetric loads, single-phase laterals) is more evident. Three-phase modeling of distribution networks is becoming the practice of modern electric utilities. Feeders are modeled in its peak loading; the actual instantaneous peak is measured on each feeder.

Models of transformer connecting T&D systems are not available either in the transmission or distribution division. The part of the utility dealing with the system protection usually has fair models of HV/LV transformers. Frequently, utilities also have MV ($12kV < V_n < 69kV$) networks usually called the sub-transmission system. Depending on utility's organization, these networks are modeled in the "transmission" or "distribution" way.

Modeling of the entire power system starts by collecting the data from different utility subdivisions. The accuracy of the obtained data is usually vague. For instance, the amount of feeder capacitors that were switched on during the feeder peak is known with 80% of accuracy (malfunctioning of switches and capacitors is always an issue); the amount of feeder capacitors switched on during transmission valley load can only be estimated. Before the T&D models can be coupled, an extensive data analysis should be

performed. The analysis includes (but is not limited to) the following:

- Balancing of the three-phase distribution models.
- Scaling of non-concurrent T&D peak loads. Distribution loads are scaled to the transmission peak load level. Scaling can be done in many ways. Keeping the constant power factor of distribution loads seems to be a logical method.
- Scaling of sub-transmission data. If MV data exist the problem usually doubles: the MV data are recorded for the MV peak that is non-concurrent with the LV or HV peak.
- Accounting for power lost in the coupling transformer (HV/LV or HV/MV and MV/LV). Exact tap position of these transformers is usually unknown.

Despite the considerable amount of uncertainty, setting the integral system model is possible if proper engineering judgment is applied. Nevertheless, these difficulties, coupled with foreseen mathematical complexity (common for the high-order systems), are often the main factors for dismissal of the integral T&D approach.

4.2. System Decoupling

Solution of the problem (3) on the integral T&D system model suffers from the dimensionality curse due to the system size. The following example illustrates T&D system's related problem. The test system elaborated in Chapter 9 contains approximately 300 transmission buses. The sub-transmission part of the system consists of nineteen 44 kV feeders; if these are included in the transmission system, the number of buses more than doubles. The distribution system consists of 247 LV feeders. Using a realistic assumption of 400 nodes per feeder, the number of buses (nodes) in the system reaches

up to 100,000. The power flow solution of such a system is still possible; however, any computationally efficient optimization of it becomes a challenge. Even the power flow problem becomes difficult to solve if dozens of similar systems are put together.

As a consequence of the above discussion, system decoupling is proposed. The decoupling principle is depicted in Figure 3. Resources are split between the transmission and distribution systems. Optimization is performed separately on each system. Solutions from both systems are combined with an appropriate algorithm to filter a unique Pareto-optimal solution front (optimal set for the overall system).

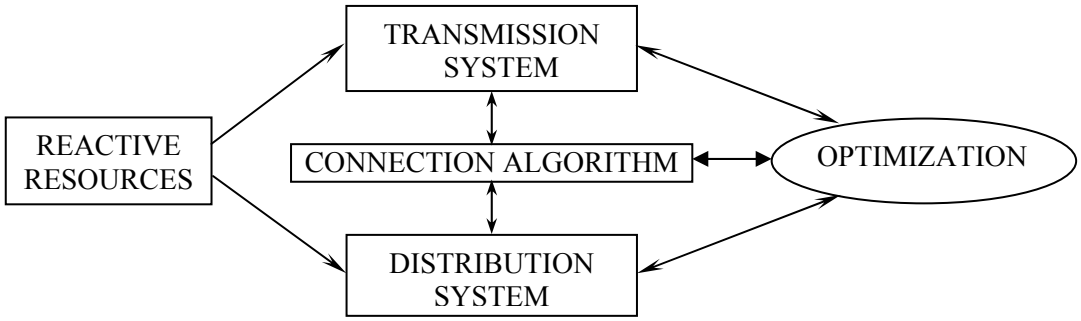

Figure 3. Flowchart for multi-objective optimization of reactive resources.

If the problem (3) could be fully decoupled, it would be possible to represent it with *d+1* independent optimization problems shown in (5-1) and (5-2). Formulation (5-1) corresponds to the transmission system optimization; subscript *T* refers to transmission system quantities. The formulation assumes that transmission loads do not depend on the solution of (5-1); furthermore, it assumes that the loads do not depend on the solution of problem (5-2) which is totally unrealistic. Optimization problem (5-2) considers *d* independent distribution systems (connected to transmission buses). Subscript *D* refers to distribution system quantities. The formulation (5-2) assumes not only mutual autonomy of distribution systems but also their independence from the transmission system.

However, important distribution controls, such as voltage on the source end of a distribution system, are dependent on the solution of (5-1). To that end, (5-1) and (5-2) should be augmented with the set of equation (5-3). The role of the connection algorithm (Figure 3) is to implement equations (5-3) during optimization of decoupled T&D systems.

$$\text{Minimize:} \quad f_T(x_T, u_T, p_T) \qquad f_T : R^{N_T} \to R^{k_T}. \tag{5-1}$$

$$\text{Subject to:} \quad g_T(x_T, u_T, p_T) = 0 \qquad g_T : R^{N_T} \to R^{n_T},$$

$$h_T(x_T, u_T, p_T) \geq 0 \qquad h_T : R^{N_T} \to R^{m_T}.$$

$$\text{Minimize:} \quad f_{Di}(x_{Di}, u_{Di}, p_{Di}) \qquad f_{Di} : R^{N_{Di}} \to R^{k_{Di}}. \tag{5-2}$$

$$\text{Subject to:} \quad g_{Di}(x_{Di}, u_{Di}, p_{Di}) = 0 \qquad g_{Di} : R^{N_{Di}} \to R^{n_{Di}},$$

$$h_{Di}(x_{Di}, u_{Di}, p_{Di}) \geq 0 \qquad h_{Di} : R^{N_{Di}} \to R^{m_{Di}},$$

$$\text{Interface equations:} \quad \left.\begin{array}{l} x_T = [x_{TT}\ x_{TD}]^T \\ u_{Di} = [u_{DDi}\ u_{DTi}]^T \end{array}\right\} \to x_{TD} = \bigcup_{i=1}^{d} u_{DTi}, \tag{5-3}$$

$$p_T = [p_{TT}\ p_{TD}]^T \to p_{TD}(i) = \Psi_{Di}(x_{Di}, u_{Di}, p_{Di}).$$

Here:

i - distribution system index; $i \in \{1,2,...,d\}$

x_{TD} - voltage phasors on transmission buses connected to distribution system

x_{TT} - voltage phasors on the rest of transmission buses

u_{DTi} - voltage phasors on source-end of feeder i

u_{DDi} - the rest of the feeder i controls (capacitors, taps…)

p_{TD} - transmission system loads

p_{TT} - the rest of transmission parameter vector

Ψ_{Di} - dependence of load on transmission bus *i* on appropriate feeder quantities

Compact formulation of optimization problem (5-1)-(5-3) is presented with (6).

$$\text{Minimize:} \quad F = \left[f_T(x_T, u_T, p_T), f_{D1}(x_{D1}, u_{D1}, p_{D1}), .., f_{Dd}(x_{Dd}, u_{Dd}, p_{Dd})\right]^T. \tag{6}$$

$$\text{Subject to:} \quad G = \left[g_T(x_T, u_T, p_T), g_{D1}(x_{D1}, u_{D1}, p_{D1}), ..., g_{Dd}(x_{Dd}, u_{Dd}, p_{Dd})\right]^T = 0,$$

$$H = \left[h_T(x_T, u_T, p_T), h_{D1}(x_{D1}, u_{D1}, p_{D1}), ..., h_{Dd}(x_{Dd}, u_{Dd}, p_{Dd})\right]^T = 0,$$

$$X_{TD} = \left[u_{D1}, u_{D2}, ..., u_{Dd}\right],$$

$$p_{TD} = \left[\Psi_{D1}(x_{D1}, u_{D1}, p_{D1}), ..., \Psi_{Dd}(x_{Dd}, u_{Dd}, p_{Dd})\right],$$

$$I_R(u_T, u_{D1}, ..., u_{Dd}) = constant,$$

$$P = \left[p_T, p_{D1}, ..., p_{Dd}\right]^T = P(t).$$

Different techniques for solving problem (6) are discussed in following chapters. The superiority of the integral T&D approach to current industry practice is already illustrated in the motivational example (Chapter 2). However, a logical question arises from system decoupling: How distant are the solutions of the original and decoupled problems? In other words, what is lost by decoupling?

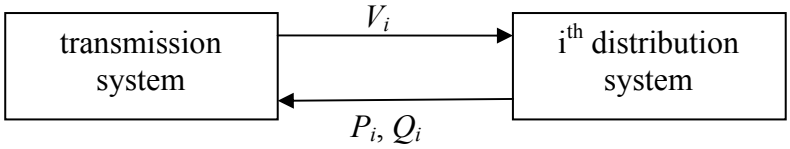

Figure 4. System decoupling; shared variables.

Figure 4 illustrates system decoupling from the physical standpoint. If the voltage phasor, V_i, at interconnection point is known, the distribution system could be solved independently. If the transmission loads, P_i and Q_i, at interconnection point are known, the transmission system could be optimized independently. Coupling of T&D systems is

caused by dependence $P_i(V_i)$ and $Q_i(V_i)$. If the distribution solutions are found for the set of discrete values V_i, distribution consumption P_i and Q_i, can be considered constant within one discrete step δV, formula (7). The only error induced in the decoupling procedure comes from the assumption of constant distribution consumption. If $\delta V \rightarrow 0$, decoupling vanishes from the problem, systems are solved in the original form (3). Proper size of δV can be chosen by its variation; if the decrease in δV does not improve the optimization results, decoupling does not induce error.

$$V_i \in \{V_{i\_\min}, V_{i\_\min} + \delta V, V_{i\_\min} + 2\delta V, ..., V_{i\_\max}\}. \quad (7)$$

4.3. Algorithm Synthesis

Two kinds of optimization techniques are used in this research, deterministic and probabilistic. Deterministic optimizations rely on derivatives while searching for function optimum; they are very fast but tend to converge to local optima. Probabilistic techniques use different probability rules for transition from one to another (usually better) solution. When carefully tailored they are capable of locating the global optima; however, they are very, sometimes extremely, time consuming.

The solution space of the attacked problem, even with decoupled systems, is very large. For an illustration a system with n buses can be used; the system is to be compensated with k identical capacitor banks. The solution space of such a problem (the number of different capacitor scenarios) is $\binom{n+k-1}{k}$. Table 3 provides an insight into the size of the solution space for systems used throughout this research. When the solution spaces are that large, it does not seem wise to rely on any of the above techniques alone.

Probabilistic techniques may last forever, deterministic techniques will converge to a local optimum. Therefore, the following strategy, Figure 5, is applied. A deterministic algorithm is used to find the set of locally best solutions. These are then fed into a probabilistic algorithm to proceed toward the global optima. This procedure keeps the solution space, left for the probabilistic optimization, reasonably small.

Table 3. Solution space dynamics for different sizes of the problem.

System	10-node feeder	10-node feeder	39-bus system	39-bus system	284-bus system
Reactive support	4 banks of 0.3MVA	20 banks of 0.3MVA	20 banks of 10MVA	200 banks of 10MVA	500 banks of 1 MVA
Size of solution space	715	10 millions	$1.8*10^{15}$	$1.7*10^{44}$	$9*10^{220}$

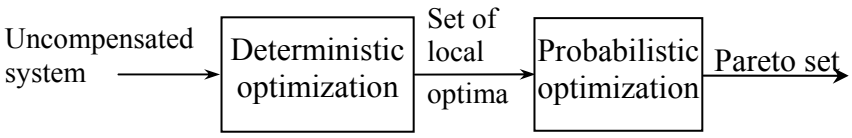

Figure 5. Algorithm synthesis; deterministic and probabilistic algorithms combined to reduce solution space.

CHAPTER 5

5. OPTIMIZATION TOOLS

This section explains the necessary mathematical details of the optimization tools: linear programming (LP) and genetic algorithm (GA). LP is a well-known optimization method used in linear problems. It efficiently optimizes linear functions subjected to sets of linear constraints. In order to apply LP the power system has to be linearized. Linearization, as usual, induces an error; therefore, the technique is not capable of finding the global optima. Their results can be enhanced using GA. GA is a probabilistic method. GA converges slowly; it tends to find the global optima, though. Both tools have originally been developed for the case of single-objective optimization problems. However, they can be extended to the multi-objective optimization.

5.1. Linear Programming

Linear programming is a popular tool in engineering optimization [31]. The simplex method is a widely used linear-programming algorithm. This section gives a brief introduction to the simplex method. Before proceeding with the algorithm the definition of a linear program in standard form is given. Transfer of any linear problem into standard form is briefly explained.

Linear problem in standard form. An optimization problem with a linear objective function and linear constraints is called a linear problem. A standard form of the linear problem includes three additional requirements:

1. Objective function is to be minimized.

2. All the variables are nonnegative.

3. All the constraints must be equality constraints.

Therefore, a linear problem written in standard form looks like:

$$\text{Minimize} \quad c^T x \tag{8}$$

$$\text{Subject to} \quad Ax = b$$

$$x \geq 0$$

where c and b are vectors and A is a constrain matrix of proper dimensions.

Any linear problem can be converted into standard form. If the problem is maximization it is easily converted into minimization by changing the sign of vector c^T. Inequality constrains of the linear problem are transferred into equality constraints by addition of slack variables. A free variable, x_i, is split into two non-negative variables $(x_i = x_i^+ - x_i^-)$. These practices are illustrated with the example in Figure 6.

Linear problem	***Linear problem in standard form***
Maximize $3x_1 - 4x_2$	Minimize $-3x_1 + 4x_2$
s.t. $2x_1 + x_2 \leq 5$	s.t. $2x_1 + x_2^+ - x_2^- + s_1 = 5$
$x_1 + 3x_2 \geq 2$	$x_1 + 3x_2^+ - 3x_2^- - s_2 = 2$
$x_1 \geq 0$	$x_1, x_2^+, x_2^-, s_1, s_2 \geq 0$

Figure 6. Transferring a linear problem into standard form.

Basic feasible solution. The main reason for using the standard form (8) is the latter discussion of the system $Ax = b$. The usual case in optimization problems is that $rank(A) = m < n$ (n is dimension of vector x). In that case the system $Ax = b$ has infinitely many solutions. If the n-m x_i's are set to zero, then the system can be solved uniquely (providing that columns of A are not linearly dependent). Such solution is called the *basic solution*; if the basic solution of the system $Ax = b$ is also the feasible solution of problem

(8) it is called the *basic feasible solution* (BFS). The variables that are set to zero are called non-basic variables; the others are called basic variables. The following theorem lays the foundation of the simplex method.

Theorem: *A point in the feasible region of a linear problem is an extreme point if and only if it is a basic feasible solution for the linear problem.*

Simplex method. The simplex method uses elementary row operation, similar to Gaussian elimination, to detect the optimal solution of linear problem. It does so by going from one to another basic feasible solution. The algorithm is capable of detecting unbounded problems as well. Without going into details, the core of the simplex method is presented next.

The simplex method consists of the following steps:

- Linear problem is converted to standard form.
- Basic feasible solution is calculated.
- If the BFS is optimal, the algorithm is terminated. The BFS is optimal if all the coefficients in objective functions are greater than zero.
- If the BFS is not optimal, the variable that enters and the variable that leaves set of basic variables are to be found. A variable with a positive coefficient value (in the objective function) is chosen to enter the set. The variable that leaves the set is chosen by checking the coefficients of entering variables throughout the set of constraints. For all positive coefficients the ratio coefficient / (right hand side) is found. The minimum ratio determines the leaving variable.
- Elementary row operations are used to find new basic feasible solution.

5.2. Linearization of the Optimization Problem

Nonlinear features of the reactive optimization problem, (3), are numerous: optimization functions are nonlinear, system of power flow equations is nonlinear, constraints are nonlinear as well. In order to apply the LP-based optimization, the problem should be transformed into linear standard form. State variables should be eliminated from the problem as well; linearized optimization problem should look like:

Minimize $f(u)$. (9)

Subject to $LB \le u \le UB$,

$K(u) \ge 0$.

where

$f(u)$ is linear objective function (u is the control vector)

LB, UB are the lower and upper bounds on system controls

$K(u)$ is linearized set of constraints

Objective function linearization. Linearization of any function $F(x, u)$, x being the state vector, is performed in the usual way:

$$F \approx F^0 + \frac{dF}{du}(u - u^0)$$

Minimization of F is equivalent to minimization of $\frac{dF}{du}u$. Total derivative of F with respect to control vector is found using the chain rule and auxiliary function $g(x,u) = 0$

$$\frac{dF(x,u)}{du} = \frac{\partial F(x,u)}{\partial u} - \frac{\partial F(x,u)}{\partial x} \cdot \left(\frac{\partial g(x,u)}{\partial x} \right)^{-1} \cdot \frac{\partial g(x,u)}{\partial u}. \quad (10)$$

Sensitivity of system's losses with respect to capacitor bank installed at bus i. Formula (10) is general; it applies to any function $F(x,u)$. The formula can be utilized to decide to which transmission bus to assign a capacitor ($u_i = Q_{Ci}$), in order to optimize the

particular objective. The bus with the highest sensitivity of the objective function is the logical candidate for the capacitor installment. The following choice of functions and variables is needed to calculate the sensitivity of system losses with respect to a capacitor bank installed at bus i:

- $F(x,u)$ - system losses
- $g(x,u)=0$ - set of power flow equations
- $x = [\delta\ V]^T$ - state vector of system voltages (angles and magnitudes)
- u_i - control variable (Q_C to be installed at bus)

The system losses can be defined as the sum of active power flowing into both ends of each system's branch. Therefore:

$$F(x,u) = P_{loss} = \Sigma(P_{ij} + P_{ji}). \tag{11}$$

Formula (10) can be simplified. In particular: $\frac{\partial F(x,u)}{\partial u_i} = 0$, $\frac{\partial g(x,u)}{\partial x}$ is the system's Jacobian and $\frac{\partial g(x,u)}{\partial u_i}$ is easily computable from the power flow equations. The only challenge is finding an analytic expression for $\frac{\partial F(x,u)}{\partial x}$. After defining system losses as in (11), the appropriate power flow equation (4) can be utilized to find $\frac{\partial F(x,u)}{\partial x}$.

The above derivations presents all of the necessary mathematical tools needed to perform sensitivity analysis of system losses with respect to an installed capacitor bank. A similar procedure can be applied to other objective functions.

Linearization of system constraints. A set of typical power system constraints contains line flow limits, reactive and active generation limits and limits of the system's voltages. Linearization of apparent line flow is depicted next; other, simpler, constraints are omitted to avoid unnecessary repetitiveness. The apparent power flow in the line

connecting buses “i” and “j”, measured at bus “i” can be expressed as:

$$S_{ij} = \sqrt{P_{ij}^2 + Q_{ij}^2}$$

The apparent flow at both ends of the line has to be less than the line transfer limits.

$$S_{ij} \le S_{\max}$$
$$S_{ji} \le S_{\max}$$

Linearized above inequalities look like:

$$\frac{dS_{ij}}{du} u \le S_{\max} - S_{ij}^{\ 0} + \frac{dS_{ij}}{du} u^0$$
$$\frac{dS_{ji}}{du} u \le S_{\max} - S_{ji}^{\ 0} + \frac{dS_{ji}}{du} u^0$$

The next step illustrates calculation of $\frac{dS_{ij}}{du}$ ($\frac{dS_{ji}}{du}$ is found accordingly).

$$\frac{dS_{ij}}{du} = \frac{\partial S_{ij}}{\partial u} - \frac{\partial S_{ij}}{\partial x}\left(\frac{\partial g}{\partial x}\right)^{-1} \frac{\partial g}{\partial u}.$$

The partial derivatives $\frac{\partial S_{ij}}{\partial u}$ and $\frac{\partial S_{ij}}{\partial x}$ are calculated from:

$$\frac{\partial S_{ij}}{\partial u} = \frac{P_{ij}}{S_{ij}} \frac{\partial P_{ij}}{\partial u} + \frac{Q_{ij}}{S_{ij}} \frac{\partial Q_{ij}}{\partial u}$$
$$\frac{\partial S_{ij}}{\partial x} = \frac{P_{ij}}{S_{ij}} \frac{\partial P_{ij}}{\partial x} + \frac{Q_{ij}}{S_{ij}} \frac{\partial Q_{ij}}{\partial x}$$

The above partial derivatives are calculated from the power flow equations (4). The above procedure applied to each branch, at both ends, linearizes line flow constraints.

5.3. Genetic Algorithm (GA)

GA belongs to the class of artificial-intelligence based optimization methods known as evolutionary algorithms. “Genetic algorithms are search algorithms based on the mechanics of natural selection and natural genetics.” [32]. GAs differ from traditional

(calculus-based) optimization and search procedures in following ways:

- They use probabilistic transition rules rather than deterministic;
- They do not use derivatives or any other auxiliary knowledge of the objective function; they use only the objective function values at given points;
- They work with a population of points rather than with a single point.

Perhaps the most distinguishing feature of GAs is that they do not deal with derivatives. Calculus-based techniques need gradient information of the objective function while searching for the optima. This process has two major weaknesses: it depends on the existence of derivatives and it seeks for the local optima. On the contrary, GAs do not need this auxiliary information. While performing the search for a better solution, they only need the objective function values for the given arguments.

Single-objective GAs were developed first. However, because they operate with populations of solutions, their extension to a multi-objective optimization is straight forward.

Single-objective GA. While a genetic algorithm can include many different operators, needed for fine adjustment, the following three operators capture the core of every GA: reproduction, crossover and mutation. The mechanics of a GA that contains only these three basic operators are quite simple; it only contains copying and swapping of strings.

At the beginning of every GA, an *initial population* is to be chosen. In order to demonstrate the power of genetic algorithm, the initial population is often chosen randomly. The GA is then applied to obtain a new generation of solutions with enhanced properties. The initial population (and subsequently every generation) contains a set of

possible solutions to a problem. Each solution is modeled by a fixed length string of coded decision variables. *Coding* is done in various ways; binary coding is very often used. Integer coding, or floating-point representation can be used as well. If the goal of a GA is to find the maximum of function $f(x) = -x^2$ on a domain $D = \{x \mid 0 < x < 63\}$, a randomly chosen four-member initial population, could look as in Figure 7.

Member	x	Binary coded string	$f(x)$
1	10	0 0 1 0 1 0	-100
2	31	0 1 1 1 1 1	-961
3	2	0 0 0 0 1 0	-4
4	25	0 1 1 0 0 1	-625

Figure 7. Binary coded initial population.

The first step in every GA is *reproduction*. This is a process in which the individuals of the current generation are copied according to their "wellness". For each generation member, the objective function (called *fitness* by biologists) is calculated. A higher probability of reproduction is assigned to individuals with higher fitness; a lower probability is assigned to the low-fitness individuals. After defining probabilities of reproduction to each individual, the reproduction operator may be applied in numerous ways. Probably the easiest way to implement reproduction is to create a roulette wheel in which each member of the population has its wheel slot proportional to its fitness. Reproduction is then performed by spinning the wheel, as many times as needed. After performing the reproduction, an intermediate population is obtained. It usually has the same size as the original population; some of the originals are repeated, some are omitted.

The intermediate population is then entered into a mating pool where the *crossover* is performed. Similar to reproduction, crossover can be performed in numerous ways: single-point crossover, two-point crossover, arithmetical crossover, etc. The first

step of crossover (irrespective of its type) is random mating between the members of the intermediate population. In the second step, each pair of members undergoes crossing according to a chosen rule. The mechanism of single-point, crossover is demonstrated in Figure 8. It is expected from this operation to preserve good substrings from parents and, by combining them, to improve the children's fitness.

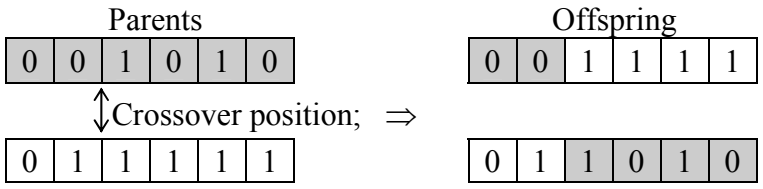

Figure 8. Single-point crossover upon two mated population members.

The *mutation* operator plays a secondary role in GAs. As in nature, mutation happens rarely and its role is to prevent the loss of potentially useful genetic material, or to introduce new information to the population (in capacitor placement problems, mutation could serve to put the capacitor on the certain node that was omitted in the initial population). The mutation rate is usually not pre-determined; it should be tailored for each particular optimization problem. In binary coding, mutation represents flipping of a single bit in a string (from 0 to 1, or vice versa).

Multi-objective genetic algorithms. Multi-objective GAs are quite similar to single-objective ones. The mechanisms of crossover and mutation work exactly as explained. However, the process of reproduction needs to be altered to take into consideration two additional phenomena: solution fronts and density of solutions inside the fronts. There are several ways to approach the problem, and they are all based on giving the higher reproduction probability to the individuals closer to the Pareto-optimal front and to individuals that are widely separated from their neighbors. A technique for applying the algorithm, based on *binary tournament* [28, 30] can be chosen.

The algorithm starts with a randomly chosen initial population. After each generation, the population is classified as shown in Figure 9. Non-dominated solutions are extracted from the set and assigned to the subset called *front of rank 1*. After these individuals are ignored, non-dominated solutions of the rest of the set are found and assigned to the *front of rank 2*. This process is repeated as many times as necessary to assign each member of the population to the front of the appropriate rank.

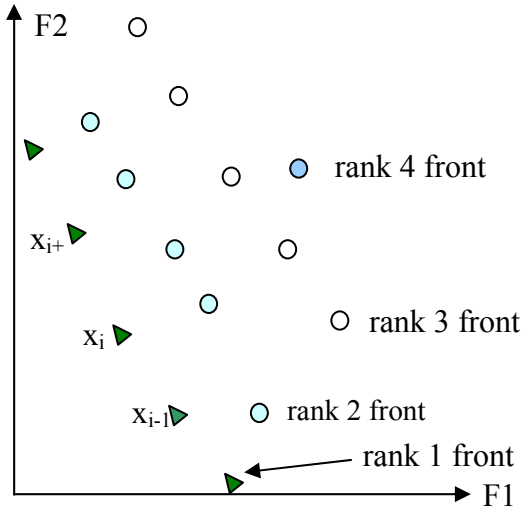

Figure 9. Population classification.

After the population is classified, the "crowded distance" of each solution inside its front is to be calculated according to:

$$cd(x_i) = \prod_j cd_j(x_i)$$

Where :

$$cd_j(x_i) = (F_j(x_{i+1}) - F_j(x_{i-1}))/(F_{jmax} - F_{jmin}), \quad j=1,2$$

The value $cd_j(x_i)$ is a measure of the distance between the *i*-th individual and his neighbors (Figure 9) in the particular front, with respect to the *j*-th objective function.

Following the classification, a binary tournament is performed as follows:

- Two individuals are randomly chosen from the population.

- The one from the lower-rank front is entered into the mating pool. If individuals are from the same front, the one with the higher crowded distance is entered into the mating pool. The later selection prevents scattering of solutions around a few points.
- The previous steps are repeated N times, where N is population size.

5.4. Efficiency of GAs in high dimensional solution spaces

This section provides an insight in the behavior of genetic algorithms on the problems with high solution spaces. This section is added posteriori, after the work on the algorithm was completed. This discussion is initiated by a member of the proposal committee. Optimization presented in this research was difficult because of high-dimensionality of the search space and the lack of knowledge of the global optima. Basically, the research has proven that the proposed algorithm finds the better solutions than the one currently used in the real system. However, it is not possible to say (at least at this point) how close the obtained solutions to the global optima are. The literature research has not revealed a solution to the particular problem, but it has provided some insight in the desirable organization of GA when the optimization time (solution space) is an important optimization constraint.

Several properties of genetic algorithms have been investigated thoroughly: encoding problems, selection strategies, crossover, mutation, various models of genetic algorithms, etc. However, population size and the number of generations have not been discussed much. This can be contributed to the stochastic nature of genetic algorithms. It has been recognized [33-36] that the proper choice of the population size and number of generations can greatly help in reducing the time needed for algorithms to converge.

Work presented in [33] tackles a similar problem. The authors are trying to improve the convergence speed by identifying the global optimum that is being found in the current population but it has not been identified as such. Due to the lack of identification of the global optimum many steps are performed needlessly. Different stop criteria usually used in GAs (total number of generation, stability of the fitness of the best individual, convergence of the population, etc.) are discussed and compared against the stop criterion proposed by the authors. The proposed solution is to build an approximation of the objective function; the approximation should be mathematically well defined so its global maximum can be located quickly. GA algorithm is performed on the original problem and GA is terminated once the error between the objective function and the global optimum of the approximation is low enough. Work discussed in [33] has deficiencies in that it only tackles single-objective optimization and that the proposed stop criterion outperforms conventional methods only on the particular problem (optimization of superconductor magnetic energy storage).

Lee et al. in [34] propose a new algorithm for assessing of GA performance. They recognize that if the optimal solution is not known GA performance is difficult to measure accurately and the reliability of the final solution is always a concern. Based on defined fuzzy goal the concept of a fuzzy stop criterion is developed. The fuzzy stop criterion is based on achieving a user-defined level of performance for the given problem. Data from past performance of the GA is used as a frame of reference for the current GA performance. The algorithm provides a higher level of user-GA interaction allowing the user to request a certain level of performance and reliability. Authors prove that their method locates faster optimal solutions than the convectional GAs. As in the case of the

[33], the work is done in single-objective framework and only on a single, well-researched, optimization problem: traveling salesman problem.

Cvetkovic and Muhlenbein investigate optimal population size in [35]. The optimal population size is defined as a minimum population size to converge to the optimum with high probability. The optimal population size is empirically calculated, by numerical fitting of data, for a given optimization function (ONEMAX function). For a specific genetic algorithm (called breeder genetic algorithm in the paper) the expected number of generation, GEN, until convergence is computed. It is shown that GEN is independent of the population size if population size is greater than the minimal population size. While the paper provides the empiric formulae for the minimal population size and minimum number of function evaluation (GA generation), the work is performed, again, only for a particular single-objective function. Moreover, the results are valid just for the specific genetic algorithm (mutation rate = 0, etc.).

Tsoy discusses in [36] the number of function evaluations, FE; FE is obviously FE = G·N; where, G- generation number limit and N is population size. In general, the higher the population size, the better solution is found in G generation; however, the higher the population size the more time will be spent performing evaluation function. Author tries to answer a question what is better, large population and small generation number or, vice versa. The author relays on the work given by [35] and work of several other authors to conclude that increase of the population size improves the performance of genetic algorithm since it reduces genetic drift (tendency of population to converge to a single genotype) and increases parallelism of the algorithm. After performing several experiments the authors conclude that in most cases largest populations with less number

of generations are better than the small population with a high number of generation.

Common denominator of the work presented in this section is that it focuses on single-objective optimization functions and that authors were focused each on a particular single optimization function. Common difficulty is that no analytic formula for reduction of search space exists, [36]. The main cause of this is a great variety of GAs and the necessity to take into account numerous parameters that influence genetic algorithm. While there is no final conclusion how to better organize the algorithm to more efficiently research high solution spaces, some hints from this research could have been used in the original GA implementation: greater population sizes, approximation of the objective function for measurement of convergence, etc.

5.5. Metrics for Comparison of Pareto Sets

A metric is never an issue in single-objective optimization; there is no dilemma as to which of the two solutions is better. However, metrics that allow meaningful comparison of the multi-objective optimization results should be developed. Coello et al. [30] present a useful survey of available metrics. When developing multi-objective metrics, researchers usually generate true PF, PF_{true}, and measure performance of the solutions based on relations between PF and PF_{true}. Two suitable metrics [30] are shown next.

Error rate (ER) measures the number of solutions that are not in PF_{true}. $ER = 0$ indicates that all the solutions are optimal; $ER = 1$ indicates the opposite.

$$ER = \frac{\sum_{i=1}^{n} e_i}{n}; \qquad e_i = \begin{cases} 0 & PF(i) \in PF_{true} \\ 1 & otherwise \end{cases}.$$

Generalized distance (GD) measures distance between PF and PF_{true}.

$$GD = \frac{\left(\sum_{i=1}^{n} d_i^p\right)^{1/p}}{n},$$

for $p=2$, d_i is Euclidian distance (in objective space) between the PF(i) and the nearest member of PF_{true}.

The above metrics are additionally tailored to better suit the particular problem. The size of the solution space is large (Table 3); therefore, it is neither justifiable nor possible to search for PF_{true}. Optimization is performed several times; all solutions are gathered and the optima are extracted to find approximate PF (used as an approximation of PF_{true}).

Since one of the objectives in subsequent optimizations is discrete (investment), overall PF can be sliced into finite number or sub-Pareto fronts (SPF), each having the same investment. *GD* is calculated using the distance to the closest solutions inside the appropriate SPF. Normalization of objectives is used to compare different values of objective functions (P_{loss} and ΔV for instance). Spreading, *SP*, is proposed as a third metrics to augment results of *ER* and *GD*. Wider solution fronts have bigger values of *S*P. Spreading are calculated for each SPF and than added as follows:

$$SP_{SPFi} = \left(\sum_J \left(F^i_{J\max} - F^i_{J\min}\right)^p\right)^{\frac{1}{p}}.$$
$$SP = \sum_i SP_{SPFi}.$$

Here, $F^i_{J\max}$ is normalized maximum value of J^{th} objective function inside the i^{th} SPF.

Only the combination of all the proposed metrics enables meaningful comparison of multi-dimensional solution fronts. An example showing how the use of only one or

two metrics can be misleading is shown in Figure 10. Solution front 1 has excellent values of *GD* and *ER*; *SP=0* shows that the front is degenerate. Solution front 2 has great *SP* and ambiguous *ER*; high *GD* shows its weakness. Despite having the worst *ER*, solution front 3 is the best.

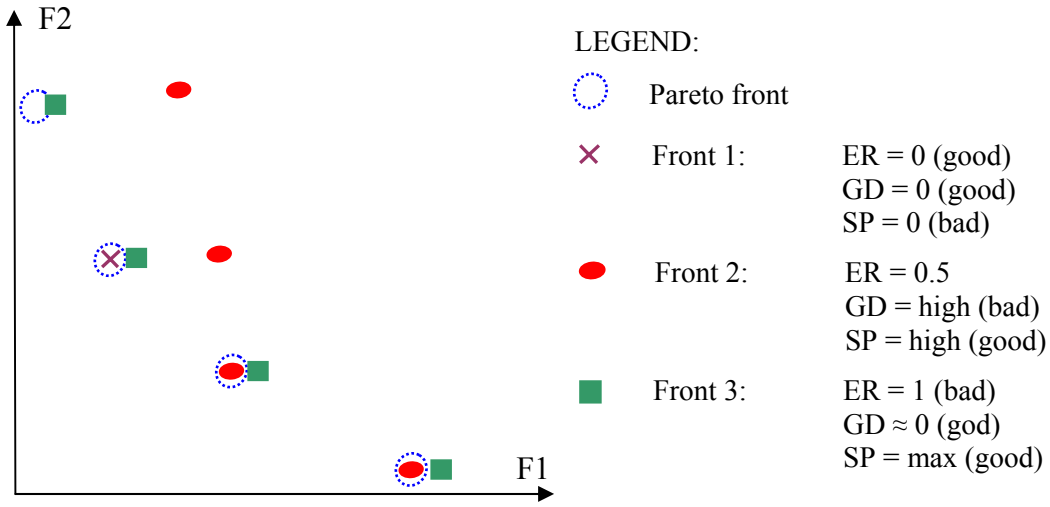

Figure 10. Comparison of solution fronts.

CHAPTER 6

6. CUSTOM-DESIGNED OPTIMIZATION ALGORITHMS

The optimization algorithms explained in the previous section are well known and frequently used. The algorithms are custom-tailored to fit the multi-objective reactive power-planning; the algorithms are presented next in detail.

6.1. Multi-objective linear programming

Two-objective LP-based capacitor placement. Limitation on investment resources (IR) is the main optimization constraint. The decoupling principle pushes IR into the list of objectives on the both system sides (further proof of this claim is illustrated in Section 7.2.). The simplex method is by nature single-objective. The fact that one of the unavoidable objectives, IR, is a discrete function linearly dependent on the amount of reactive support, is used to extend the optimization into two-dimensional (2D) framework. Pseudo code in Figure 11 shows 2D-LP algorithm for minimization of IR and system losses; any other objective from Table 1 can be used instead.

Non-compensated feeder; reactive support (RS) = 0.
Perform power flow. Calculate P_{loss}. Define the optimization step ΔQ.
New loss (NL) = P_{loss}. Old loss (OL) = P_{loss} + 1. Initial solution = (P_{loss}, RS).
While NL < OL.
    OL = NL.
    Solve LP: min P_{loss};
        s.t. power flow constraints; *operational constraints;*
        $RS = RS+\Delta Q$.
    Create a new solution: round controls to the closest feasible values.
    Perform power flow. Calculate P_{loss}. NL = P_{loss}.
    New solution = (NL, RS).
End
Ignore last solution (overcompensated feeder).

Figure 11. **Pseudo code of 2D_LP algorithm.**

Three-objective LP-based capacitor placement. The two-objective LP algorithm was easy to derive and understand. It is based on the fact that one of the two objectives translates to number of applied capacitor banks. The 2D-LP algorithms easily fill out the entire two-dimensional solution fronts: IR vs. losses or IR vs. voltage deviation (ΔV). However, these fronts constitute only two envelopes of the entire 3D solution set (IR vs. losses vs. ΔV). Yet, the entire solution subset lies hidden between these envelopes. 3D-LP algorithm is designed to populate this subspace. Every solution from one of the 2D fronts is enhanced in the direction of optimization of the other objective. For example the optimal solution, with respect to ΔV, with one capacitor bank is enhanced by adding additional capacitor banks to minimize P_{loss}. Graphical presentation of the process is shown in Figure12.

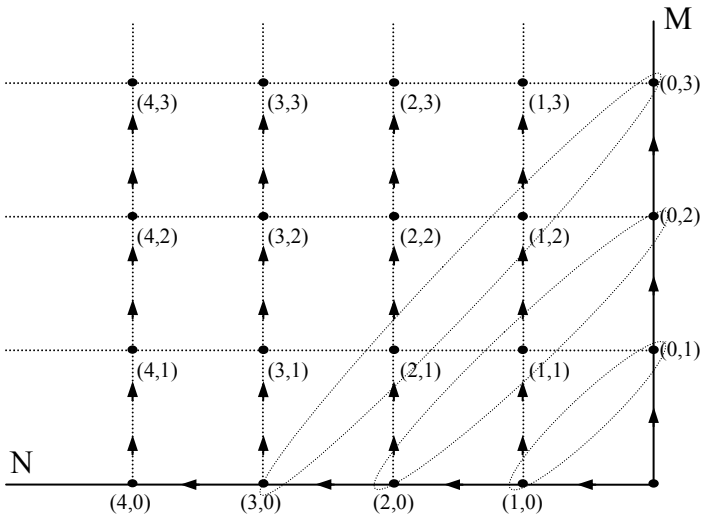

Figure 12. Illustration of 3D-LP algorithm. M (N) counts the number of capacitors applied to optimize first (second) objective. Single arrows show optimization path during 2D-optimisation. Double arrows show the 3D-optimisation paths. Coordinates of solutions (*n, m*) give number of banks applied to minimize particular objective. Sub-fronts with the same number of banks are encircled.

The above example depicts optimization of feeder losses, voltage deviation and investment in the reactive support. It is obvious that any other combination of objectives can be used in the same framework. Moreover a similar algorithm can be designed for optimization of four (or more) objectives.

6.2. Linear-Programming based Optimal Power Flow

The algorithm discussed in the previous section is focused only on the major controls, the shunt capacitors. However, the reactive optimization problem is influenced by other system controls as well (active power injections, voltage set points, etc.).

An algorithm that minimizes the overall system generation using the system active power injection and generator voltages as controls has been developed and is

presented in this section. This optimization is chosen for two reasons. First, in the case of constant power loads, minimization of the overall generation is equivalent to minimization of system losses. Second, the results of the above optimization can be compared with results obtained by any commercial optimal power flow software.

Optimal power flow is usually formulated as:

$$\text{Minimize} \qquad F = \sum_{i=1}^{n} f_i(P_{gi})$$

$$\text{subject to} \quad C$$

where

P_{gi} is the real power output of the unit i

$f_i(Pgi)$ is the production cost of the unit i

n is the number of units;

C is the set of optimization constraints.

The variables in this problem are:

- Voltage angle at the slack bus; assumed $\delta_{slack} = 0$
- State variables $x = [\delta\ V]^T$; δ's and V's are voltage angles (on PV and PQ buses) and magnitudes (at PQ buses in the system)
- Control variables: $u = [V_{slack}\ V_{PV}\ P_{PV}]^T$
    - V_{PV} is the vector of voltage magnitudes at all PV buses
    - P_{PV} is the vector of active power injection at all PV buses
- Dependent variables: P_{gslack}, Q_{PV} (Q_{PV} reactive power injection at all PV buses)

The set of constraints consists of:

- $g(x,u) = 0$ set of power flow equations
- allowable voltage magnitude values

- production limits of generator (active and reactive)
- line flow limits

Both the optimization function and the constraints are nonlinear. Nevertheless, the optimal power flow problem can be solved using LP. The optimization function and the constraints are linearized around the working point and LP is then applied. Successive linearization yields to the solution that is close to the optimal one. The linearized problem looks like:

Minimize $F(u)$

s.t. $LB \le u \le UB$

$C(u)$

where

$F(u)$ is the linear objective function (function of system controls only)

LB, UB are the vectors of lower and upper bounds on system controls

$C(u)$ is the linearized constraints vector

Minimization of the system's active injection is a nonlinear optimization formulated as:

$$\begin{aligned} &Minimize \quad F = F(x,u) = \sum_{i=1}^{n} P_{gi} \\ &subject\ to \quad LB_U \le U \le UB_U \\ &\qquad LB_V \le V(x,u) \le UB_V \\ &\qquad LB_Q \le Q_g(x,u) \le UB_Q \\ &\qquad LB_P \le P_{gslack}(x,u) \le UB_P \\ &\qquad LB_S \le S_{ij}(x,u) \le UB_S \end{aligned} \tag{12}$$

where:

U - Control vector $U = [V_{slack}\ V_{PV}\ P_{PV}]^T$

V - Vector of voltages on PQ buses

Q_g - Vector of reactive power generation of system machines

P_{gslack} - Active power generation of slack bus.

S_{ij} - Vector of apparent line flows, for all the system lines.

The only linear features in (12) are control constraints. In order to solve the above problem via LP it is necessary to linearize nonlinear optimization function and constraints; state variables should be eliminated from the problem as well. The process is explained in Section 5.2. Upon linearization, the optimization problem becomes linear (13). All of the functions in (13) are linearly dependent on the system controls.

$$\begin{aligned} &\textit{Minimize} && F(u) \\ &\textit{subject to} && LB_U \le U \le UB_U \\ & && LB_V \le V(u) \le UB_V \\ & && LB_Q \le Q_g(u) \le UB_Q \\ & && LB_P \le P_{gslack}(u) \le UB_P \\ & && LB_S \le S_{ij}(u) \le UB_S \end{aligned} \tag{13}$$

The flow chart of the optimization algorithm is shown in Figure 13. The algorithm linearizes the nonlinear optimization problem and optimizes it using LP-based algorithm.

Verification and comparisons. Developed LP-based OPF algorithm is compared with the optimal power flow routine of Matpower software package (Table 4). Matpower uses a nonlinear optimization routine. Since the optimization is based on the linearized model it is expected that it gives the approximate results; however, the results are very close to the optimal even for the biggest system. On the other hand, the computational effort of LP algorithm increases linearly with the size of the system. The non-linear algorithm, while being much faster on the small systems, becomes computationally inefficient when the system size increases.

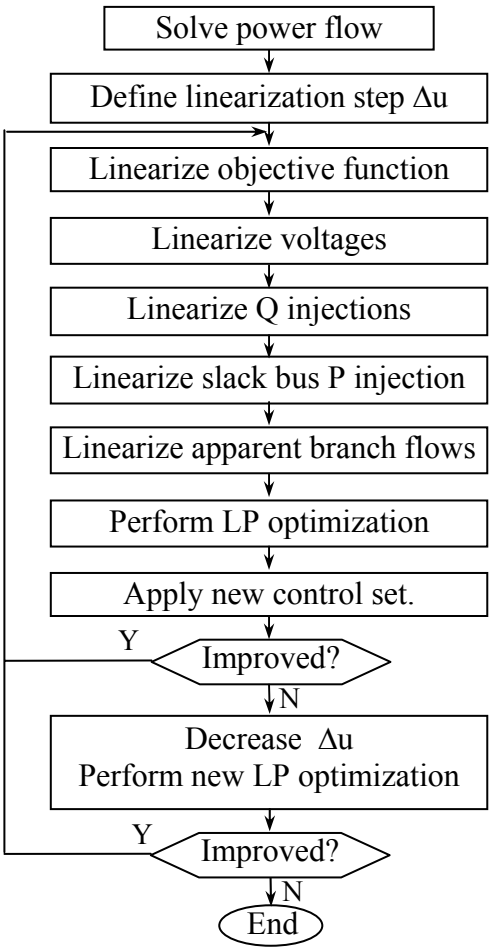

- Start from any power flow solution
- Model valid for: $u - \Delta u \le u \le u + \Delta u$
- OF $\approx c_1u_1 + c_2u_2 + \ldots + c_nu_n$
- For PQ buses linearize $V_{imin} \le V_i \le V_{imax}$
- For each generator linearize: $Q_{min} \le Q \le Q_{max}$
- Linearize $P_{min} \le P_{gslack} \le P_{max}$
- For every branch linearize: $S_{min} \le S_{ij}, S_{ji} \le S_{max}$
- Optimize linear objective function, subject to control limits and set of (linear) constraints
- Solve power flow
- Find new control set; solve power flow

Figure 13. Flow chart of LP-based OPF algorithm.

Table 4. LP-based OPF versus non-linear OPF.

	LP-based OPF		Matpower OPF	
	ΣP_G [MW] P_{loss} [MW]	Execution time	ΣP_G [MW] P_{loss} [MW]	Execution time
IEEE 9-bus system	317.8923 2.8923	3.61 sec	317.8924 2.8924	0.55 sec
IEEE 39-bus system	6179.226 28.726	26 sec	6179.220 28.720	5.5 sec
283-bus system	2119.676 38.392	**4.9 min**	2119.667 38.383	**2.7 hours**

6.3. Multi-objective Genetic Algorithm for reactive power planning

As already explained, GA qualifies naturally as a multi-objective optimization tool. The general approach of GA application to multi-objective problems is already explained. Its particular application to the capacitor allocation is given next.

Integer *coding* is usually used for capacitor allocation. Each solution is modeled by a fixed length integer string. The position of each integer in the string corresponds to the appropriate feeder bus. The value of each number in the string corresponds to the size of the capacitor applied at the appropriate bus (number of minimal capacitor banks). For example, in the case of a 10-node feeder, a population member may look as in Figure 14. The solution of the figure corresponds to capacitor placement on nodes 2, 4, 5, 7 and 8 of the feeder; for instance, the capacitor placed at node 4 is $Q_4 = 2 \cdot Q_{min}$.

0	1	0	2	3	0	2	1	0	0

Figure 14. An integer-coded population member.

The following set, of GA operators and properties, is applied in common fashion. The *initial population* contains N randomly chosen integer-coded strings. Reproduction is done via *binary tournament*. A fixed-rate *mutation* is used. A fixed number of iterations is used as a *termination criterion*.

Single-point arithmetical *crossover* is applied. For each pair of mated solutions, a random integer, k1, ($0 < k1 < N$) is generated. It defines the position of the crossover in the string of N integers. The part of the string to the right of the k1-th integer is called the tail. The second random number, k2, ($0 < k2 < 1$) is generated next. It defines the weighting of tails in the crossover. Crossover is performed as shown in Figure 15.

tail1_new = k2 * tail1_old + (1-k2)*tail2_old

tail2_new = k2 * tail2_old + (1-k2)*tail1_old

Figure 15. **Single-point arithmetical crossover.**

Elitism is a GA operator that forces the GA to keep the best individuals. Without elitism applied, the GA can lose the best individuals by spoiling them via reproduction, crossover and mutation. The algorithm applies elitism using nondominated sorting. When the new generation is obtained, it is compared (using ranks and crowded distances) with the old one. Only the best N individuals from both generations are transferred to the next generation. The pseudo-code of the two-objective GA is given in Figure 16.

```
Initialize population.
    Random population generation (N members).
    Objective functions evaluation.
     Assign ranks based on Pareto dominance.
     Determination of crowded distances between the points on each front
For i = 1 to # of generations
     Binary tournament selection.
     Crossover.
     Mutation.
     Evaluation of  objective functions.
     Combined population (added parents and offspring). Size of population is 2N.
     Assigned ranks to combined population.
     Determination crowded distances inside the combined population.
     New generation extraction.
     Additional non-dominated sorting.
End of loop.
```

Figure 16. Pseudo code of multi-objective GA.

Sparse GA. Unlike the LP, the structure of GA does not depend on the number of objectives. Inclusion of the third or fourth objective does not influence the basic GA

operators. However, even 3D Pareto fronts are of considerable sizes; for example a feeder of moderate size and significant reactive load can have several hundred Pareto solutions. Rich Pareto fronts may cause an overwhelming computational burden when a power system with thousands of feeders is to be solved. GA can be tailored to yield a Pareto subset of a predetermined size. Sparse realization of GA saves time during the feeder optimization, as well as during the subsequent optimization on the overall system.

The limited population size is used in sparse GA. To insure a good dispersing of solutions and existence of all dominant compensation levels (numbers of capacitor banks) the following is implemented:

- While choosing individuals to be placed into the mating pool, maximum fitness is given to the ones on the boundaries (extreme values of objective functions).
- Higher fitness values are given to solutions in less crowded areas.
- If the number of solutions in any segment (subset with a constant number of capacitor banks) exceeds a predetermined value, excess solutions are given lowest fitness.

6.4. Voltage Stability Assessment and Control

Continuation power flow (CPF), [37], is used to assess the voltage stability margin of the system. A by-product of the CPF calculations is the detection of the weakest bus, the bus that triggers voltage instability. Reactive support applied to this bus is expected to move the system farthest from instability, [5].

Dependence of the voltage stability margin on feeder reactive support is also investigated. The margin is usually found by increasing the transmission loads. A change in feeder reactive support induces significant changes in the corresponding transmission

reactive load. Simple proportional scaling of the reactive transmission loads, without consideration of the distribution reactive support, can yield misleading results. For instance, if the feeder is compensated up to unity power factor, the appropriate transmission Q-load is equal to zero. This load, if simply scaled, will always stay at zero. This corresponds to the inaccurate assumption that with a feeder load increase the feeder reactive support increases proportionally.

An algorithm which includes the feeder support in calculation of stability margin is developed. It relies on the decomposition of the transmission load into three components, the sum of feeder loads (Q_{Load}), feeder losses (Q_{Loss}) and feeder reactive support (Q_C).

$$Q_T = Q_{Load} + Q_{Loss} - Q_C.$$

Component Q_{Load} changes with the load increase; Q_C stays constant. Therefore, the voltage stability margin part of the reactive load should increase (according to active load), while another part should stay constant. If the feeder losses are neglected the following could be written:

$$P_{TS\ base\ case} \rightarrow P_{TS\ increased} = \lambda\, P_{TS\ base\ case}$$

$$Q_{TS\ base\ case} = Q_{Load} - Q_C \rightarrow Q_{TS\ increased} = \lambda\, Q_{Load} - Q_C \neq \lambda\, Q_{TS\ base\ case}$$

A test of the above hypothesis was performed using detailed CYME feeder models. For a particular feeder, all of the loads are varied and the feeder consumption is found for each case. A prediction of the feeder consumption is made using the classical method ($\lambda\, Q_{base\_case}$) and the proposed formula ($\lambda\, Q_{Load} - Q_C$). The results are shown in Figure 17.

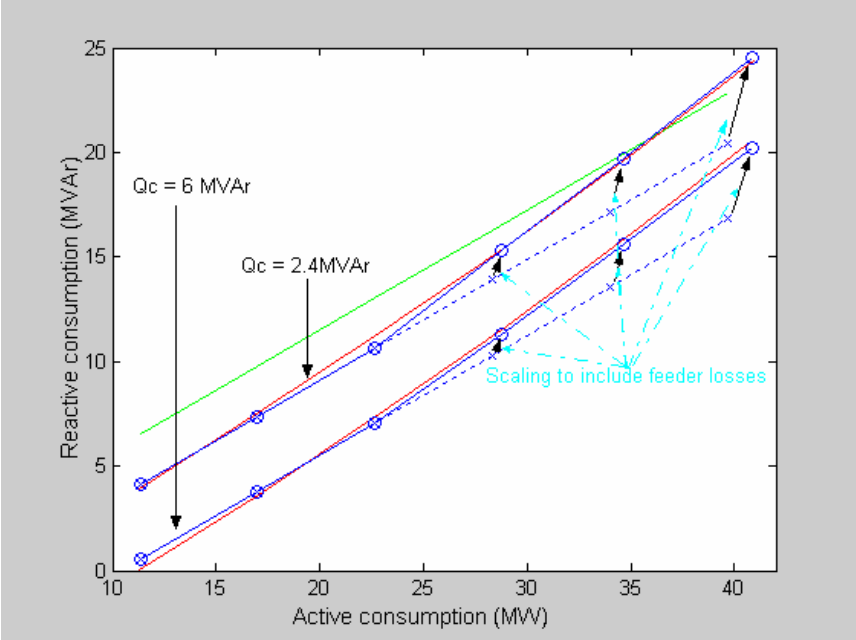

Figure 17. Load prediction; losses included.

The red lines show the accurate feeder consumption while the feeder loads change from 100% up to 350%; two red lines are given for different amounts of feeder reactive support (2.4 and 6 MVAr). The green line is obtained by the classical approach (λ Q_{base_case}). The model is accurate while the loads are close to the base case. In case of higher loading, the losses become significant and should be taken into consideration. If the predicted values for feeder Q and P are multiplied with the coefficients shown in Table 5, the solid blue lines are obtained. They predict the feeder consumption very well; the same accuracy is obtained when calculation is repeated on several other feeder models.

Table 5. Scaling coefficients for inclusion of feeder losses.

	$2.5 < \lambda < 3.0$	$3.0 < \lambda < 3.5$	$3.5 < \lambda$
P coefficient	1.015	1.02	1.03
Q coefficient	1.1	1.15	1.20

It should be noted that the search for the accurate feeder consumption (red line) using CYME models cannot be performed for each feeder in the system (and for each

level of reactive support as well). It is achievable, but impractical. However, the proposed prediction of load can be done without any additional computational cost; instead of using λQ_{Tbase_case}, the formula $\lambda Q_{Load} - Q_C$ is used.

CHAPTER 7

7. CAPACITOR ALLOCATION ON A DISTRIBUTION FEEDER

This section is used to demonstrate the optimization algorithm on a small system. To that end the 11-node feeder is used (Figure 18, Table 6). This model is derived from the IEEE 13-node test feeder by performing the following modifications: existing switches and low voltage transformers are removed from the model, distributed load is neglected, loads are balanced and doubled. Despite being geometrically simple, the 11-node feeder is highly loaded. This enables various capacitor solutions and therefore, its Pareto front contains a large number of solutions.

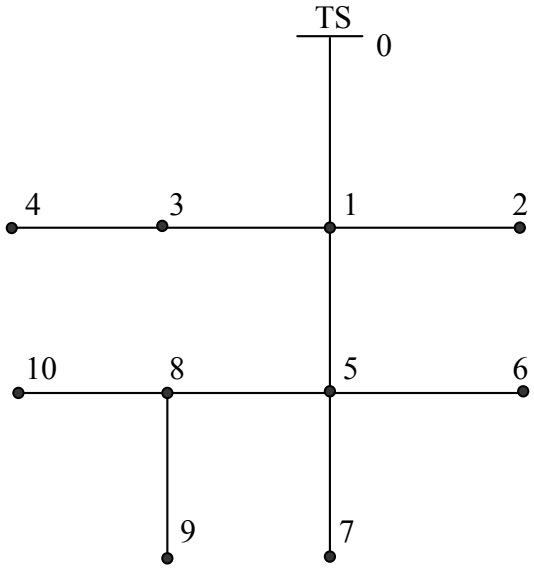

Table 6. 11-node feeder data.

Node A	Node B	Length [ft]	Conductor	P [kW]	Q [kVAr]
0	1	2000	556 ACSR	0	0
1	2	500	266 ACSR	800	580
1	3	500	266 ACSR	340	250
3	4	300	266 ACSR	460	264
1	5	2000	556 ACSR	2310	1320
5	6	500	266 ACSR	2026	1226
5	7	300	266 ACSR	0	0
5	8	300	266 ACSR	0	0
8	9	800	266 ACSR	252	172
8	10	300	266 ACSR	340	160

Figure 18. 11-node distribution test feeder.

Different capacitor allocation techniques are developed and their strengths and weaknesses are discussed. Verification of the proposed principle of "Algorithm Synthesis" is presented in section 7.2.

7.1. Three-objective optimization on balance feeder models

Problem formulation. The optimization problem is formulated as:

$$\text{Optimize:} \quad \boldsymbol{F} = \begin{bmatrix} I \\ P_{loss} \\ \Delta V \end{bmatrix}. \tag{14}$$

$$\text{Subject to:} \quad g(x,u) = 0.$$

$$pf \geq pf_{min}.$$

$$u_{min} \leq u \leq u_{max}.$$

$$Q_{ci} = k \cdot Q_{cmin} \qquad k = 0, 1, 2 \ldots$$

Here:

$\boldsymbol{F}$ - Vector of objectives

I - Investment in feeder reactive support

P_{loss} - Feeder active losses

ΔV - Feeder voltage deviation

$g(x,u)$ - System of power flow equations

Q_{ci} - Reactive support at node "i";

Q_{cmin} - Minimum bank size

tap - Voltage set point of distribution transformer

pf - Power factor at feeder substation

Investment is assumed to be proportional to the amount and type of reactive support:

$$I = C_1 \cdot \Sigma Q_{cifixed} + C_2 \cdot \Sigma Q_{ciswitced}. \tag{15}$$

Here C_1 and C_2 are unit prices of fixed and switched banks, respectively.

Feeder losses are defined as in (11). The expression can be simplified if the feeder serves

constant power loads. Minimization of losses utilizing $P_{loss} = P_G - \Sigma P_{load}$ corresponds to minimization of substation active injection P_G.

Feeder voltage deviation can be expressed in numerous ways [23, 28]. Most of the available formulas are good for balanced feeders. Demonstration of the algorithm on a single balanced feeder is done by using $\Delta V = \Sigma(1-V_i)^2$.

The power factor constraint ignores all possible solutions with power factor less than the minimal (0.95 for example). Control constraints account for the fact that the size of shunt capacitors is discrete value, and vary between the minimum (economic issue) and maximum value (power quality issue). Usual operational constraints, such as feeder voltages and line flows, are not considered in this example. This is done to enlarge the Pareto front. Rich Pareto fronts are needed to enable the effective comparison of different optimization techniques.

7.2. Verification of proposed Algorithm Synthesis

The necessity of coupling distribution and transmission solutions forces the investment in reactive devices, I, as an objective that cannot be omitted. Feeder loss, P_{loss}, and voltage deviation, ΔV, are chosen as additional objectives. All the capacitors are considered switchable and cost \$26/kVAr. Minimal size of the capacitor banks is assumed to be 100kVA/phase, with an identical incremental capacitor step. Maximum capacitor size in this case is not imposed. Three-objective algorithms, described in Chapter 6, are applied to construct the three-dimensional solution fronts. The use of GA revealed that full Pareto front of the given feeder contains approximately four hundred solutions. If the sparse GA is used, a sparse Pareto-solutions front, Figure 19, of hundred

solutions spread throughout the entire solution space is obtained.

A comparison of the available techniques LP, GA and their synthesis (LP+GA) is presented in Table 7. Proposed algorithm synthesis on average generates only 8% dominated solutions. The dominated solutions are very close to Pareto-dominant ($GD_{LP+GA} << GD_{GA} < GD_{LP}$). Spreading of solutions is a little lower than in the case of pure GA; this is contributed to the higher number of dominated solutions in GA results.

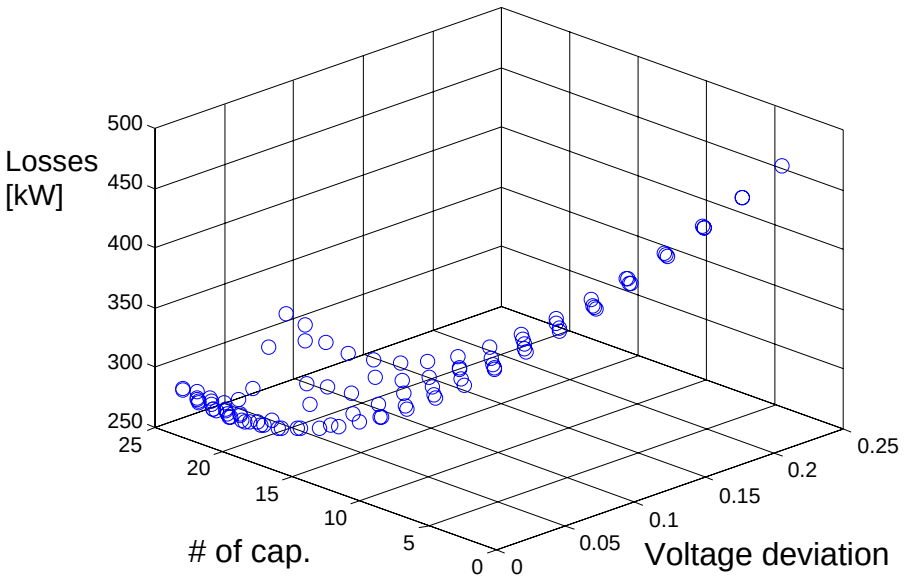

Figure 19. Sparse three-dimensional Pareto-optimal solution front.

Table 7. Comparison of optimization methodologies; 3D optimization.

Technique	Error rate [pu]	Generalized distance [pu]	Spreading of solutions [pu]
LP	0.444	1.311	2.066
GA	0.123	0.392	2.779
LP + GA	0.083	0.024	2.660

An additional illustration of the results is shown next. Enhancement of LP results using GA is demonstrated on one segment of Pareto front. Figure 21 compares convergence of randomly initialized GA and GA initialized with LP results. As expected,

in a long run GA approaches LP+GA. However, in the short run LP+GA outperforms GA significantly. The latter makes the methodology favorable to high order systems.

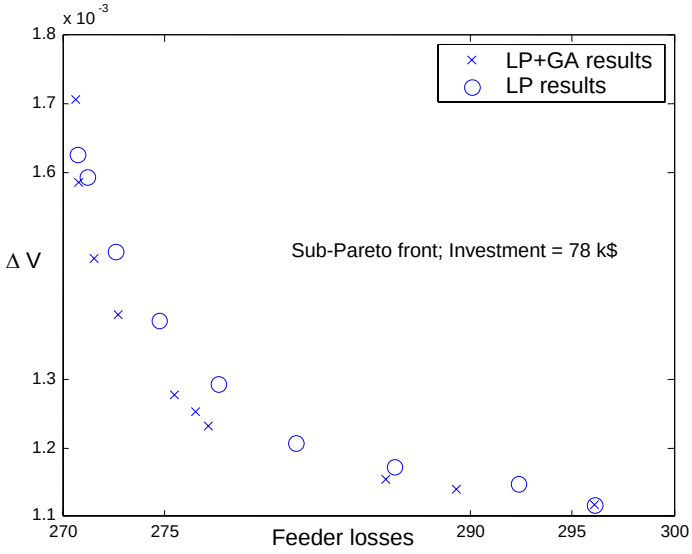

Figure 20. Comparison of LP and GA+LP. Pareto sub-fronts with same investments (corresponding to 10 capacitor banks) are shown. GA+LP enhance the LP results.

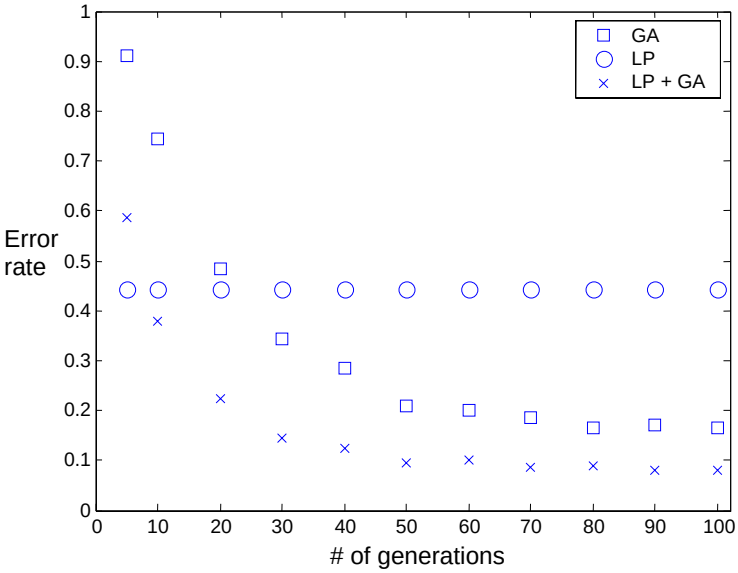

Figure 21. Convergence of algorithms measured by ER.

7.3. Extension of algorithms to Three-phase feeder models

Extension of the algorithm to asymmetric feeders (asymmetric loads, single-phase laterals, etc) is depicted in Figure 22. GA part of the algorithm is easily adapted. Since the only connection of the GA and the optimization problem is objective function evaluation, the GA only needs a three-phase power flow solver. There are few such solvers available on the market; unfortunately, all of them are part of large analysis packages with their own graphical user interfaces, created to be used as standalone applications. They are, therefore, ill-equipped for the desired type of interaction with the GA module and for repetitive use (GA run on a single feeder needs several thousand power-flow calculations). CYMEDIST power flow software is used in this research as a three-phase power flow solver. This choice is made because most of the available feeders are modeled in the same environment. Moreover, a part of the software is accessible through component object module (COM). CYMEDIST COM provides means that allow the user to run the software as a calculation engine within different environments [38]. Therefore a COM oriented GA optimization, that uses CYMEDIST power-flow solver, can be built.

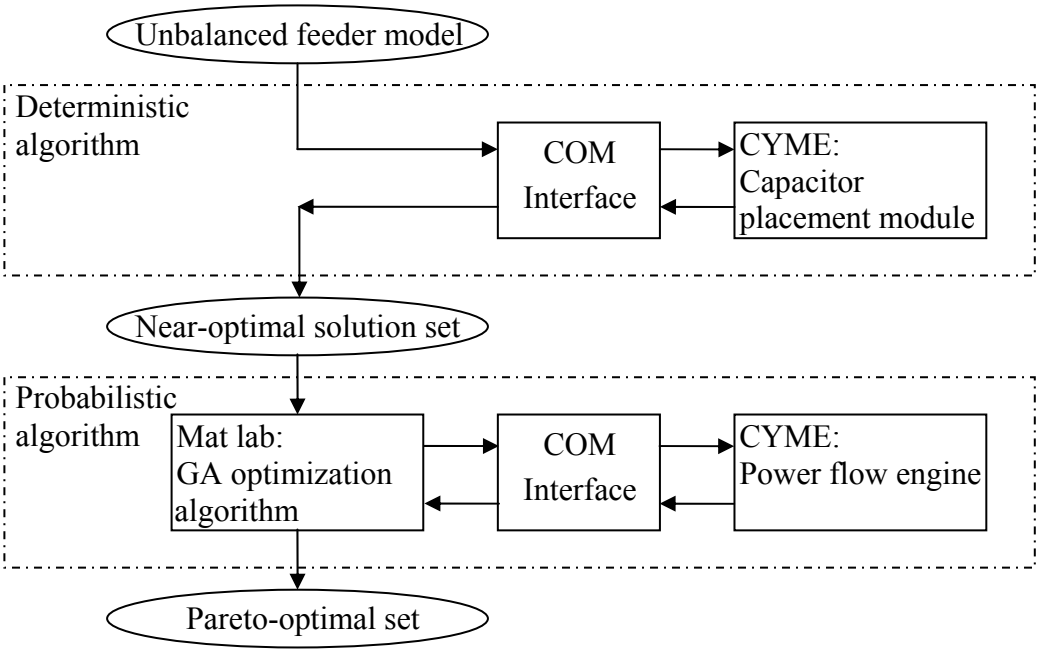

Figure 22. Optimization of unbalanced feeders; structural design of the algorithm.

The extension of the LP part of the algorithm to the unbalanced models would be more demanding. A modification of the conventional form of power-flow system of equations should be made. Fortunately, capacitor placement routine exists in the CYMEDIST. The routine utilizes LP, and performs single objective optimization (objectives are P_{loss} or ΔV). Using the COM interface this routine can be used to produce 2D and 3D Pareto fronts in the same way as shown in Section 6.1.

CHAPTER 8

8. OPTIMIZATION ALGORITHM; DETAILED OVERVIEW

General formulation of the problem is given in (3). The research is focused on the following set of objectives: distribution losses, distribution voltage deviation, transmission losses and voltage stability of the system. T&D losses are combined into single objective, total system losses. Different loading and different switching configurations of the system are also addressed. High-dimensionality of the problem prevents the consideration of all of these topics within the single optimization process; therefore the algorithm is divided in several interacting routines. One implementation of the algorithm is depicted in Figure 23. The optimization of reactive resources is performed on the peak-case of the system loading. Performance of the obtained results under different loading and switching configuration is evaluated *a posteriori*. According to these evaluations and expert knowledge of the system, the size of the Pareto set is reduced. The reduced Pareto set is still optimal with respect to the entire set of the objectives, it has satisfactory performance within different systems configurations and it satisfies other preferences of the system owner.

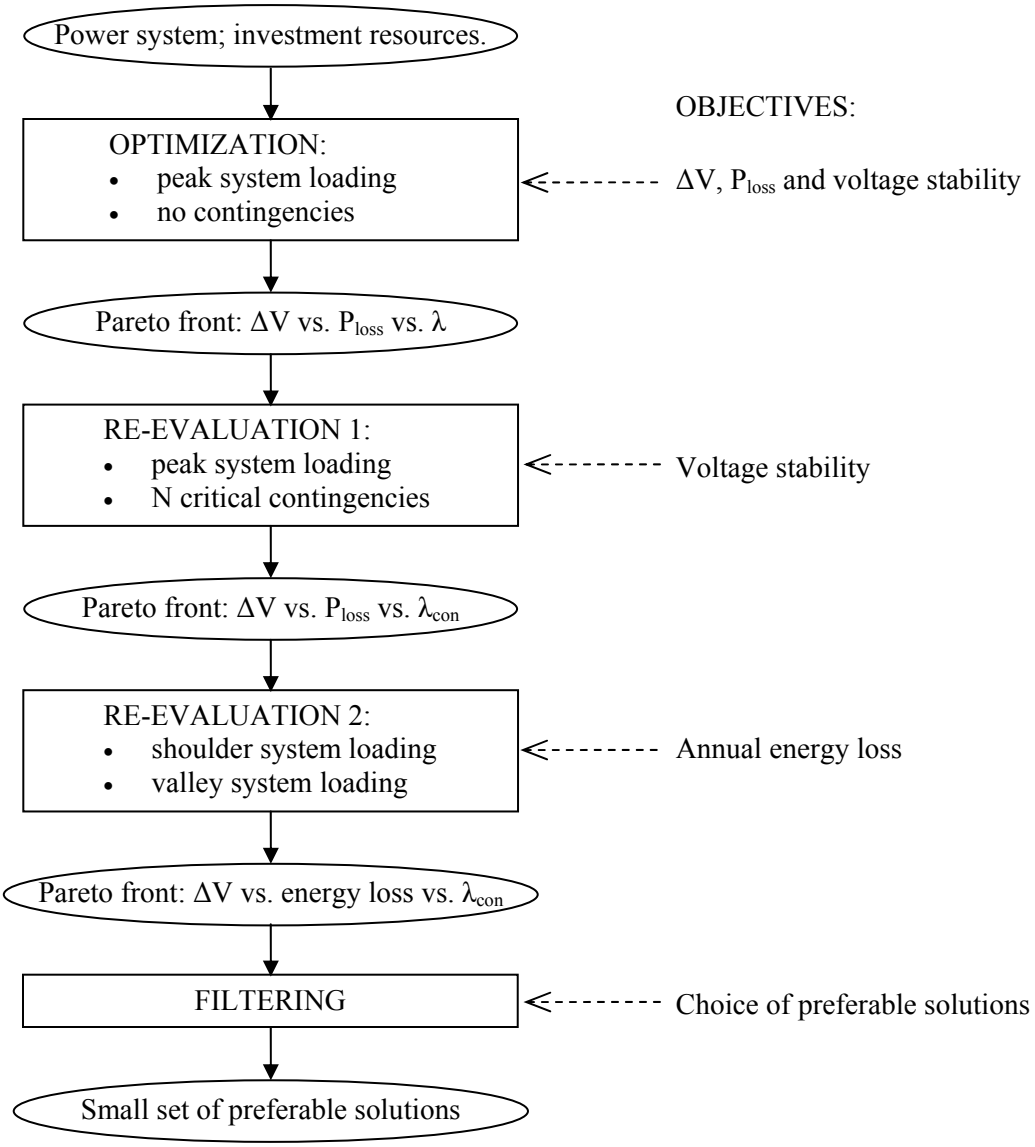

Figure 23. Detailed overview of the algorithm; routines, results and objectives.

8.1. Optimization of the System During Peak Loading

The optimization problem is simplified if a single load level within single switching configuration is considered. The simplified problem becomes:

$$\text{Optimize:} \quad F(x,u,p) = [\Delta V(x,u,p)\ P_{loss}(x,u,p)\ \lambda(x,u,p)]^T \qquad f: R^N \rightarrow R^3. \tag{16}$$

$$\text{Subject to:} \quad g(x,u,p) = 0, \qquad g: R^N \rightarrow R^n,$$

$$h(x,u,p) \geq 0, \qquad h: R^N \rightarrow R^m,$$

$$I_R(u) = C^T \cdot Q_c = constant, \qquad Q_c \subseteq u,\ Q_c(i) \in \infty,$$

$$p = constant.$$

Same notation as in (3) is used.

Additional consideration is needed when quantifying voltage deviation of the unbalanced three-phase feeder networks. To that end, the following method is used:

$$\Delta V = norm\left(\left|\Delta V_1 \quad ... \quad \Delta V_i \quad ... \quad \Delta V_n\right|\right) \tag{17}$$

$$\Delta V_i = \frac{\sum_{j=1}^{\phi_i} k_{ij} \left|V_{ij} - 1\right|}{\phi_i}$$

Here:

n - Number of nodes in the network;

ϕ_i - Number of phases at node i ($\phi_i = 1, 2$ or 3);

V_{ij} - Voltage on node i, phase j;

k_{ij} - Penalty factor ($k_{ij} = 1$ if $0.95 < V_{ij} < 1.05$; $k_{ij} > 1$ otherwise).

Voltage deviation, ΔV_i, is calculated for each node in the network. An appropriate norm of vector of nodal voltage deviations is used to quantify feeder voltage deviation. Choice of the norm in (18) depends on practice and preference of the system owner.

8.2. Accounting for Network Topology Changes

The system undergoes different switching configuration either intentionally or by accident. Since the intentional system reconfigurations (e.g. maintenance) usually happen during light system loading, their influence on the optimization can be ignored. The accidental switching reconfigurations are caused by faults. While being random, the occurrence of these contingencies has the strongest impact during the peak-loading of the system. Due to the short duration of such fault-induced reconfigurations, losses and voltage deviation are not considered during contingencies. Contingencies, however, cause instantaneous changes of voltage stability margin; therefore, their influence on voltage stability must be considered.

The following procedure is proposed for re-evaluation of the peak Pareto solution:

- Rank contingencies with respect to voltage stability.
- Isolate the set of critical contingencies C_C.
- Evaluate voltage stability margin $\lambda(C_C, u)$ of Pareto solutions in the set C_C. The solution i is characterized with vector norm $\lambda_{i,cont} = \left|\lambda_{i,base.case} \quad \lambda_{i,c1} \quad \lambda_{i,c2} \quad \ldots \quad \lambda_{i,cn}\right|$; $\lambda_{i,cj}$ being voltage stability margin of the i^{th} solution with respect to j^{th} contingency. Use of the "*–infinity"* norm ($min(\lambda_{i,cont})$) is proposed because the minimum is indeed the bounding critical solution that should be known.
- All infeasible solutions are discarded; the solution i is considered infeasible if $\exists\ j$ such that $\lambda_{i,cj} = 0$.
- All dominated solutions in the new objective space (ΔV vs. P_{loss} vs. λ_{cont}) are also discarded.

8.3. Variable system loading

System loading, p_L, is a part of the parameter vector of optimization problem (3); $p_L \subseteq p$. p_L is a probabilistic quantity. Its probability density function $f_{p_L}(P_L)$ could be expressed in different ways depending on the desired accuracy and type of the analysis. To access system energy balance, electric utilities model three load levels: peak, shoulder and valley (Sections 2 and 3.1.1.). Commonly assumed distribution of peak, shoulder and valley load is 5, 70 and 25% of the year respectively. Therefore, $f_{p_L}(P_L)$ can be expressed as follows:

$$f_{p_L}(P_L) = \begin{cases} P(p_L = p_{peak}) = 1/20 \\ P(p_L = p_{shoulder}) = 12/20 \\ P(p_L = p_{valley}) = 7/20 \end{cases} \tag{18}$$

The same load distribution can be assumed for assessment of voltage deviation. Since voltage stability is not an issue for light system loading, it is not considered here. The variable system loading is taken into account with the optimization problem (19):

$$\begin{aligned} \text{Optimize:} \quad & F(x, u, p_L) = [\Delta V(x, u, p_L)\ \mathrm{E}_{\mathrm{loss}}(x, u, p_L)]^{\mathrm{T}} && f: R^N \to R^2. \\ \text{Subject to:} \quad & g(x, u, p_L) = 0, && g: R^N \to R^n, \\ & h(x, u, p_L) \geq 0, && h: R^N \to R^m. \end{aligned} \tag{19}$$

Here $\mathrm{E}_{\mathrm{loss}}$ stand for energy loss in the system; other notation same as in (3).

Solving (19) is set as re-evaluation of Peak Pareto-solutions during different load cases. Solutions of (16) are "scaled down": since the system is overcompensated the objective functions decrease with switching-off the peak support. Linear programming

can be used to decide the switching strategy. The process should be terminated once the objectives start increasing again. After all the solutions are scaled down to the valley load the investment is relaxed. All the capacitors used in valley case are fixed, and therefore cheaper. The difference in investment can be used for several purposes; to simply reduce investment, or to further improve the overall peak solution.

8.4. Multi-dimensional Connection Algorithm

Detailed description of multi-objective algorithm is shown in Figure 24. The algorithm optimizes four objectives: transmission losses, voltage stability margin, distribution losses and distribution voltage deviation. If the T&D losses are combined into a single objective (total system losses), the outcome of the algorithm is a 3D solution Pareto front. All the solutions in this front employ the same investment.

Exhaustive search (ES) is used for the minimization of distribution objectives, Figure 24. Since all the feeders are already pre-solved, ES is actually a lookup of feeder tables. If T&D systems are maximally decoupled (connecting transformer is equipped with tap changer), ES is truly just the table lookup. If this is not the case, ES involves additional power flow solution (a change in feeder consumption induces a change in transmission bus voltage, which induces additional change in feeder losses). In either case, ES is possible and it is not time-consuming; at worst, it may require a number of power flow solutions equal to the number of transmission load buses.

Linear programming (LP) as a part of transmission optimization algorithm is not different from the algorithm explained in Section 6.1. The algorithm optimizes the entire transmission control set in order to find the optimal capacitor scenario.

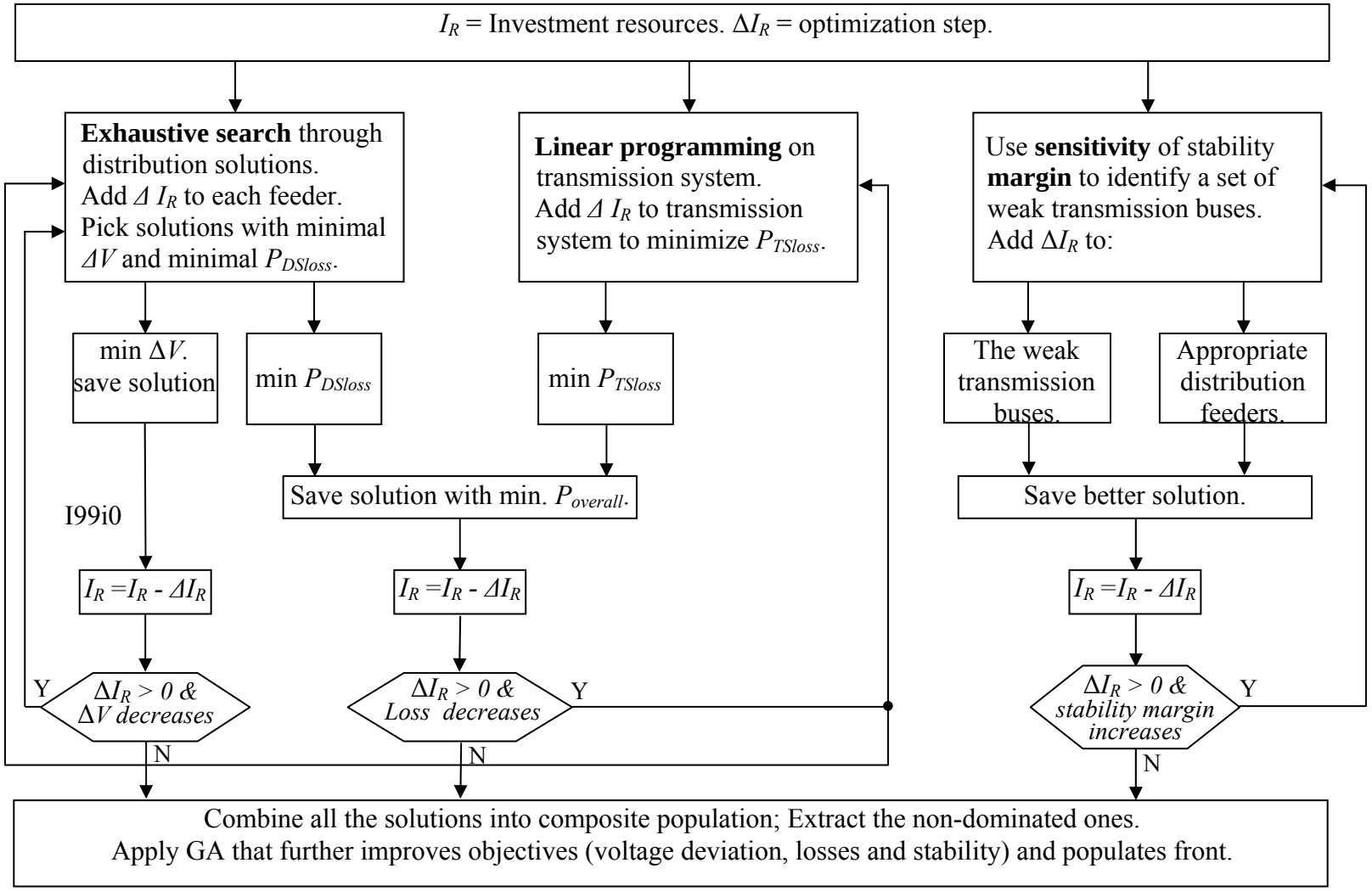

Figure 24. Detailed presentation of applied three-dimensional optimization.

8.5. Contingency Screening

Contingency ranking can be performed in many ways. If absolute accuracy is requested and speed is not an issue, ranking can be performed directly: the stability margin can be found for each particular contingency. Conversely, if the analysis is done on-line, different approximate methods could be used to extract a small set of critical contingencies. This research is done off-line and high accuracy is expected. However, since the overall T&D algorithm is already computationally highly demanding, the contingency ranking should be performed in the fastest possible way.

Vaahedi et al. [42] propose an approach based on contingency filtering. The algorithm combines both speed and accuracy. Its main idea is depicted in Figure 25. The outer, bold, PV curve belongs to the system without contingencies. The inner curves represent the system with different contingencies; some of them more severe (dashed line) than others. The critical contingencies are filtered in three steps:

- The original system is solved first; a working point close to λ_{max} is obtained (point 1).
- Working point with $k\lambda_{max}$ (for instance k =0.8) is obtained next (point 2).
- Using point 2 as initial condition contingency cases are solved. Cases with stability margin grater than $k\lambda_{max}$ are solved successfully; other cases (dashed lines) are not.

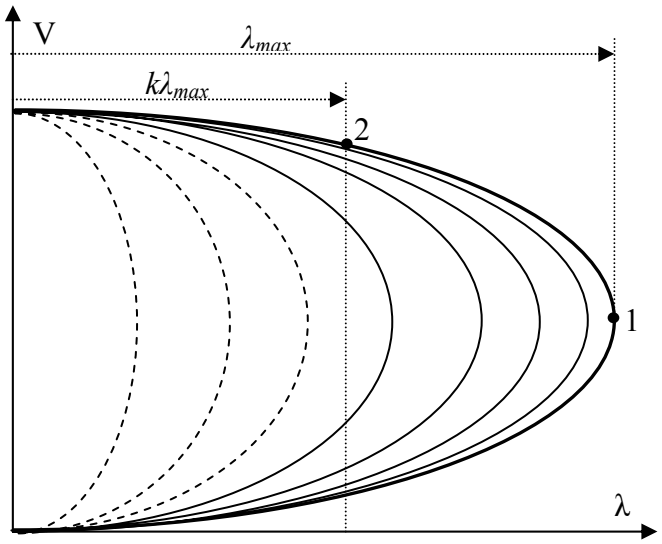

Figure 25. Contingency filtering.

The algorithm was tested on IEEE 39-bus system and no mis-rankings were observed. However, the algorithm does not consider reactive power limits of the machines in the system. Once a generator hits the reactive power generation limit, the system undergoes a PV-PQ transition, as depicted in Figure 26. After a stable transition, the system continues to serve the load. If an unstable transition occurs, the system undergoes immediate instability [39].

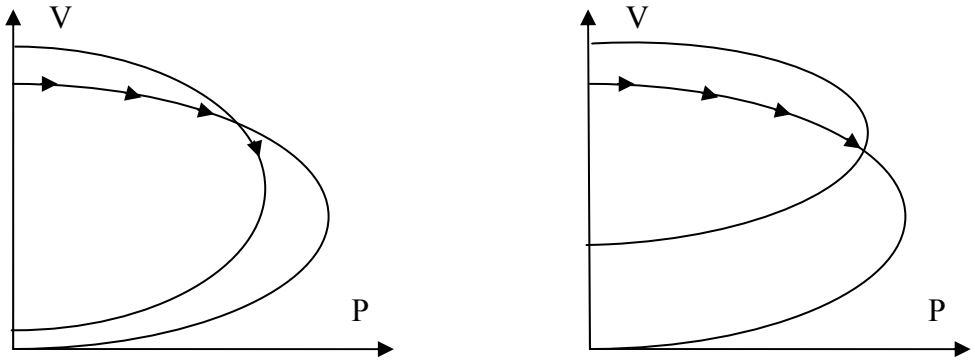

Figure 26. PV-PQ transitions; left – the stable transition, right – the unstable transition.

Filtering algorithm is modified, to include the PV-PQ transitions, as follows:

- The original system is initially solved including the reactive generation limits.
- The working point with $k\lambda_{max}$ is obtained next.
- Each contingency is solved (if possible) without imposing reactive limits.
- If the contingency is solved, the generator limits are checked. The violated limits are imposed and the contingency solved again.
- If the system has undergone PV-PQ transition and if it has been solved successfully, the bus voltages are compared with the original solution ($k\lambda_{max}$, no contingency). If the voltages have increased, the solution is unstable and therefore ignored, Figure 28.

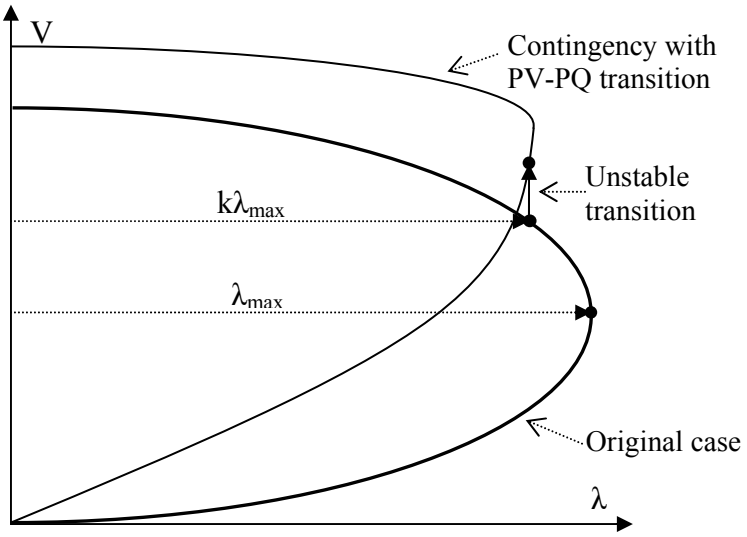

Figure 27. Detection of unstable contingency.

8.6. Path from the Pareto Front to the Particular Solutions

The result of any multi-objective optimization is a Pareto set of solutions. The size of power systems coupled with several optimization objectives, will invariably produce a very large Pareto-front. The choice of a single solution, from the multitude of possibilities left to the owner of the system, may cause his ambivalence regarding making

a single choice. If the solution is chosen arbitrarily, without the owner's expert knowledge, it might turn out to be unsatisfactory, even infeasible. Therefore an interactive procedure, engaging the planner and the owner, should be developed to reduce the size of the Pareto set.

The proposed optimization algorithm, Figure 23, is designed to partially perform this task. The very large solution front obtained using the peak system optimization (ball of diameter R0 in Figure 28) is reduced by two re-evaluations. The first re-evaluation excludes all the solutions which behave unsatisfactory during contingencies (solutions between spheres R0 and R1); second excludes those which do not perform well under light loading (solutions between spheres R0 and R1). The owner's preference in some objective values (for instance $\lambda_{cr} < 2$), or the owner's reluctance/enthusiasm to put reactive support in specific regions, will further reduce the solution set (ball R3).

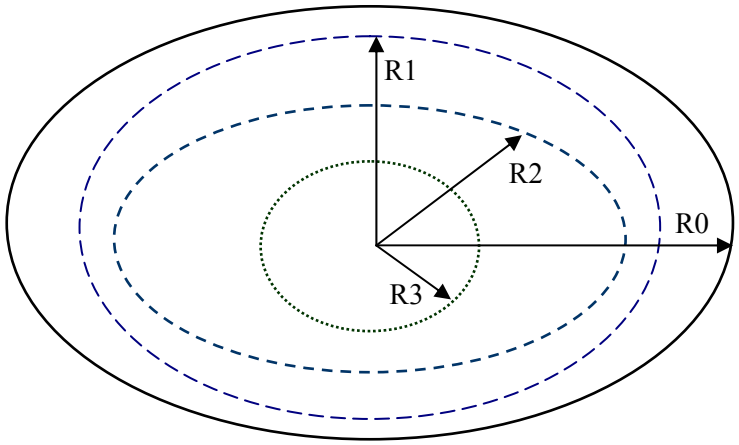

Figure 28. Reduction of very large Pareto sets.

If the reduced solution set still offers too many possibilities, a mathematical procedure for its reduction can be developed. An algorithm which performs a similar task has been presented in [27]. Here, the authors choose one objective as primary, and convert the other objectives into constraints which are allowed to vary within the ε

boundaries. The Pareto solutions are evaluated within a single objective ε-constrained optimization until a single solution is found. This procedure is essentially a departure form multi-objective framework, but it is a necessary departure to converge to a single solution. The exact procedure should be discussed and developed in tight collaboration with the system owner.

CHAPTER 9

9. RESULTS

9.1. Power System models

Various models have been used throughout this research; few of them are presented in this section. Algorithm is also implemented on a test system provided by one of US electrical power utilities (referred to as test system in this chapter). As the test system data are proprietary they could not be published here. However, a general description of the model and obtained results will be shown.

IEEE 9-bus system data.

For graphical presentation of the system see Figure 1.

Table 8. IEEE 9-bus system, bus data.

bus #	bus type	P_{load} (MW)	Q_{load} (MVA)	V_{max} (pu)
1	slack	-	-	1.1
2	PV	-	-	1.1
3	PV	-	-	1.1
4	PQ	-	-	1.1
5	PQ	90	30	1.1
6	PQ	-	-	1.1
7	PQ	100	35	1.1
8	PQ	-	-	1.1
9	PQ	125	50	1.1

Table 9. IEEE 9-bus system, generator data.

bus #	P_{gen} (MW)	Q_{max} (MVA)	Q_{min} (MVA)	V_{gen} (pu)	P_{min} (MW)	P_{max} (MW)
1	-	300	-300	1.0	10	300
2	163	300	-300	1.0	10	300
3	185	300	-300	1.0	10	270

Table 10. IEEE 9-bus system, branch data.

bus from	bus to	r (pu)	x (pu)	b (pu)	S_{max} (MVA)
1	4	-	0.0576	-	250
4	5	0.0170	0.0920	0.1580	250
5	6	0.0390	0.1700	0.3580	250
3	6	-	0.0586	-	250
6	7	0.0119	0.1008	0.2090	250
7	8	0.0085	0.0720	0.1490	250
8	2	-	0.0625	-	250
8	9	0.0320	0.1610	0.3060	250
9	4	0.0100	0.0850	0.1760	250

IEEE 39-bus system data.

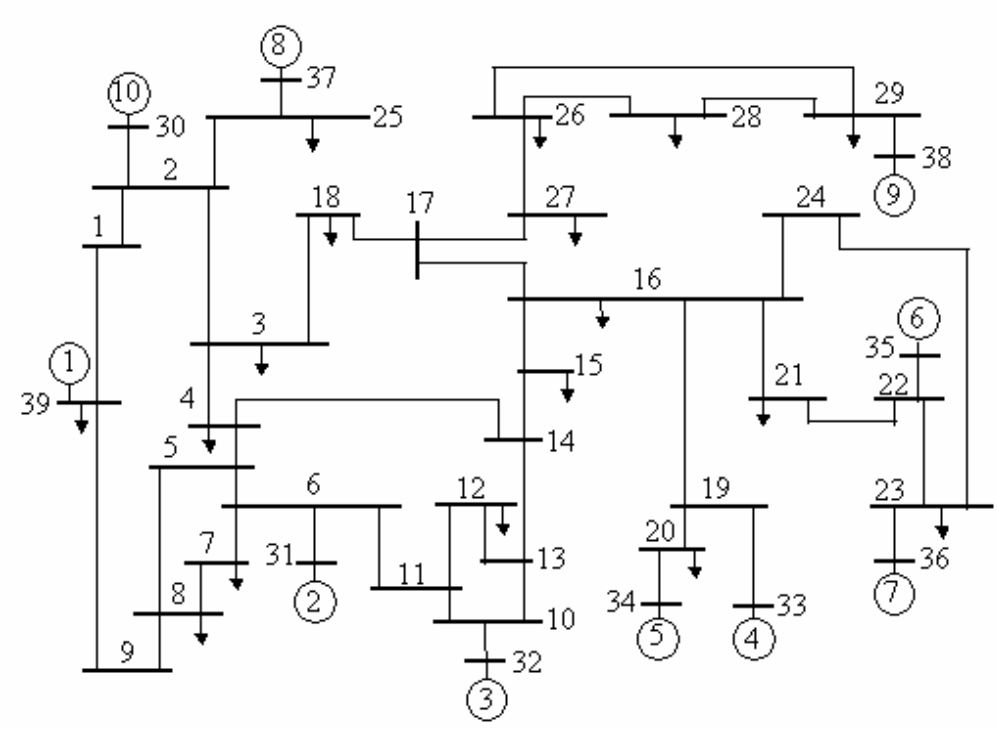

Figure 29. IEEE 39-bus System.

Table 11. IEEE 39-bus system, branch data.

Line		Line resistance (p.u.)	Line reactance (p.u.)	Line susceptance (p.u.)	Line		Line resistance (p.u.)	Line reactance (p.u.)	Line susceptance (p.u.)
From node	To node				From node	To node			
1	2	0.0035	0.0411	0.6987	16	24	0.0003	0.0059	0.068
1	39	0.001	0.025	0.75	17	18	0.0007	0.0082	0.1319
2	3	0.0013	0.0151	0.2572	17	27	0.0013	0.0173	0.3216
2	25	0.007	0.0086	0.146	21	22	0.0008	0.014	0.2565
3	4	0.0013	0.0213	0.2214	22	23	0.0006	0.0096	0.1864
3	18	0.0011	0.0133	0.2138	23	24	0.0022	0.035	0.361
4	5	0.0008	0.0128	0.1342	25	26	0.0032	0.0323	0.513
4	14	0.0008	0.0129	0.1382	26	27	0.0014	0.0147	0.2396
5	6	0.0002	0.0026	0.0434	26	28	0.0043	0.0474	0.7802
5	8	0.0008	0.0112	0.1476	26	29	0.0057	0.0625	1.029
6	7	0.0006	0.0092	0.113	28	29	0.0014	0.0151	0.249
6	11	0.0007	0.0082	0.1389	12	11	0.0016	0.0435	0
7	8	0.0004	0.0046	0.078	12	13	0.0016	0.0435	0
8	9	0.0023	0.0363	0.3804	6	31	0	0.025	0
9	39	0.001	0.025	1.2	10	32	0	0.02	0
10	11	0.0004	0.0043	0.0729	19	33	0.0007	0.0142	0
10	13	0.0004	0.0043	0.0729	20	34	0.0009	0.018	0
13	14	0.0009	0.0101	0.1723	22	35	0	0.0143	0
14	15	0.0018	0.0217	0.366	23	36	0.0005	0.0272	0
15	16	0.0009	0.0094	0.171	25	37	0.0006	0.0232	0
16	17	0.0007	0.0089	0.1342	2	30	0	0.0181	0
16	19	0.0016	0.0195	0.304	29	38	0.0008	0.0156	0
16	21	0.0008	0.0135	0.2548	19	20	0.0007	0.0138	0

Table 12. IEEE 39-bus system, bus data.

Bus #	Bus type	Power demand		Power output		Voltage set point (p.u.)
		P_d(MW)	Q_d(MVA)	P_g(MW)	Q_g(MVA)	
1	PQ	-	-	-	-	1
2	PQ	-	-	-	-	1
3	PQ	322	2.4	-	-	1
4	PQ	500	184	-	-	1
5	PQ	-	-	-	-	1
6	PQ	-	-	-	-	1
7	PQ	233.8	84	-	-	1
8	PQ	522	176.6	-	-	1
9	PQ	-	-	-	-	1
10	PQ	-	-	-	-	1
11	PQ	-	-	-	-	1
12	PQ	8.5	88	-	-	1
13	PQ	-	-	-	-	1
14	PQ	-	-	-	-	1
15	PQ	320	153	-	-	1
16	PQ	329.4	32.3	-	-	1
17	PQ	-	-	-	-	1
18	PQ	158	30	-	-	1
19	PQ	-	-	-	-	1
20	PQ	680	103	-	-	1
21	PQ	274	115	-	-	1
22	PQ	-	-	-	-	1
23	PQ	247.5	84.6	-	-	1
24	PQ	308.6	-92.2	-	-	1
25	PQ	224	47.2	-	-	1
26	PQ	139	17	-	-	1
27	PQ	281	75.5	-	-	1
28	PQ	206	27.6	-	-	1
29	PQ	283.5	26.9	-	-	1
30	PV	-	-	250	146.9	1.048
31	Slack	9.2	4.6	573.3	207.5	0.982
32	PV	-	-	650	205.8	0.983
33	PV	-	-	632	109.1	0.997
34	PV	-	-	508	166.7	1.012
35	PV	-	-	650	211.1	1.049
36	PV	-	-	560	99.8	1.063
37	PV	-	-	540	1.0	1.028
38	PV	-	-	830	22.0	1.026
39	PV	1104	250	1000	87.9	1.03

Test System.

1. Geographical description
    a. Enough generation in the system
    b. Area interchange disabled
    c. Urban and rural area included
2. Voltage levels
    a. Generation: 6.6-22 kV
    b. Transmission: 44-500 kV
3. Constant Power loads
4. Peak / Shoulder / Valley case

busses:	288 / 283 / 280		loads:	133 / 133 /133	
plants:	37 / 34 / 37		machines:	40 / 32 / 30	
branches:	322 / 313 / 313		transformers:	55 / 52 / 54	
	MW		MVAR		
From generation	2296 / 2160 / 733		113 / 402 / -854		
To constant power load	2234 / 2081 / 711		460 / 433 / 46		
To bus shunt	0.0 / 0.0 / 0.0		88 / 121 / 0.0		
From line charging	0.0 / 0.0 / 0.0		1274 / 1230 / 1233		

5. Feeder loads
    a. 474 belonging feeders (>3 per load bus)
    b. Complete feeder models (3-phase unbalanced)

9.2. Test System – Detailed Description

Test system consists of 288 transmission buses; general system data are shown in Table 13. System feeds 133 loads; 72 of them are modeled as feeder networks (consisting of 44kV and/or 12kV feeders). The rest of the loads belong to the customer-operated substations; no reactive support was assigned to these circuits. While the number of these loads is considerably high (sixty-one); they are usually small and their overall consumption (733 MW) does not exceed one-third of the system load.

Table 13. Transmission system Peak Case; load summary.

	P [MW]	Q[MVAr]
Load	2238	460
Losses	55	-
Generation	2293	-263

The entire system is well compensated with reactive support; amount of support and the system losses are depicted in Table 14. The last column in the table is obtained by scaling feeders to the transmission peak-load level. The losses on any feeder during its peak load are higher than (or equal to) the losses on the same feeder during the transmission peak; therefore, the values in last column are slightly smaller than the original data (the third column). As-is state of the transmission network (system before the optimization) is depicted in the Figure 30.

Table 14. Transmission system Peak Case; loss and support summary.

		Support [MVAr]	Losses [MW]	Losses - scaled [MW]
Transmission system	reactors	201	55.05	55.05
	capacitors	237.6		
Subtransmission system (44kV feeders + belonging 12kV feeders)		225	17.24	16.88
Distribution system (12 kV feeders only)		271.8	23.03	19.14

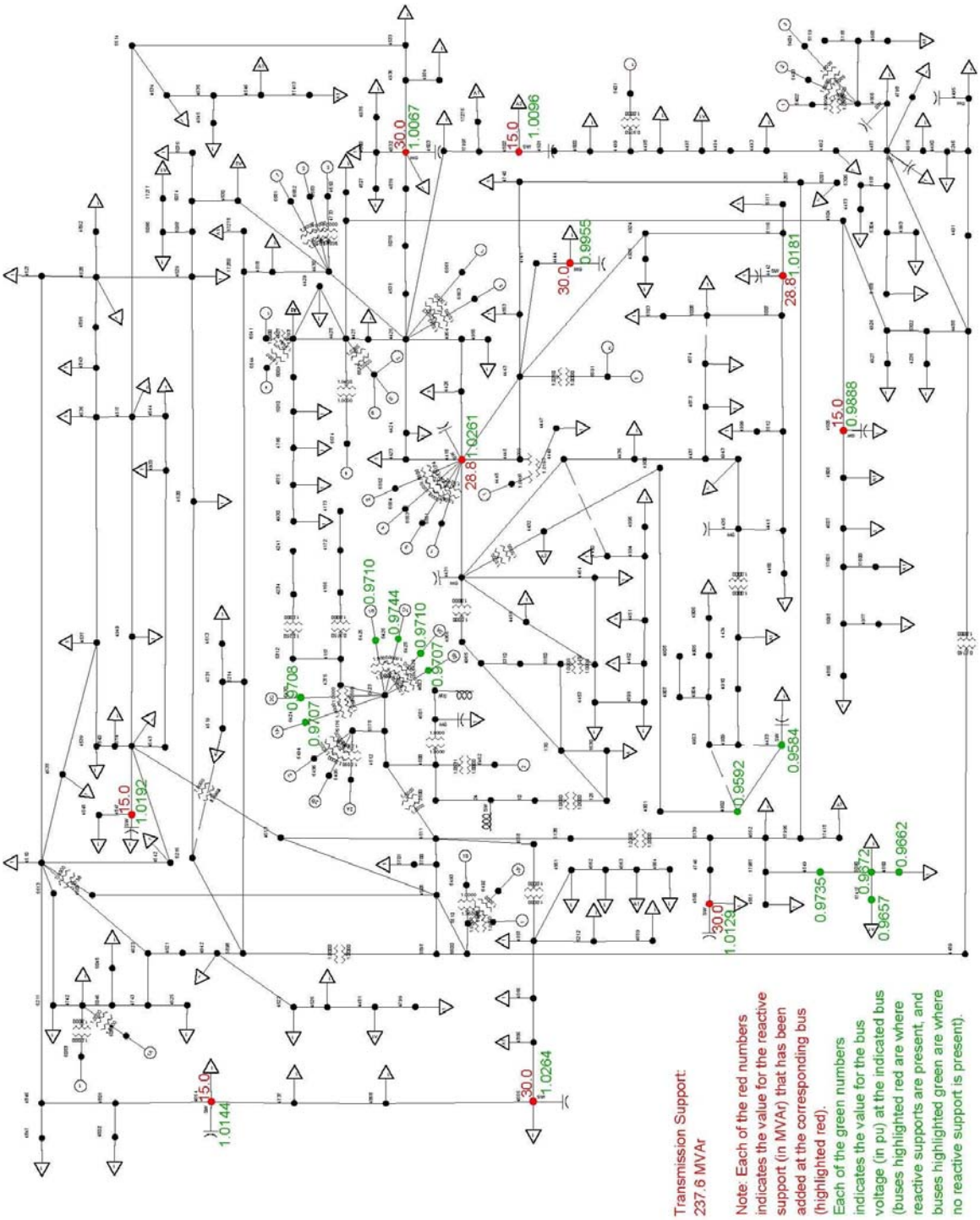

Figure 30. As-is (Before the Optimization) State of the Transmission System.

The existing reactive support has been ignored during this project. Starting from the uncompensated system, the same amount of reactive support is applied to the system and the resulting solution is compared with the existing system. It was confirmed that the integral T&D optimization reaches superior solution with respect to all system objectives.

Feeder optimization is performed first; each feeder is solved separately from the rest of the system. Each feeder is represented with the set of the Pareto solutions called Pareto-front and depicted in Section 7. During transmission optimization the particular feeder solutions are chosen and coupled with the transmission system.

The starting point of optimization was the system with feeder power factors increased up to 0.95. Therefore, the first step was the choice of particular feeder solutions (for each feeder in the system) that will boost the power factor of appropriate transmission loads over 0.95. Comparison of this initial solution with the existing system state is shown in Table 15 (unit costs of $26/kVAr and $20/kVAr are supposed for distribution-switched capacitors and transmission capacitor banks respectively).

Table 15. Comparison of the existing system support and a state obtained by compensating all the feeders up to the power factor of 0.95.

		System loss [MW]	**Reactive support [MVAr]**	**Investment [M$]**
Existing state	Transmission system	55.05	237.6	4.8
	Distribution + subtransmisssion	36.01	496.8	12.9
	Total	**91.06**	**734.4**	**17.7**
“0.95” state	Transmission system	58.97	0	0
	Distribution + subtransmisssion	33.25	331.2	8.6
	Total	**92.22**	**331.2**	**8.6**

A brief comparison of the two states reveals that the distribution system is overcompensated. Actually, some of the feeders are overcompensated (support is designed for feeder peak conditions) while others do not have any support. Reduction and shuffling of reactive support could yield decrease in LV and MV losses.

9.3. Feeder Scaling

The first step in feeder optimization is scaling the feeder data to the transmission peak level. The necessity of scaling and its consequences are already discussed in Section 2 (motivational example) and Section 4. The following two examples provide detailed description of the scaling process.

Example 1: Transmission Bus 89

Distribution network connected to transmission bus 89 consists of three 12 kV feeders. The basic transmission and feeder data are given in the next two tables. All the numbers in the tables in Sections 9.3 and 9.4 are given in MVA (MW or MVAr). It is necessary to scale the feeder loads to the transmission system load level. The scaling is done using the active power as the reactive power is highly dependent on the number of capacitors that were ON at the given working point – this data was not readily available.

Table 16. Transmission data bus 89 (115kV side)

Bus #	Valley load	Peak load
89	6.2 + j 0.4	17.3 + j 3

Table 17. Feeder peak loads; bus 89 (12kV side)

Feeder	Consumption	Existing Capacitors
89 - 1	9.378 + j 3.071	4.5
89 - 2	6.391 - j 2.233	4.2
89 - 3	3.330 - j 1.132	2.7
Overall:	19.1 - j 0.294	11.4

Feeders are scaled for peak conditions. Feeder loads are reduced by 9.4%; (19.1-17.3)/19.1. Losses of 115/12kV coupling transformer are added to the feeder consumption. The first row in Table 18 corresponds to the case when all the feeder capacitors are switched ON; second row corresponds to the case when all the capacitors are switched OFF. Transmission reactive load (j 3) is within the transmission Q range. It roughly occurs when 3 MVAr (out of 11.4) is switched OFF, which seems reasonable.

Table 18. Feeders scaled for peak conditions (scaling -9.4%)

Reactive support	12kV load	Transformer losses	115kV load
Capacitors ON	17.23 - j 1.611	0.138 + j 1.725	17.37 + j 0.114
Capacitors OFF	17.36 + j 10.34	0.188 + j 2.352	17.55 + j 12.692

Feeder loads are next scaled by 67.5% to match the valley load (Table 19). Transmission reactive load (j 0.4) is within the above range; it roughly occurs when 7.7 MVAr (out of 11.4) is switched off; reasonable again.

Table 19. Feeders scaled for valley conditions (scaling -67.5%)

Reactive support	12kV load	Transformer losses	115kV load
Capacitors ON	6.107 - j 8.798	0.053 + j 0.661	6.160 - j 8.140
Capacitors OFF	6.050 + j 3.283	0.022 + j 0.273	6.072 + j 3.556

Example 2: Transmission bus 28

There is only one 12kV feeder connected to the transmission bus 28. The basic transmission and feeder data are given in the next two tables. Even without scaling the feeder load, it was obvious that feeder reactive power will never match the transmission reactive load; the difference will only become worse. Capacitors are not to blame; if they are switched OFF, the difference will increase more.

After additional review of the case, the system owner has discovered an error in feeder model. After the correction the feeder model was “scalable” to the transmission level. The purpose of this example is to support the claim from Section 2: Even though the process of coupling T&D models may be time-consuming, the discovered modeling errors are enough to pay off for this process.

Table 20. Transmission data bus 28 (115 kV side)

Bus #	Valley load	Peak load
28	0.7 - j 0.1	2.4 + j 0.8

Table 21. Feeder peak loads; bus 28 (12kV side)

Feeder	Consumption	Existing Capacitors
28 - 1	3.115 + j 0.181	0.6

9.4. Feeder Optimization

This example explains the optimization of two feeders connected to the transmission bus 69. The appropriate transmission loads (at 115kV bus) are:

- Peak load 8 + j 3.1
- Shoulder load 7.36 + j 2.83
- Valley load 1.6 - j 0.4

As the feeders are modeled as unbalanced three-phase networks, capacitor allocation is performed using COM interface to the industrial-grade software. After ignoring the existing capacitors on the feeders, the optimization is performed for the peak feeder loads. The results are shown in the following figure:

Feeder 69-1: ***P_{loss} minimization*** ***ΔV minimization***

Section	Size	Type	Section	Size	Type
5140778.2	0.3	Switched	No solution		

Feeder 69-2: ***P_{loss} minimization*** ***ΔV minimization***

Section	Size	Type	Section	Size	Type
5178165.3	0.3	Switched	5177976.2	0.3	Switched
5178728.2	0.3	Switched	5177976.2	0.3	Switched
5179018.3	0.3	Switched	5179709.3	0.3	Switched
5178032.1	0.3	Switched	5178056.1	0.3	Switched
5178448.2	0.3	Switched	6359073.1	0.3	Switched
5177898.1	0.3	Switched			

Figure 31. A typical result of feeder optimization.

After the optimization the feeder loads are scaled down to the transmission peak (shown in the next table), shoulder and valley cases. These results will be used by the transmission optimization algorithm. One example of the two-dimensional feeder Pareto front is shown in Figure 33; a feeder with rich Pareto front is chosen for this illustration. One may notice a "tail" of dominated solution in Figure 33. These solutions were non-dominated during the feeder peak optimization; they have become dominated after scaling the feeder loads. In other words, feeder is overcompensated for the transmission peak load.

Table 22. Feeder Pareto front; results scales to the 115kV level

Support (MVAR)	P_{115KV} (MW)	Q_{115KV} (MVAR)	P_{loss} (MW)	ΔV (%)
0.0	8.057	2.550	0.308	2.288
0.3	8.051	2.236	0.304	2.042
0.3	8.051	2.240	0.304	2.029
0.6	8.048	1.920	0.302	1.957
0.6	8.047	1.919	0.301	1.969
0.9	8.048	1.602	0.301	1.975
0.9	8.045	1.598	0.299	2.021
1.2	8.047	1.282	0.302	1.993
1.2	8.043	1.285	0.297	2.044
1.5	8.049	0.963	0.304	2.035
1.5	8.043	0.969	0.296	2.054
1.8	8.042	0.651	0.296	2.139
2.1	8.041	0.329	0.295	2.174

Once the feeder optimization is performed, a few additional things need to be done. If the feeder is fed from the substation with tap changer the results can simply be stored in a simple file for the subsequent optimization of the transmission system. In this case, the substation secondary voltage will be maintained on a constant level and equal to the voltage used for feeder optimization. In this case, the feeder is only loosely coupled

with the transmission system; the transmission optimization algorithm will choose one of many feeder solutions.

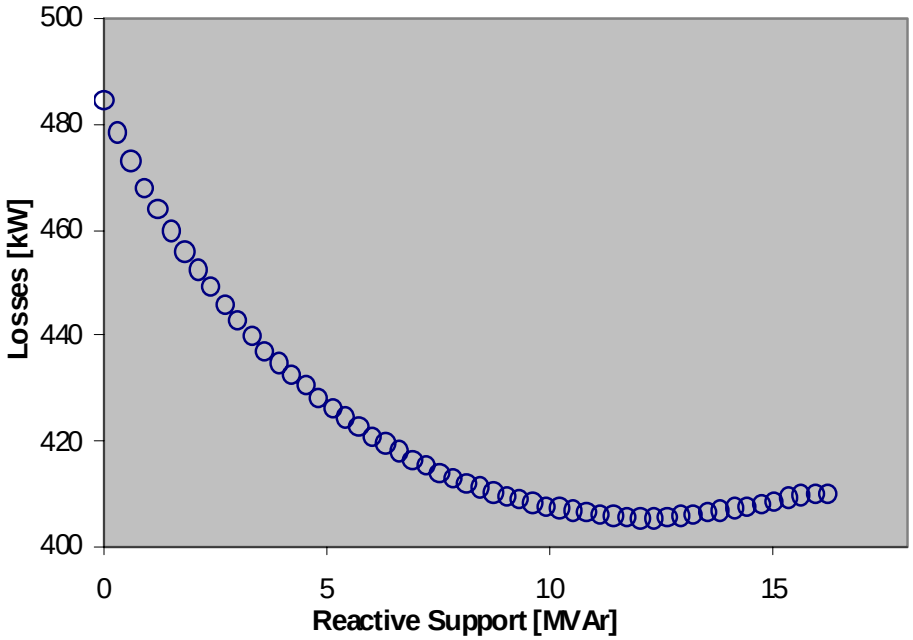

Figure 32. Results of deterministic optimization

However, if substation's secondary voltage is variable all the solutions from the above graph have to be reevaluated for a different set of feeder voltages (e.g. 0.95-1.05 with the step of 0.01). This is a fast and straightforward process as there is no optimization involved. The optimization is performed only for feeder voltage of 1pu. Reevaluation is only the set of power flow solutions. Table 23 provides the structure of the feeder solutions that should be available in the transmission network computations. This table contains all of the necessary information needed in the further calculations and when generated there is no need for any additional computations on the distribution level of the system.

Table 23. Structure of Needed Complete Feeder Solution

Support (# of banks)	Feeder Voltage	P_{115KV} (MW)	Q_{115KV} (MVAR)	P_{loss} (MW)	ΔV (%)
0	0.95				
	0.96				
	0.97				
	0.98				
	0.99				
	1.00				
	1.01				
	1.02				
	1.03				
	1.04				
	1.05				
1	0.95				
	0.96				
	0.97				
…					

9.5. Results on the Overall System

Results of deterministic optimization on Test System are presented in two dimensional solution space losses vs. stability. Figure 33 shows the results for five different investment levels. These levels are spread between "0.95" state (feeders compensated to 95% power factor) and the existing system state (the amount of support equal to the support already existing in the system). Each point on Figure 33 represents a unique system state, i.e. each solution has a different amount of capacitors for any given transmission bus or distribution feeder.

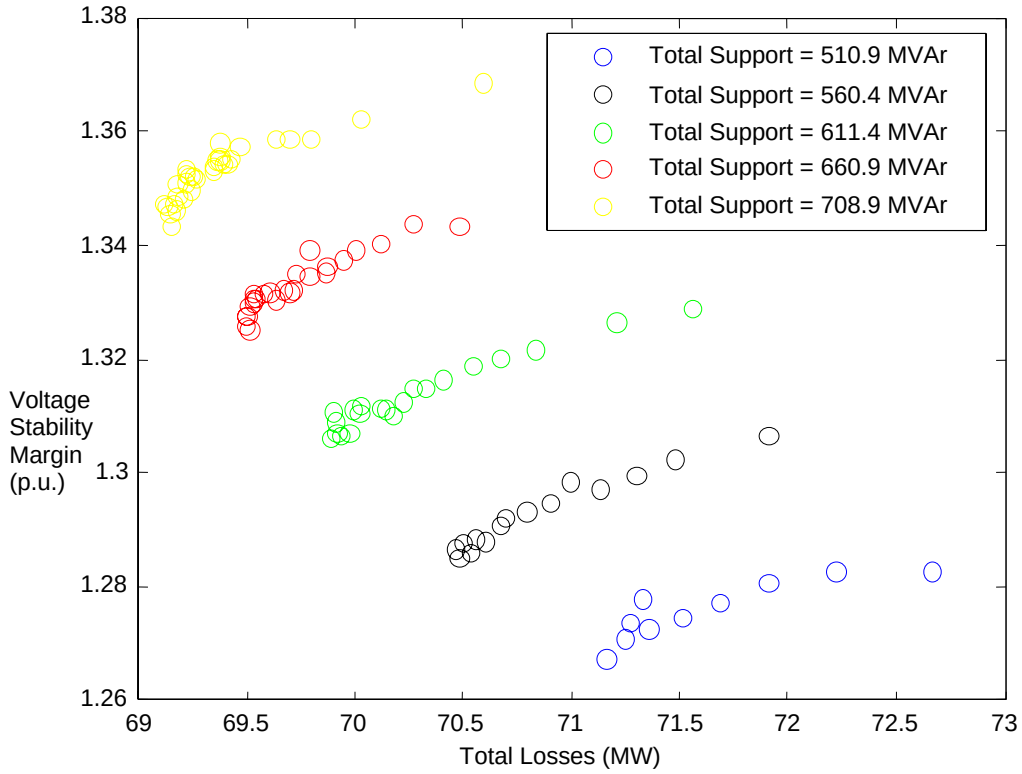

Figure 33. Results of deterministic optimization.

Results obtained by Genetic Algorithm are presented in Figures 34 and 35. Figure 34 shows migration of the solution though 15 iterations of the algorithm. Solution front 708.9 MVA, obtained by deterministic optimization, is shown after 3 iterations (GA3), 6 iterations (GA6), 9 iterations (GA9), 12 iterations (GA#12) and 15 iterations (GA#15). Fronts are progressing toward the global optima. Figure 35 shows the comparison of deterministic optimization and GA for the investment level of 708.9 MVA. It is obvious that Genetic Algorithm improves the solutions toward global optima; in addition it populates the front and spreads it nicely throughout the solutions space.

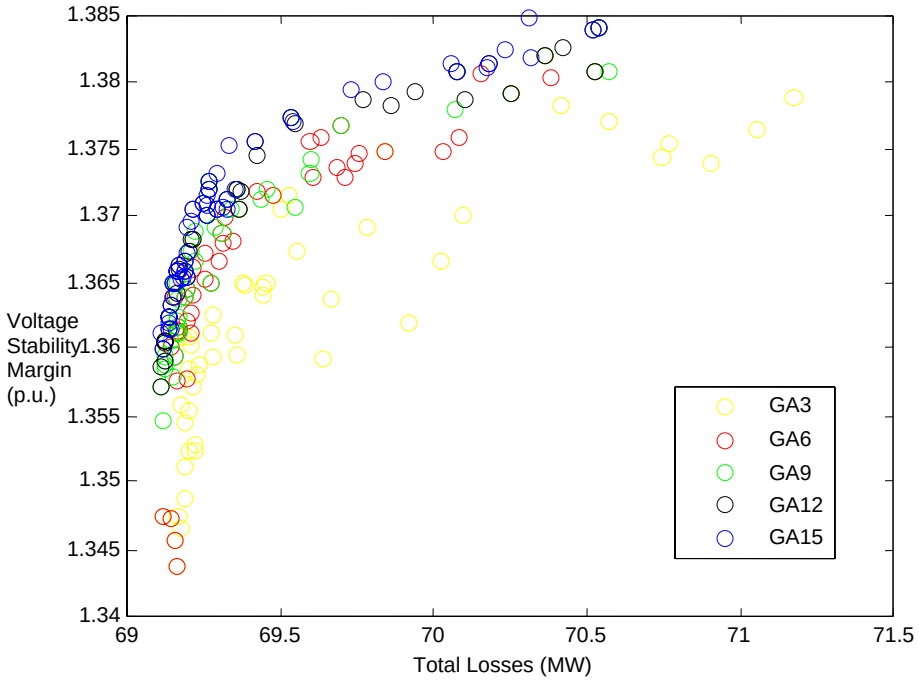

Figure 34. Results of Genetic Algorithm.

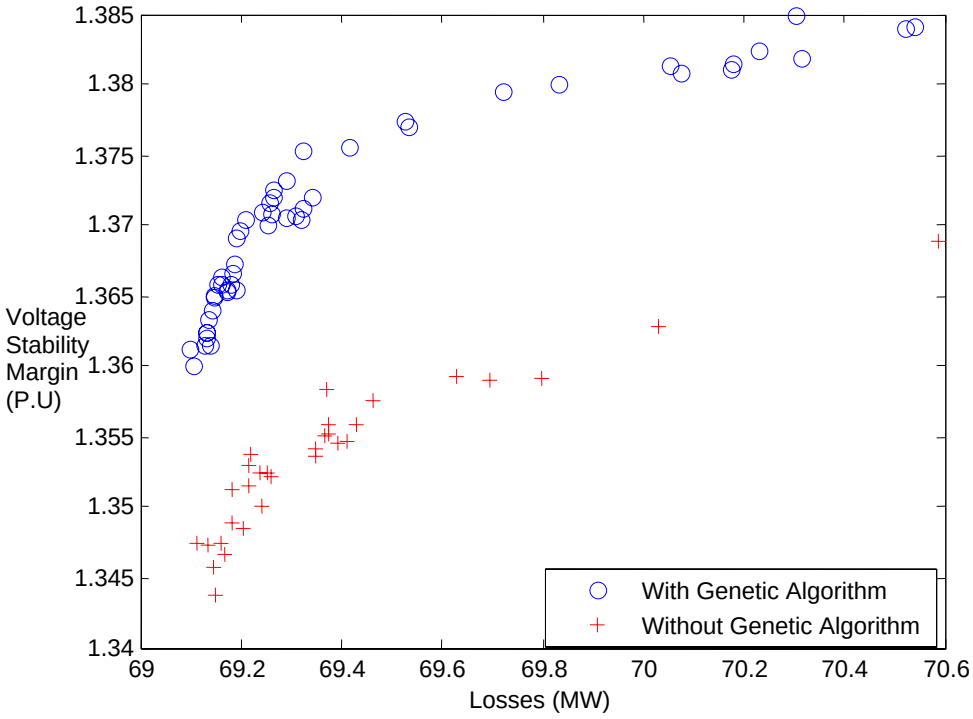

Figure 35. Comparison of GA and LP.

An additional comparison of the results is presented in the following three figures. Figure 36 shows how distribution and transmission losses decay with the addition of the reactive support in the system. Five points presented in the figure are the five best solutions from the five fronts shown in Figure 33. Higher rate of the decay of transmission losses is expected as distribution support reduces both: transmission and distribution losses.

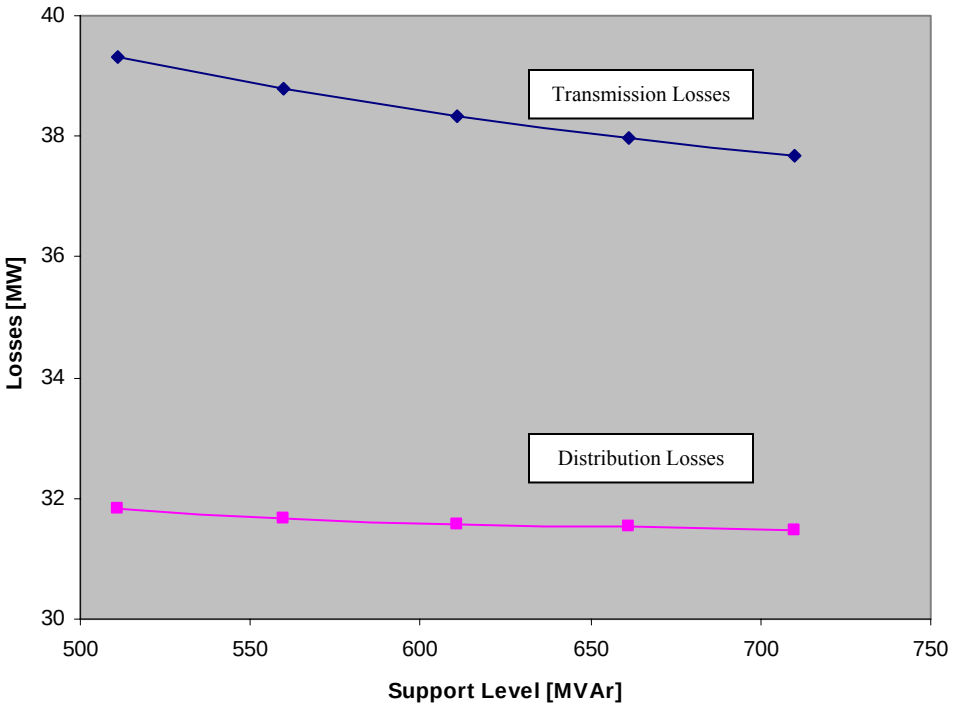

Figure 36. Distribution and Transmission Losses as Functions of the Support Level.

Figures 37 and 39 present respectively the overall system losses and voltage stability margin. Points presented in the figure are five best solutions for losses and five best solutions for voltage stability margin from the five fronts of Figure 33. Last point in both figures comes from the front in Figure 35; it shows the improvement of the objectives due to the genetic algorithm part of the optimization. The solution has same amount of the support than its predecessor, but better losses or stability margin.

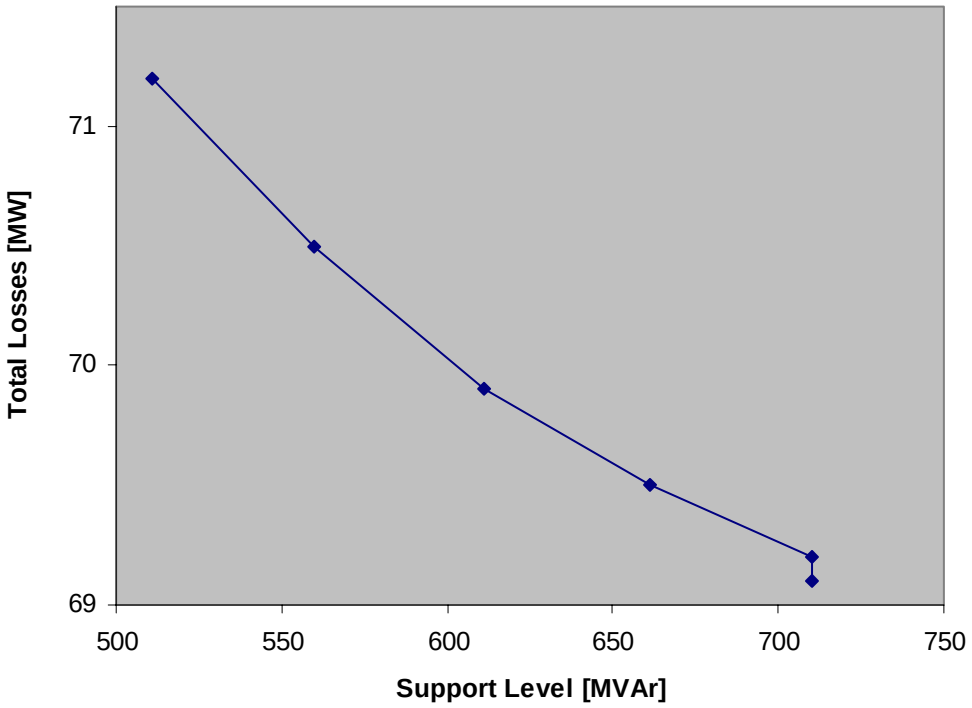

Figure 37. Total System's Losses as Functions of the Support Level.

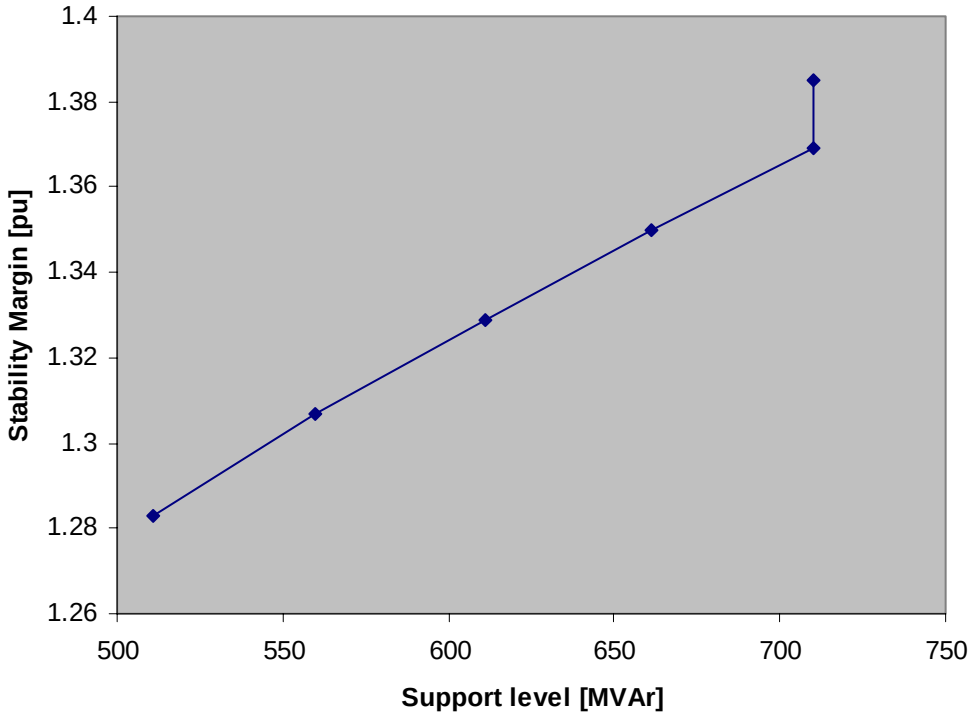

Figure 38. Voltage Stability Margin as Functions of the Support Level.

Additional consideration of the solutions presented in Figures 33-35 are given in [44]. They include discussion on voltage profile in the system, verifications that all the system constraints (branch loading, generation limits, etc.) are satisfied, and detailed information about location and sizing of capacitor banks. Only few of the solutions are presented in the following section in order to demonstrate the feasibility of the solutions and depict the capacitor allocation schemes. One such a solution is also graphically presented in Section 9.7.

Choice of a single solution

The algorithm is designed to produce a set of the solutions rather than a single solution. It is left to the system owner to choose a single solution from the set. The system owner can utilize different criteria while making the choice; the following discussion depicts a few ways of doing it. The first step is discarding the dominated solutions; all the green solutions (unfilled solutions) in Figure 39 are dominated and should be discarded.

To simplify the decision process only three of the solution will be discussed further (red solutions, Figure 39); it should be understood that the same logic can be applied to entire Pareto front or a chosen cluster of the solutions. A detailed analysis of the solution is given in the next section and summarized in Table 24.

Table 24. Analysis of three Pareto solutions.

Solution #	Losses [MW]	Stability Margin [pu]	Voltage-mean [pu]	Voltage-STD [pu]
1	69.13	1.362	1.0063	0.0246
2	69.53	1.377	1.0072	0.0245
3	70.30	1.385	1.0074	0.0234

User should decide if one criterion is more important than the other. For instance, if

stability margin of 36% is acceptable, solution #1 should be chosen as it generates minimal losses. Contrary, if voltage stability is essential, solution # 3 should be chosen. Finally, if user wants a solution that keeps stability on the high side, yet does not generate high losses, any solution from the middle of the front will work (solution # 2 for instance).

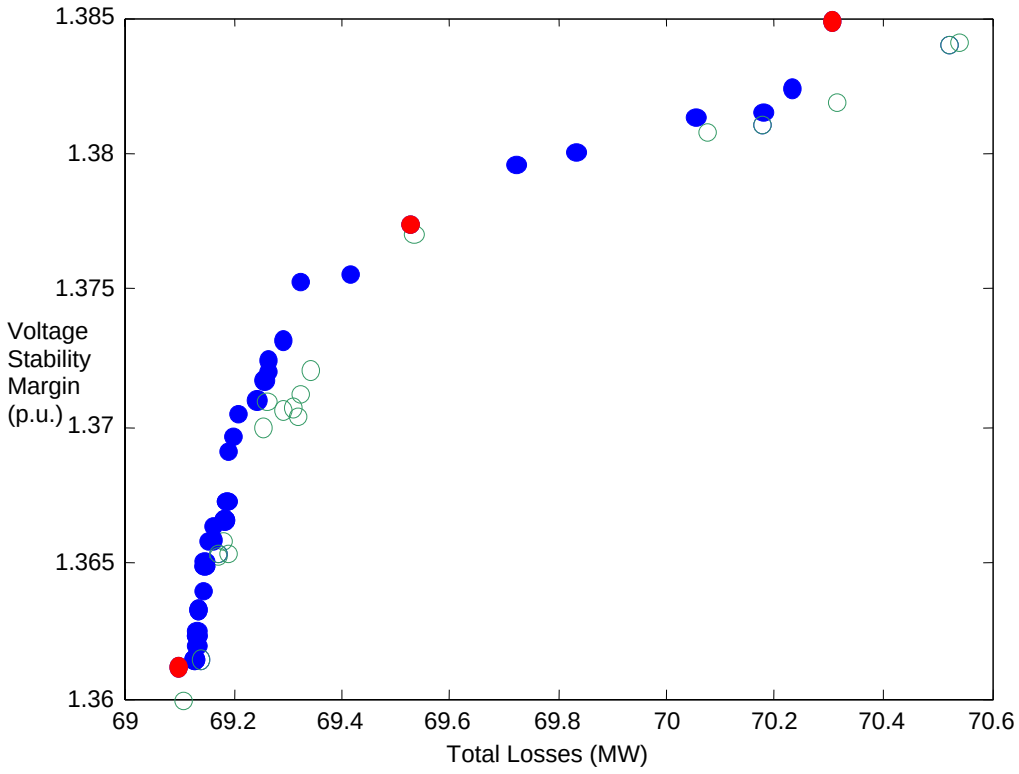

Figure 39. Choice of one solution from the front.

If both of the criteria, losses and stability, are within the desired range for all three solutions, the decision can be based on any other auxiliary criteria, voltage profile for example. Table 24 gives the mean value and standard deviation for transmission system voltages for all three solutions. Standard deviation of voltages can be used to measure "flatness" of the voltage profile. Solution # 3 dominates solutions 1 and 2 as it has the smallest standard deviation.

9.6. Case Studies

A detailed analysis of the three cases depicted in Table 24 is performed in this section. The purpose of this analysis is to demonstrate feasibility of the solutions and provide confirmation that the designed algorithms have performed accurately (system voltages are within the desired levels, branches are not overloaded, support is scattered on both systems, etc.).

Each case begins with a table showing the amount of capacitors and losses in both system as well as the voltage stability margin in this state. This is followed by graphs showing the reactive support on 72 distribution subsystems. Histogram of transmission bus voltages and graph showing the amount of transmission support is shown next. Finally the percent of line emergency ratings is shown.

The analysis of the results shows different capacitor distributions on both systems. Voltage histogram shows no voltage violations. Finally the histogram of % line emergency ratings shows a consistent problem. In all the obtained solutions two identical lines have been overloaded. In a subsequent conversation with the system owner it has been concluded that the input data for the line ratings was wrong for these two lines.

Case-I

Table 25. Case I – System State**.**

Network	Total Capacitor Support (MVAr)	Losses (MW)	Voltage Stability Margin (pu)
Transmission	108.0	37.608	-
Distribution	593.4	31.52	-
Total	701	69.132	1.3624

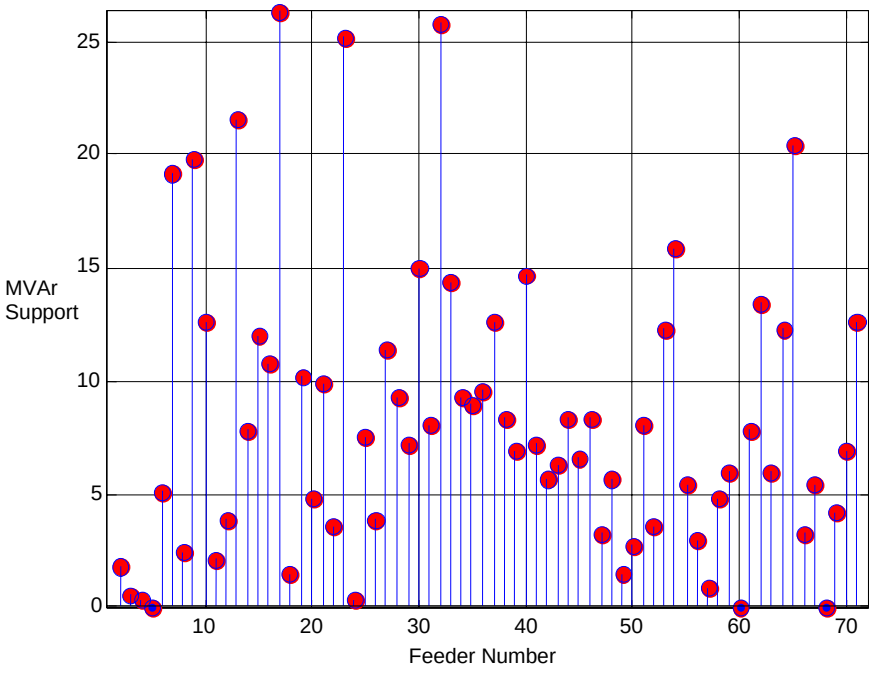

Figure 40. Reactive Support on each feeder- Case I.

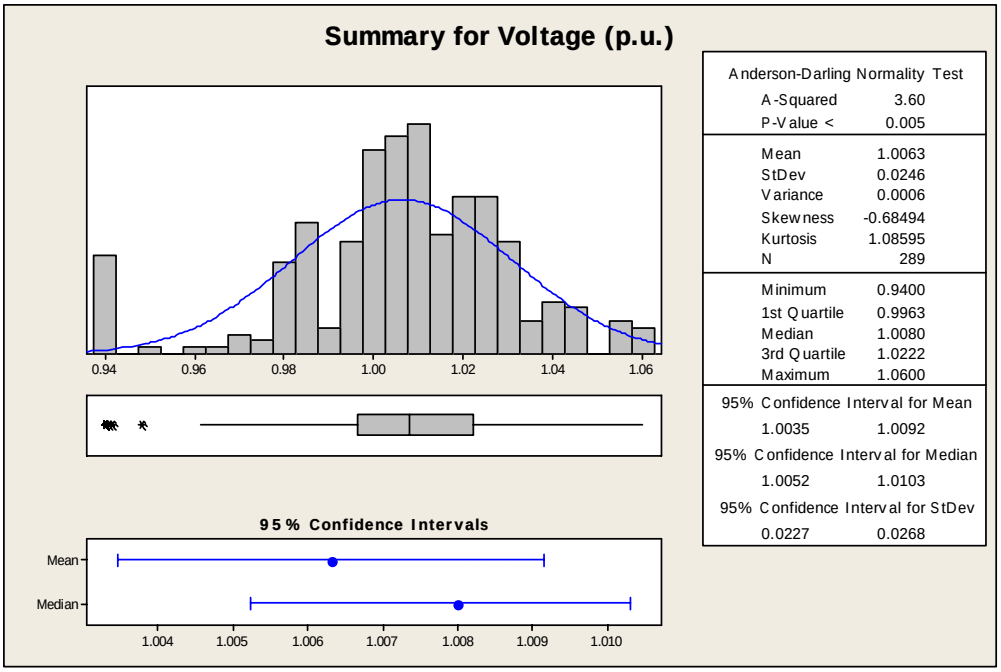

Figure 41. Histogram of Bus Voltages - Case I.

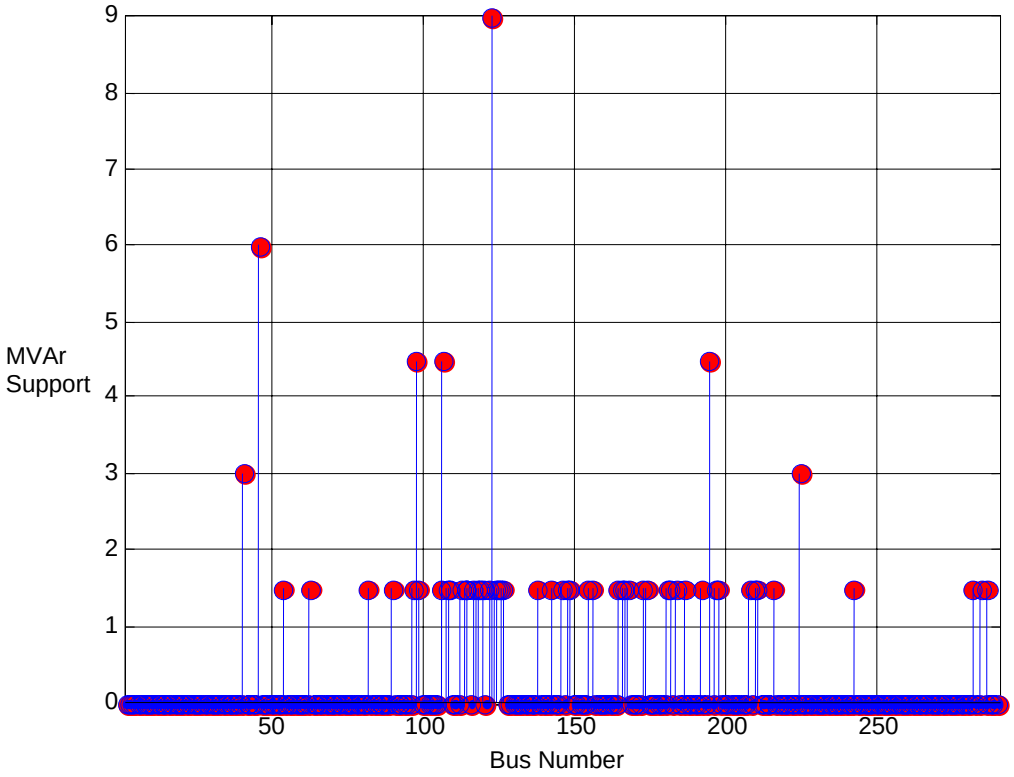

Figure 42. Reactive support on Each Transmission Bus – Case I.

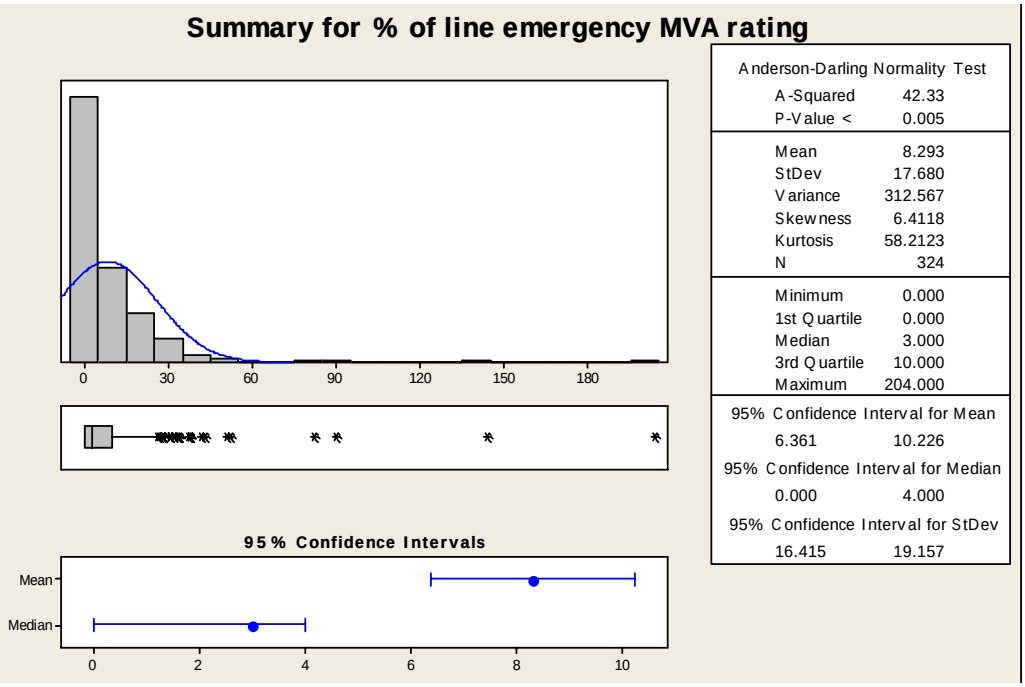

Figure 43. Histogram of Apparent Power Flow as percent of emergency rating

Case-II

Table 26. Case II – System State.

Network	Total Capacitor Support (MVAr)	Losses (MW)	Voltage Stability Margin (pu)
Transmission	156.0	38.485	-
Distribution	605.1	31.82	-
Total	761	70.304	1.3849

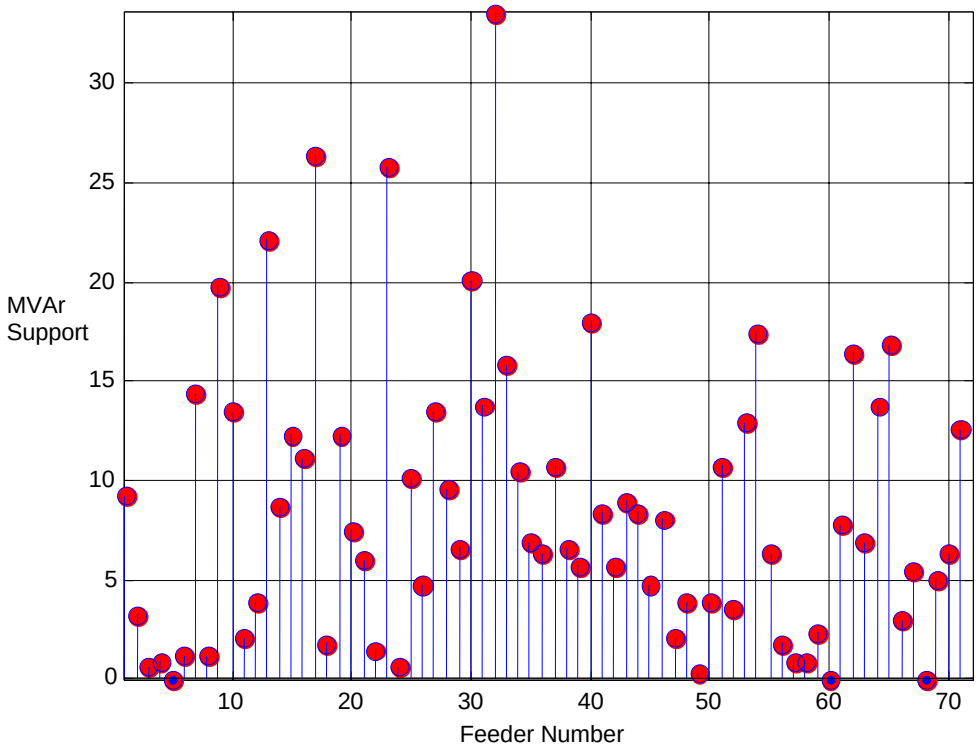

Figure 44. Reactive Support on each feeder – Case II.

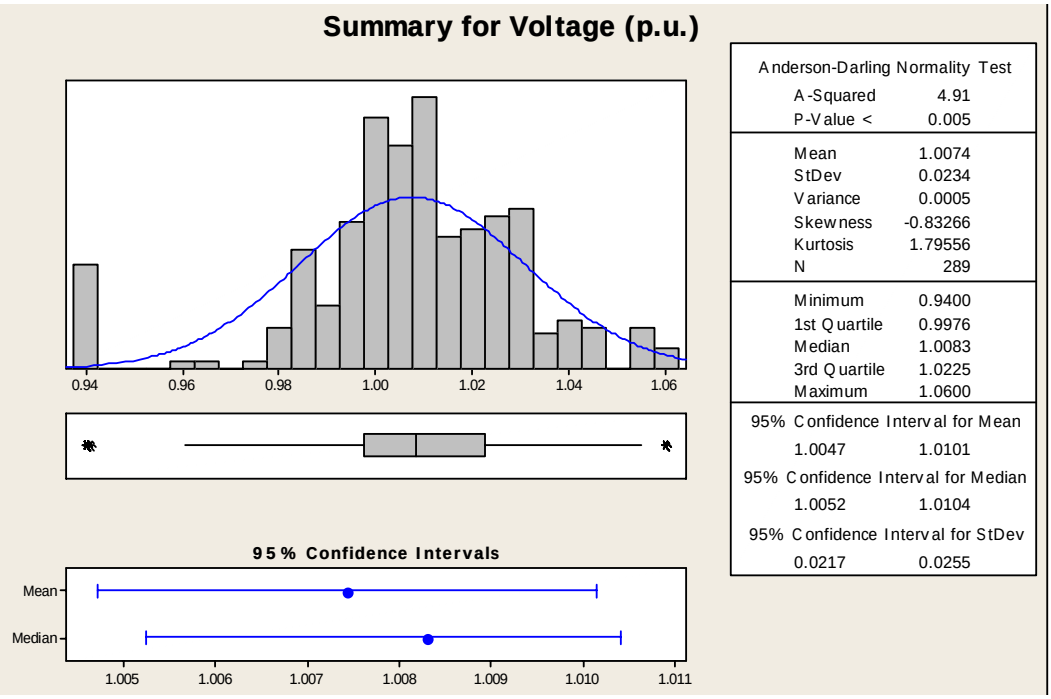

Figure 45. Histogram of Bus Voltages – Case II.

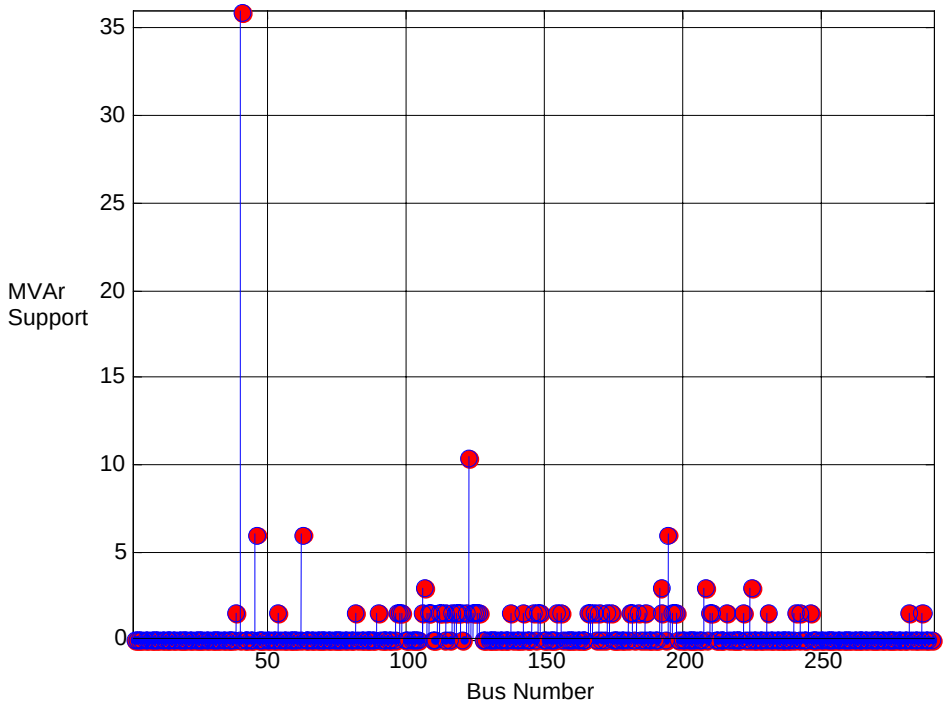

Figure 46. Reactive Support on Each Transmission Bus – Case II

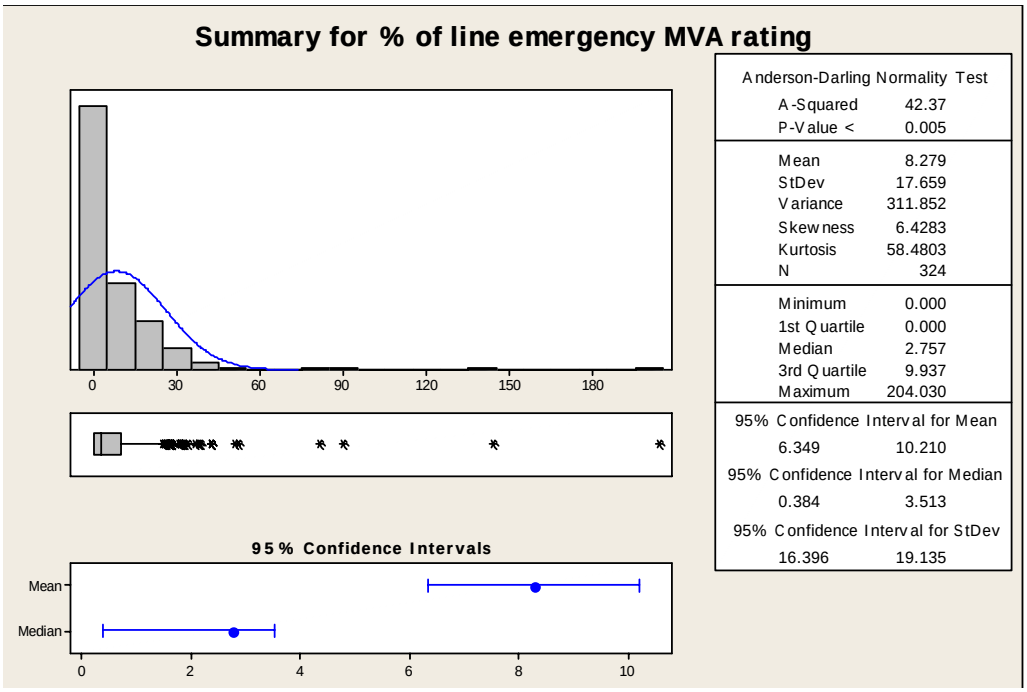

Figure 47. Histogram of Apparent Power Flow as percent of emergency rating

Case-III

Table 27. Case III – System State.

Network	Total Capacitor Support (MVAr)	Losses (MW)	Voltage Stability Margin (pu)
Transmission	114.0	37.905	-
Distribution	607.2	31.62	-
Total	721.2	69.527	1.3774

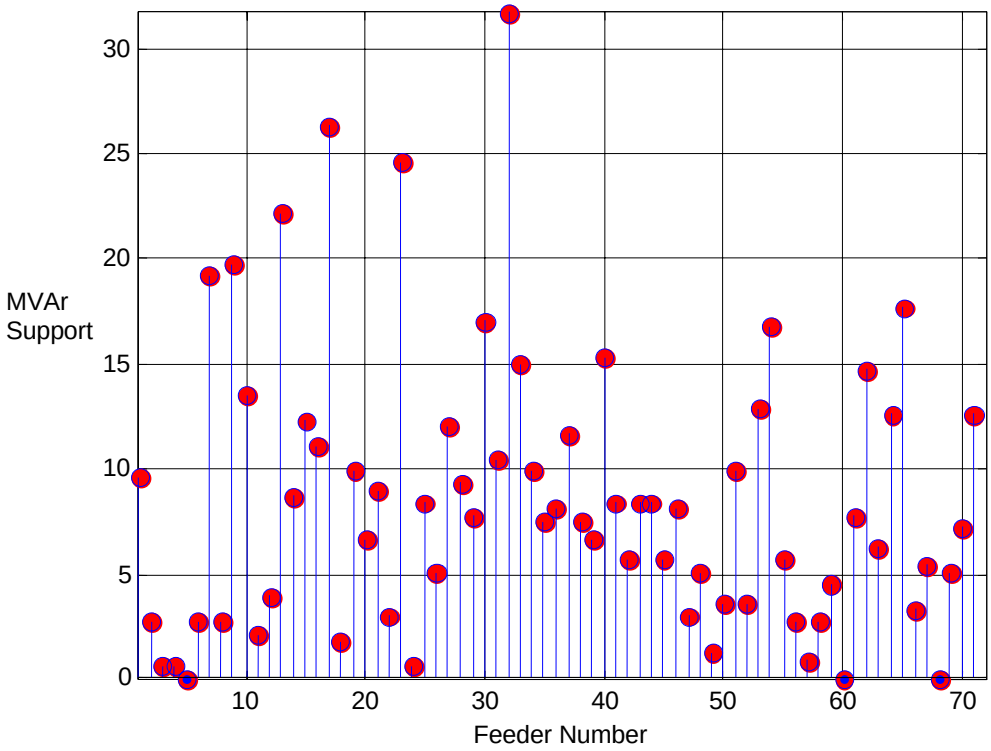

Figure 48. Reactive Support on each feeder – Case III.

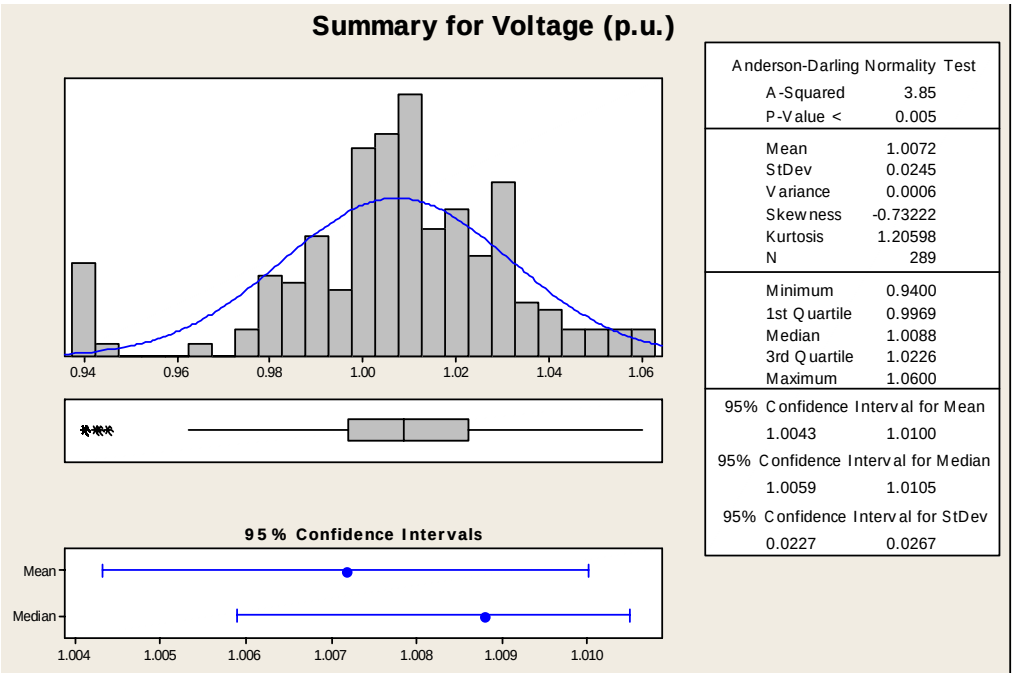

Figure 49. Bus Voltages.

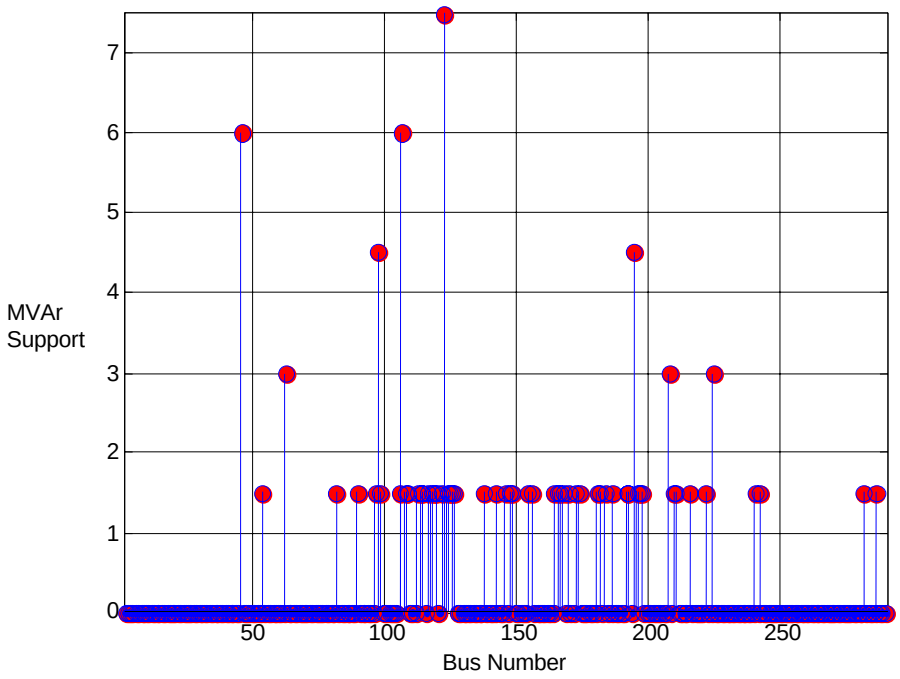

Figure 50. Reactive support on each Transmission Bus – Case III.

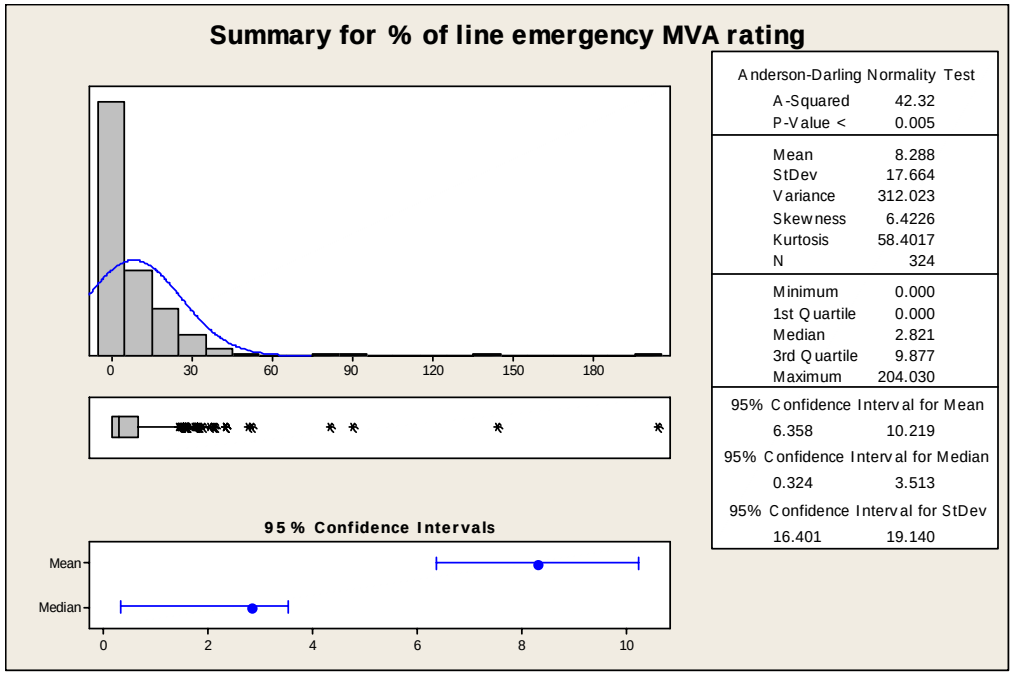

Figure 51. Histogram of Apparent Power Flow as percent of emergency rating

9.7. Conclusion

The algorithm presented in Sections 2 through 8 has been applied on multiple systems: IEEE 9-bus system, IEEE 39-bus system, IEEE 13-node test feeder and on the Test System comprised of several hundred of transmission buses and several hundred of distribution feeders. The algorithm has been tailored to each particular system due to the different properties of the different systems. For example, distribution optimization of feeders in the Test System was performed utilizing industrial-grade code for capacitor optimization, while the optimization of IEEE 13-node feeder was performed using developed Mat Lab based multi-objective optimization algorithm. In all cases the optimization has performed as expected and better than the existing optimization practices.

Proof of the concept was done using the IEEE 39-bus system and IEEE 13-node feeders. The details of this work are published in [43]. This part of the work was focused on the system decoupling explained in the Section 4.2 and algorithm synthesis explained in Section 4.3. The work yielded promising results which propelled this research in the real-field systems.

The feasibility study was performed on the Test system obtained from one US electric utility company. The details of this work are published in [44]. It is expected that, in future, the algorithm presented here been developed as a part of an industrial-grade software. To bring the algorithm to that level the developed code (programming language-wise and speed-wise) must be optimized and the process of coupling T&D models should be automated. It is also expected that the future work on this problem will

include transient stability phenomenon and the dynamic reactive support.

The feasibility study has revealed some general conclusions that are worth presenting here:

First, it has been demonstrated that the algorithm reaches a set of solutions that outperform the one currently used in the Test System. Detailed comparison of "as-is" solution and the solutions obtained by integral optimization is available in [44]. Only one aspect of the comparison is tackled here. A comparison of the total system losses of case #1 (Table 25) and the "as-is" solution (Table 15) shows the decrease of losses of 21.93 MW. Assuming the cost of losses of 6 cents/kWh and assuming the load distribution of 5% peak, 70% shoulder and 25% valley, the annual energy savings are calculated at $9.1 million.

It is very important to notice that the above savings should not be only contributed to the developed integral approach. "As-is" solution of the system was not obtained by simply assigning given amount of the support separately to transmission and distribution systems. This solution was developed over the years, even decades, by adding capacitors to the system as it was growing and changing. Each capacitor addition was done to solve a different problem at hand. Therefore, "non-optimality" of "as-is" solution is natural and inherent to any system that this algorithm would deal with. On the other hand, the algorithm does not have a problem with the addition of the support to such systems; it is capable (as demonstrated in Figures 37-38) of improving the system starting from any solution. Finally, the above savings are not net savings. There is a considerable amount of engineer-hours involved in setting the model of transmission and distribution systems together. The beneficial side-effects of this work illustrated in Section 9.3 are deemed

enticing enough for such a venture.

The second important conclusion concerns the amount of the reactive support applied on transmission and the distribution system respectively. Information obtained by several electric utilities reveal that the current practice is to use twice as much support at the distribution level than at the transmission level. All the results provided, fronts of optimal solutions for different levels of reactive support (investment), have this ratio between 4 and 6.5. Therefore, the more the reactive support is applied to the distribution system the better the overall system. In general, if all the distribution models were controllable (no customer owned substation), the optimization would set all the support on the distribution side of the system.

The next important conclusion is that in most of the cases the optimization favors small capacitor banks on the transmission system. One transmission solution (Case 1 from the previous Section) is graphically presented in the next figure. Figure 52 shows together the existing capacitors in the system (red numbers) and the capacitor scheme that should be applied according to Case 1 (blue numbers). All the numbers in the figure show capacitor size in MVAr. The algorithm has used the smallest available capacitor bank (1.5 MVAr) in most of the cases. The biggest capacitor bank used in this solution is 9MVAr. It is worth noting that the minimal capacitor bank of 1.5 MVAR is industry standard and its use in this project has been approved by all the electric utilities supervising the project.

Further comparison of these two solutions reveals that the algorithm has applied the support in the same areas of the system as in the case of the current solution. The main difference is that the amount of the transmission support is significantly lower

(most of the support is on the distribution side) and the proposed solution additionally distributes the resources.

Finally, it is worth repeating that none of the above conclusions diminishes the value of the "as-is" solution currently existing in the system. This solution is a product of historical development of power systems and capacitor allocation techniques. As no other work on integral optimization of transmission and distribution systems was available during this research, the "as-is" solution was the only possible choice for comparisons with the developed solutions.

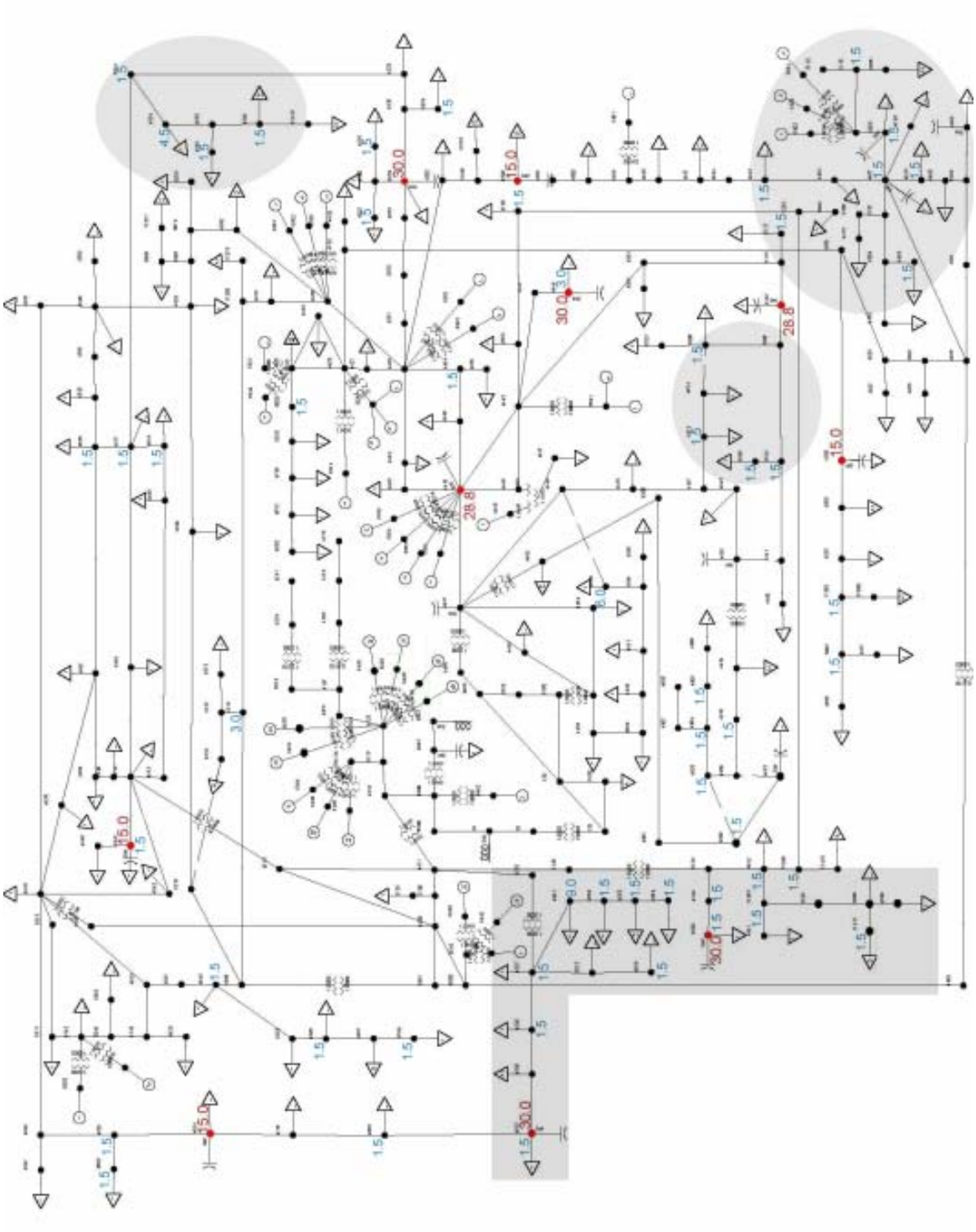

Figure 52. Test case: Comparison of “As-is” state with the Case #1

9.8. Contributions

The main contributions of the work presented here are proof of the concept that multi-objective reactive-optimization of T&D network is possible, [43], and the example of the feasibility of such an optimization on a real-system as demonstrated in [44]. It has been shown, [44], that the developed algorithm converges to the superior solutions when compared to the conventional solution that has been applied in the test system.

The novel approach comprises integral T&D system modeling, problem decoupling and algorithm synthesis. It has been shown that the modeling of the entire power system is possible despite the fact that it has not been performed in the past. Problem decoupling decreases the optimization search space. Algorithm synthesis is used to improve the efficiency of the optimization algorithm.

The optimization algorithms used are customized for the problem at hand. While the used optimization algorithms are well known, they have never, or very seldom, been used in multi-objective framework combined with very large solution spaces. Linear programming is extended in multi-objective framework; customized genetic algorithm was started with the locally-optimal initial population and the linear optimal power flow is developed.

The following customized algorithms have been developed to better accommodate the entire optimization process:

- LP-based optimal power flow (fully verified and validated)
- Fast contingency filtering algorithm with the recognition of unstable PV-PQ transition

- Voltage stability assessment of the transmission system via scaling of the loads of adjacent distribution systems
- An algorithm that automates execution of industrial-grade software using COM interface.

Comparison of the developed algorithms with available software (public or industrial) has shown that all the developed algorithms perform as expected and better than the available software.

Work presented here has resulted in two papers, [45] and [46], two reports, [43] and [44], and two additional papers are being prepared for submittal to IEEE.

REFERENCES

[1] M.M. Saied, "Optimal long line series compensation (HVAC transmission lines)" *IEEE* Trans. Power Delivery, Vol.PWRD-1, Issue 2, April 1986, pp. 248-253

[2] O. Ojo, "Optimal series capacitor compensation of high voltage transmission lines", Proc. 23rd Southeastern Symposium on System Theory, March 1991, pp. 550–554

[3] C.S. Indulkar, B. Viswanathan, and S.S. Venkata, "Maximum power transfer limited by voltage stability in series and shunt compensated schemes for AC transmission systems", IEEE Trans. Power Delivery, Vol. 4, Issue 2 , April 1989, pp. 1246-1252

[4] M.M. Begovic, and A.G. Phadke, "Control of voltage stability using sensitivity analysis", IEEE Trans. Power System, Vol. 7, Issue 1 , February 1992, pp. 114-123

[5] V. Ajjarapu, L.L. Ping, and S. Battula, "An optimal reactive power planning strategy against voltage collapse", IEEE Trans. Power Systems, Vol. 9 Issue 2 , May 1994, pp. 906 –917

[6] F. Jurado, and J.A. Rodriguez, "Optimal location of SVC based on system loadability and contingency analysis", Proc. 7th IEEE International Conference on Emerging Technologies and Factory Automation, Vol. 2 , 1999, pp. 1193 -1199

[7] N.H. Dandachi, "Improved algorithm for voltage/VAr management on the NGC system", IEE Colloquium on Voltage Collapse, Digest No. 1997/101, 1997, pp. 4/1 - 4/6

[8] H.N. Ng, M.M.A. Salama, and A.Y. Chikhani, "Classification of capacitor Allocation techniques", IEEE Trans. Power Delivery, Vol. 15, No. 1, Jan 2000, pp. 387-392

[9] J.J. Grainger, and S.H. Lee, "Optimum size and location of shunt capacitor for reduction of losses on distribution feeders", IEEE Trans. Power Apparatus and Systems, Vol. 100, March 1981, pp. 1105-1118,

[10] S.H. Lee, and J. J. Grainger, "Optimum placement of fixed and switched capacitor on primary distribution feeders", IEEE Trans. Power Apparatus and Systems, Vol.100, March 1981, pp. 345-352

[11] J.J. Grainger, and S. Civilnar, "Volt/Var Control on Distribution Systems with Lateral Branches Using Capacitors and Voltage Regulators, Part I: Overall Problem", IEEE Trans. Power Apparatus and Systems, Vol. 104, , Nov 1985, pp. 3278-3297

[12] J.J. Grainger, and S. Civilnar, "Volt/Var Control on Distribution Systems with Lateral Branches Using Capacitors and Voltage Regulators, Part II: The Solution Method", IEEE Trans. Power Apparatus and Systems, Vol.104, Nov 1985, pp. 3278-3297

[13] J.J. Grainger, and S. Civilnar, "Volt/Var Control on Distribution Systems with Lateral Branches Using Capacitors and Voltage Regulators, Part III: The Numerical Result", IEEE Trans. Of Power Apparatus and Systems, Vol.104, Nov 1985, pp. 3278-3297

[14] Y.Y. Hsu, and H.C. Kuo, "Dispatch of Capacitors on Distribution System Using Dynamic Programming", IEEE Proc. Generation Transmission and Distribution, Vol. 140 , Issue 6, November 1993, pp. 433-438

[15] M.E. Baran, and F.F. Wu, "Optimal Capacitor Placement on Radial Distribution Systems", IEEE Trans. Power Delivery, Vol.4, November 1985, pp. 725-734

[16] M.E. Baran, and F.F. Wu, "Optimal Sizing of Capacitors Placed on Radial Distribution Systems", IEEE Trans. Power Delivery, Vol.4, November 1985, pp. 725-734

[17] A. Salam, T.S. Chikani, and A.Y. Hackam, "A New Technique for Loss Reduction Using Compensating Capacitors Applied to Distribution Systems with Varying Load Condition", IEEE Trans. Power Delivery, , Vol. 9, Issue 2, April 1994, pp. 819-827

[18] M. Cris, M.M.A. Salama, and S. Jayaram, "Capacitor Placement in Distribution Systems Using Heuristic Search Strategies", IEEE Proc. Generation, Transmission and Distribution, Vol. 144, Issue 3, May 1997, pp. 225-230

[19] W.S. Jwo, C.W. Liu, C.C. Liu, and Y.T. Hsiao, "Hybrid expert system and simulated annealing approach to optimal reactive power planning", IEE Proc. Generation, Transmission and Distribution, Vol. 142, Issue 4, July 1995, pp. 381 – 385

[20] S. Sundhararajan, and A. Pahwa, "Optimal selection of capacitors for radial

distribution systems using a genetic algorithm", IEEE Trans. Power Systems, Vol. 9, Issue 3, August 1994, pp. 1499-1507

[21] K.N. Miu, H.D. Chiang, and G. Darling, "Capacitor placement, replacement and control in large-scale distribution systems by a GA-based two-stage algorithm", IEEE Trans. Power Systems, Vol. 12, Issue 3, August 1997, pp. 1160–1166

[22] M. Delfanti, G.P. Granelli, P. Marannino, and M. Montagna, "Optimal capacitor placement using deterministic and genetic algorithms", IEEE Trans. Power Systems, Vol. 15, Issue 3, August 2000, pp. 1041–1046

[23] J. Andersson, "A survey of multiobjective optimization in engineering design", http://citeseerx.ist.psu.edu/viewdoc/summary?doi=10.1.1.8.5638 (Accessed October 22, 2008).

[24] A. Augugliaro, L. Dusonchet, S. Favuzza, and E.R. Sanseverino, "Voltage regulation and power losses minimization in automated distribution networks by an evolutionary multiobjective approach", IEEE Trans. Power Systems, Vol. 19, Issue 3, August 2004, pp. 1516-1527

[25] G. Levitin, A. Kalyuzhny, A. Shenkman, and M. Chertkov, "Optimal capacitor allocation in distribution systems using a genetic algorithm and a fast energy loss computation technique", IEEE Trans. Power Delivery, Vol. 15, Issue 2, April 2000, pp. 623–628

[26] J.T. Ma, and L.L. Lai, "Evolutionary programming approach to reactive power planning", IEE Proc. Generation, Transmission and Distribution, Vol. 143. No. 4, July 1996, pp. 365-370

[27] Y.-T. Hsiao, and C.-Y. Chien, "Optimization of capacitor allocation using an interactive trade-off method", IEE Proc. Generation, Transmission and Distribution, Vol. 148, Issue 4, July 2001, pp. 371–374

[28] B. Milosevic, and M. Begovic, "Capacitor placement for conservative voltage reduction on distribution feeder", IEEE Trans. Power Delivery, Vol. 19, Issue 3, July 2004, pp. 1360-1367

[29] B. Baran, J. Vallejos, R. Ramos, and U. Fernandez, "Reactive power compensation using Multi-objective evolutionary algorithm", 2001 IEEE Porto Power tech Conference, September 2001, Vol. 2, pp. 532-538

[30] C. A. Coello, D. A. Van Veldhuizen, and G. B. Lamont, "Evolutionary algorithms for solving multi-objective problems", New York: Kluwer Academic/Plenum Publishers, 2002

[31] D. Bertsimas, and J. N. Tsitsiklis, "Introduction to linear optimization", Belmont Massachusetts: Athena Scientific, 1997

[32] D Goldberg, "Genetic Algorithm in Search, Optimization and Machine Learning", New York: Addison Wesley, 1989.

[33] O. Hajji, S. Brisset, and P. Brochet, "A stop criterion to accelerate magnetic Optimization process using genetic algorithms and finite element analysis", IEEE Transaction on Magnetics, Volume 39, May 2003, pp. 1297-1300

[34] M. Lee, and X. Feng, "A fuzzy stop criterion for genetic algorithms using performance estimation", IEEE World Congress on Computational Intelligence, Volume 3, , Jun 1994, pp. 1990-1995

[35] D. Cvetkovic, and H. Muhlenbein, "The optimal population size for uniform crossover and truncation selection", http://citeseerx.ist.psu.edu/viewdoc/summary?doi=10.1.1.7.2680 (Accessed October 22, 2008)

[36] Y. R. Tsoy, "The influence of population size and search time limit on genetic algorithm", The 7th Korea-Russia International Symposium on Science and Technology, Volume 3, July 2003 pp: 181 - 187 vol.3

[37] V. Ajjarapy, and C. Christy, "The continuation power flow: a tool for steady state voltage stability analysis", Proc. Power Industry Computer Application Conference, May 1991, pp. 304-311

[38] Cyme International Inc., "CYMEDIST COM; Reference Manual for CYMEDIST" Dec, 2003

[39] S. Greene, I. Dobson, and F. Alvardo, "Sensitivity of the loading margin to voltage collapse with respect to arbitrary parameters", IEEE Transactions on Power Systems, Volume 12, No 1, Feb. 1997, pp. 262 – 272

[40] B. Chazelle, "An optimal convex hull algorithm and new results on cuttings",

Proceedings of the 32th Annual Symposium on Foundations of Computer Science, 1991, pp. 29-38

[41] T. Ottmann, S. Schuierer, and S. Soundaralakshmi, "Enumerating extreme points in higher dimensions", Proceedings of the 12th Annual Symposium on Theoretical aspects of Computer Science (STACS), 1995, pp. 562-570

[42] E. Vaahedi, C. Fuchs, W. Xu, Y. Mansour, and H. Hamadanizadeh, G. K. Morison, "Voltage stability contingency screening and ranking", IEEE Transactions on Power Systems, Volume 14, Issue 1, Feb. 1999 Page(s):256 - 265

[43] M. Begovic, B. Radibratovic and F. C. Lambert, "Optimization of reactive resources in transmission and distribution networks", NEETRAC Baseline Project 02-105, December 2003

[44] M. Begovic, B. Radibratovic and F. C. Lambert, "Optimization of reactive resources in transmission and distribution networks – Phase 2", NEETRAC baseline Project 04-158, December 2007

[45] M. Begovic, B. Radibratovic and F. C. Lambert, "On multiobjective volt-VAR optimization in power systems", Proceedings of 2004 IEEE HICSS, Hawaii, January 4-7, 2004.

[46] M. Begovic, B. Radibratovic, F. C. Lambert, Damir Novosel, "Optimization of Capacitor Allocation in Transmission and Distribution Networks", 2004 IEEE IREP Symposium, August 2004.

VITA

Branislav Radibratovic

Branislav Radibratovic was born in Belgrade, Serbia on December 11, 1970. He received a B.S. degree in Electrical Engineering from Belgrade University in 1997. He worked several years as a Professional Engineer in Belgrade, Serbia on the design of various kinds of power system infrastructure, substations, transmission lines, etc. He enrolled in Georgia Institute of Technology in 2002 and received his M.S. degree in Electric and Computer Engineering in December 2002. Between 2002 and 2007 he worked at Georgia Institute of Technology as a teaching and research assistant. In January 2007 he accepted the position in EDSA Micro Corporation, developer of software for design and analysis of power systems. He currently holds the position of Project Manager for the entire EDSA software family.